A STUDY OF HIGH PERFORMANCE ANTENNA SYSTEMS FOR DEEP SPACE COMMUNICATION

Status Report IV
June 15, 1969 to December 15, 1969

15 February 1970

Grant Number NGR-17-004-013

Prepared for
National Aeronautics and Space Administration
Office of Grants and Research Contracts
Washington, D.C.

CRES

THE UNIVERSITY OF KANSAS • CENTER FOR RESEARCH INC
ENGINEERING SCIENCE DIVISION • LAWRENCE, KANSAS

A STUDY OF HIGH PERFORMANCE ANTENNA SYSTEMS FOR DEEP SPACE COMMUNICATION

L.L. Bailin
Program Manager

A.A. Ksienski
Assistant Program Manager

Status Report IV
June 15, 1969 to December 15, 1969

Grant Number NGR-17-004-013

Prepared by
The University of Kansas
Center for Research, Inc.
Engineering Science Division
Lawrence, Kansas

for
National Aeronautics and Space Administration
Office of Grants and Research Contracts
Washington, D.C.

CONTENTS

A STUDY OF HIGH PERFORMANCE ANTENNA SYSTEMS FOR DEEP SPACE COMMUNICATION

I. INTRODUCTION

The objective of this program is to study the most recently defined parameters for a high data rate of communication system which can operate between an earth station and a vehicle in space over great distances. An effort will be made to describe and delineate the characteristics of radiating subsystems and their internal sub-divisions which can satisfy the requisite performance criteria for an S-band system. Considerations will be given to the advance technology concerned with the ground based antenna, and where pertinent, to the spacecraft antenna as well. An effort will be made to determine the feasible design approaches for the ground antennas and its component parts. Appropriate design criteria will be investigated analytically, and where possible a comparison will be made with empirically determined results in an effort to define areas of research and development which need long term attention. The data rates of long term interest are 10^6 to 10^7 bits/second for a Mars mission and 10^4 to 10^6 bits/second for a Jupiter mission.

The ground-based antennas are discussed in this program as components of a link designed to fulfill the specific function of providing uninterrupted communication from a spacecraft to the earth at planetary distances. For obvious reasons, the most attention is given the down link aspects using a carrier frequency of 2.3 GHz, since a frequency in this region has advantages for an all-weather ground station and is presently in use in the NASA Deep Space Instrumentation Facility. It is assumed also that future mission plans will require information rates of the order of 10^4 to 10^7 bits/second with a given probability of error, 10^{-2} to 10^{-5}. These parameters imply a specific system performance in terms of bandwidth and signal-to-noise ratio. When the characteristics of the available transmitter and receiver are evaluated or assumed, the required performance characteristics of the overall radiating system are determined either directly or by implication. The overall radiating system is taken to include the combination of the spacecraft and the ground or relay station antenna equipment in their inevitable environment. Thus, for this study, certain gain and aperture requirements will be assumed nominal as parameters to satisfy a variety of space missions.

There are two general areas of concern that must be investigated relative to the ground-based receiving system which of necessity must be large compared to wavelength to achieve the desired performance characteristics. The first involves questions about the received signal to noise level or the gain that must be provided to handle it. Considerations must be given to methods by which it may be enhanced, and the limitations that may be encountered during the various phases of a mission. The second area embraces questions about the contributions made to the noise of the communications link, the manner in which these are introduced, and

methods by which they may be minimized. These questions are, of course, interrelated, and the limitations encountered are intensely practical and economic, as well as theoretical. For this study, emphasis will be given to the first area and when necessary, results of other investigations into the questions involved in the second area will be used.

The requirement of a minimum signal to noise level forces the sum of the gains of the space and ground antennas to be of some value that can be specifically determined for a particular mission. It is important to be able to allocate the antenna gains at each end of the link according to reasonable expectations concerning the practical designs and performance characteristics that can be accomplished in the next ten to fifteen years. An optimum allocation of these gains is difficult although some progress has been made along these lines. For this study nominal values shall be used as parameters in an effort to establish quantitative relationships between pertinent dimensions and techniques. It has been shown that at 2.3 GHz, dimensions on the order of 600 to 1000 ft or more are probably realistic aperture sizes to consider for the high data rates and low error probabilities listed above. Using the plans of the communication link characteristics for the 1971 Voyager Mission at 1AU as a basis for comparison, the sum of the gains on future missions can be estimated to be about 100 dB to achieve a data rate of 10^6 bits/second or a 20 dB increase over the gains specified in the Voyager link for which a spacecraft transmitter of 50 watts has been postulated. If the spacecraft antenna is postulated to be capable of 30-40 dB of gain using a transmitter with 50-100 watts of power, then the ground based receiving system must be studied for the following range of parameters:

Antenna Gain -- 60 to 80 dB
Data Rate -- 10^4 to 10^7 bits/second
Error Probability -- 10^{-2} to 10^{-5}

Final results will be given for this entire range of parameters although nominal values will be used to illustrate and expedite the discussion of various techniques during the intermediate phase of this program.

Because of the significance of the noise level in determining the overall gain requirement, many studies have been directed to a consideration of the noise that competes with the signal and is collected and introduced at the ground end of the down link. The convention of treating the noise as resulting from an equivalent antenna temperature has followed in this program. Since the noise level is highest when the antenna beam is directed at or near a noise source, attention is being paid to techniques which can be used to mitigate these deleterious effects in certain special mission circumstances.

The characteristics of high gain techniques, either electrical or mechanical, form essential parts of tradeoffs in system accuracy, reliability, and cost. Of course practical compromises must be made for certain aspects of a particular mission. These compromises will depend on the techniques available for directing or steering the receiving beam on the ground as compared with those for controlling the vehicle attitude. Three types of steering mechanisms are possible for spacecraft antenna systems: mechanical (as for large appendage antennas); electromechanical; and electronic or inertialess. Electronic techniques offer the greatest versatility with regard to communications between a vehicle in space and earth. These are two generic types: those that require external controls to phase the elements properly and those that are self-steering. The externally controlled systems, such as the conventional phase array, need an external sensor (IR, RF, or ground station) to point the beam, and a computer, a phasing network, and an attitude sensing device to point the beam appropriately. In the self-steering system, however, attitude information is presented to the antenna system by a pilot beam from a ground station, and electronic circuitry senses the phase of incoming pilot signals to position a beam in the direction of these pilot signals. Multiple beam systems may be accommodated by the use of diplexers and multiple electronic channels. Each of these spacecraft systems is being worked on by various research and development groups throughout the country and abroad. Appropriate results of these efforts will be used to achieve stated objectives of this program.

II. PROGRAM DESCRIPTION

As has been discussed in earlier reports on this program, there are basically two fundamental kinds of antenna systems that can be used in applications requiring large apertures. The first is a large mechanically steerable paraboloidal reflector or a number of smaller reflectors of this type which are connected and fed as an array and mechanically steered as individual radiators. The second is a phased array with stationary or fixed apertures composed of subapertures whose relative phasing controls the direction of the antenna beam. Thus, this program considers the various aspects and organizations of the following generic types of large ground based antenna systems:

A. A SINGLE LARGE APERTURE -- mechanically steerable.

A system of this type will be discussed in this study only to provide a basis for the comparison of performance characteristics with the other systems listed below. Technical descriptions and data appropriate to this portion of the program have been obtained from several organizations not directly involved in this study.

B. AN ARRAY OF LARGE DISHES -- each of which is mechanically steerable.

The appropriate organization of a system of this type is considered herein with respect to the element spacing and their interaction.

C. A PHASED ARRAY OF SMALL CLOSELY SPACED ELEMENTS ORGANIZED INTO SUBAPERTURES -- electronically steerable.

Most of the effort in this program will be concerned with the various organizations, the feeding techniques, and the elements appropriate to this type of system.

D. A SELF-STEERING ARRAY -- rapidly switched multiple beams or adaptive systems.

Systems of this type can be used to mitigate the effects of high intensity noise sources and employed in conjunction with the system of type C to accomplish optimum mission performance. The feasibility of application of these techniques for a high data rate communication system is being investigated during the course of this program.

Consideration is being given to the capabilities and limitations of each of the above types during the course of this study and a report made in the above listed categories.

Although some of the results and information described herein were obtained in one research or industrial institution and some in another, this report, as have previous reports, will be written with the idea of integrating the results of various research efforts and techniques. Results of this investigation will be described in such a way as to implement the objectives of the program without regard to the actual source of the material. It will be the purpose of this report to glean as much pertinent material as possible and to organize it into a form which permits a quantitative comparison of the various high performance antenna systems. The outcome of this study will be a series of recommendations to NASA/ERC concerning the pacing technology which needs long term research and development. Appropriate design approaches and performance criteria will be suggested, primarily as they pertain to the ground based antenna subsystems and the subsystems on the space vehicle in an effort to optimize the overall performance characteristics of the down link (toward the earth) portion of the communication channel.

This program has been active for the past thirty months as a cooperative effort between the personnel of the Center for Research (CRES) at the University of Kansas, and the ElectroScience Laboratory (ESL) at The Ohio State University. It has uncovered a number of technical details that need further consideration and invention. More recent fundamental data now becoming available indicate that the performance characteristics and production costs of low loss transmission

lines, radiating elements, and other subsystem components are not yet to a level comparable with a reasonable system. This information has been assessed in terms of these relationships since they are the primary factors which govern the establishment of criteria for a large scale antenna design. Further studies of the kind described herein are needed to firmly establish a viable design approach which is both technically sound and economically feasible. Thus, this program has been extended as a NASA grant for the following work statement and personnel organization.

STATEMENT OF WORK (1969-1970)

The ElectroScience Laboratory (ESL) at The Ohio State University proposes to supply all the personnel and service necessary to continue the study program according to the following statement of work. This extension of an ongoing program includes several of the items previously listed and introduces several new or modified tasks. This extended program will include but not necessarily be limited to the following items as listed:

1. A continuing effort will be devoted to an intensive review and assessment of the research programs and techniques studies in progress or recently completed which may have influence on a high data rate communication system for space applications. This additional study is to assist ERC/NASA in assuring that no significant matters or techniques on electronic beam shaping and steering have been slighted or overlooked.

2. A continuing study will be made of the various types and sizes of radiating elements, their interaction, and their associated control circuitry in an effort to evaluate their potential in a large ground based array (or special purpose vehicle) antennas with a large number of elements. This investigation will be concerned primarily with low noise circuitry to provide the phase and amplitude control of the elements of the array. The circuits may include mechanical or ferrite phase shifters or the use of integrated semiconductor devices and heterodyning techniques. Consideration will be given to the state-of-the-art in techniques for controlling phase individual elements and groups in techniques for controlling phase individual elements and groups of elements. An assessment will be made of their adequacy in providing sufficient control to satisfy the requirements of the system.

3. A study will be made of methods for arranging, grouping, exciting and interconnecting the requisite number of elements to provide the appropriate radiation characteristics from array antennas. Particular consideration will be given to the investigation of novel feeding and phasing techniques which would either significantly reduce array costs or increase their flexibility.

4. A study will be made of methods of achieving a capability to handle several satellites at planetary distance as well as rapidly switched multiple beams for communication with near earth orbital satellites. For this purpose, an intensive study of adaptive antennas will be made to extend recent achievements, to establish the basic engineering tradeoffs involved in the design of this type of antenna, and to establish the fundamental limitations to its performance. This item will continue the present work on adaptive arrays with emphasis on the following tasks:

   a. Consolidate the results of previous experimental work on the two-element analog adaptive array, to present a unified picture of the capabilities and limitations of this scheme.

   b. Continue tests on the available digital adaptive array (4-element L-Band array) to obtain experimental data on the speed of response, convergence properties, errors due to amplitude and phase quantization, and other properties.

   c. Continue theoretical studies on extremum-seeking adaptive controls, with the goal of providing a broader conceptual framework for the experimental results and of integrating previous experimental work with previous studies in this area.

   d. Study the use of adaptive antennas with coded communication signals. Here the goal is to use coding on the signals as the basis for distinguishing between "desired" and "undesired" signals in the array.

5. A continuing study will be made of techniques for switching from a self steering or adaptive array where the pattern is determined by the size of the subaperture to one where the steering is accomplished by externally controlling the phase and amplitude between elements so that the pattern is determined by the entire radiating aperture. This switching is to be accomplished by an appropriate signal processing scheme which is actuated by the externally generated noise or interference level. Such a scheme will produce a system capable of more efficient performance in the presence of high external noise and interference levels.

6. The Electronics Research Center of NASA is currently developing the capability for computer simulation of communication systems. It is desired to expand this capability to include array antennas. The objectives of this study will be to provide the following:

a. To identify and to describe by analytical means the pertinent parameters which should be considered in the analysis of array antennas such as element type and configuration gain, beam-scan angles, noise temperatures, data rate and line loss. Also included should be the associated computer parameters.

b. The inputs to the analysis will be in the form of discrete point inputs. Data will be generated for array antennas relating weight and costs to the pertinent parameters which will have been established in a.

ORGANIZATIONAL DESCRIPTION

The proposed study program as extended will be conducted by the personnel of the ElectroScience Laboratory at The Ohio State University in cooperation with the personnel from the Optics and Microwave Research Laboratory of the Electronic Research Center/NASA. The ESL will coordinate the efforts of this team and will be responsible for reporting to the ERC/NASA the results of the studies outlined in the Statement of Work, as well as the overall recommendations for needed long term research and development along with their relative priorities. The proposed makeup of the study group is shown in the organizational chart in Fig. 1.

ElectroScience Laboratory
Ohio State University

L. L. Bailin
Laboratory Director

A. A. Ksienski
Program Manager

R. T. Compton
Principal Investigator

L. L. Bailin
R. T. Compton
C. Don
A. A. Ksienski
R.L. Riegler
N.A. Walker

LOUIS L. BAILIN

EDUCATION:	Ph.D., 1949, Physics, U.C.L.A. M.A., 1946, Physics, U.C.L.A. B.A., 1943, Physics, U.C.L.A.
PRESENT OCCUPATION: 1969-present	Director of the ElectroScience Laboratory and Professor of Electrical Engineering, at The Ohio State University.
PRESENT RESEARCH ACTIVITIES:	with S.D. Hamren of Hughes Aircraft Co., "Some Fundamental Limitations of Large Aperture Antennas," to be submitted for publication to the IEEE Transactions P.G.A.P.; with NASA/ERC, "A Study of High Performance Antenna Systems for Space Communication". Consultant, to Research and Development Laboratories Division Bendix Corporation, Southfield, Michigan; Radiation, Inc., Melbourne, Florida; and Aerospace Corp., El Segundo, California.
PREVIOUS EXPERIENCE: 1966-1969	Chairman of the Department and Professor of Electrical Engineering, University of Kansas, Lawrence, Kansas. Consultant, to the Research and Development Laboratories Division, Bendix Corporation, Southfield, Michigan; Radar Division of R.C.A., Moorestown, New Jersey; and Research and Development Laboratories, Hughes Aircraft Co., Culver City, California; Radiation, Inc., Melbourne, Florida.
1959-1966	Manager, Antenna Department, Research and Development Div., Hughes Aircraft Company. Responsible for basic research and advanced development of antenna systems and components for airborne and space vehicles.
1960-1966	Adjunct Professor of Electrical Engineering, University of Southern California, Los Angeles. Teaching undergraduate and graduate Electromagnetics.
1953-1960	Professor of Electrical Engineering and Chairman of Graduate Studies, University of Southern California, Los Angeles. Teaching of undergraduate Electromagnetics, Circuits, Applied Electromagnetic Theory, Antennas. Department of Electrical Engineering Administrative Committee.
1956-1959	Consultant to Hughes Aircraft Co., Culver City and Fullerton, Calif. In the research and development of radar systems and basic research in field of microwave antennas; Skiatron TV Corp., Los Angeles, Calif. In the research and development of closed circuit pay television.

1949-1956	Physicist, Microwave Laboratory, Hughes Aircraft Co., Culver City, Calif. Performed basic research in fields of microwave antennas, guided missiles, electromagnetic theory, and numerical analysis.
1948-1949	Mathematician, National Bureau of Standards, Los Angeles, Calif. Formulated problems for numerical analysis dealing with electromagnetic theory, microwave antennas, guided missiles, hydrodynamics, and bio-mechanics, etc.
1945-1948	Teaching Assistant, University of California at Los Angeles, undergraduate mathematics and physics.
1944-1945	Physicist. Naval Ordnance Laboratory, Washington, D.C., engaged in basic research in theoretical and experimental underwater acoustics.
1943-1944	Assistant in Physics, University of California at Los Angeles, Army Specialized Training Program and Navy V-12 Program.

PUBLICATIONS:

Papers

"A New Method of Near Field Analysis," IEEE Trans. on A. and P., December 1959, pp. S458-S467 (with R.C. Hansen).

"On Computing Radiation Integrals," Communications on Automatic Computing Machinery, February 1959 (with R.C. Hansen and R.W. Ruthinshauser).

"Convergent Representations for the Radiation Fields from Slots in Large Cylinders," IRE Trans. on A. and P., vol. AP-5, October, 1957 (with R.J. Spellmire).

"Exterior Electromagnetic Boundary Value Problems for Spheres and Cones," IRE Trans. on A. and P., vol. AP-4, January 1956 (with S. Silver).

"The Radiation Field Produced by a Slot in Large Circular Cylinders," IRE Trans. on A. and P., vol. AP-3, July 1955, pp. 128-137.

"Empirical Approximations to the Current Values for Large Dolph-Tschebyscheff Arrays," IRE National Convention Record: Part I, Antennas and Propagation, 1954 (with R.S. Wehner and I.P. Kaminow).

"Factors Affecting the Performance of Linear Arrays," Proceedings of the IRE, vol. 41, no. 2, February 1953, pp. 235-241 (with M.J. Ehrlich).

"Further Factors Affecting the Performance of Linear Arrays," IRE Transactions on Antennas and Propagation, vol. AP-4, December 1952, pp. 93-102 (with H.F. O'Neill)

"Radiation Characteristics of a Turnstile Antenna Shielded by a Section of a Metallic Tube Closed at One End," Journal of Applied Physics, vol. 23, no. 6, June 1952, pp. 688-696 (with A. Banos and D.S. Saxon).

"An Analysis of the Effect of the Discontinuity in a Bifurcated Circular Guide Upon Plane Longitudinal Waves," Jour. Res., National Bureau of Standards, vol. 47, no. 4, October, 1951, pp. 315-335.

Oral Presentations

National Radome Symposium, Presidio, San Francisco, California, August 1951.

International Scientific Radio Union, (U.R.S.I.), Montreal, Canada, June 1953.

International Scientific Radio Union, (U.R.S.I.), Washington, D.C., May 1954.

International Scientific Radio Union, (U.R.S.I), University of Michigan, June 1955.

Trident Professional Groups of Southeastern Michigan, October 1966.

National Convention of Sigma Tau, National Engineering Society, March 1967.

PROFESSIONAL ACHIEVEMENTS:

Grants, Honors, and Awards

Principal Investigator on NASA Grant NGL 36-008-138 to Ohio State University for $78,000 over a step-funded period of three years starting November 1969.

Principal Investigator on NASA Grant NGR-17-004-013 for $90,000 to University of Kansas. The technical effort on this grant started June, 1967 and continued to November 1969.

Research grant of $2,000 to the University of Kansas from the Research Laboratories Division, Southfield, Michigan, of the Bendix Corporation

Sigma Xi - Research Society of America (RESA).

Pi Mu Epsilon (Math Honorary)

Eta Kappa Nu. (Electrical Engineering Honorary).

PROFESSIONAL ORGANIZATIONS:

Senior Member of the Institute of Electrical and Electronics Engineers

Member of the Professional Technical Group on Antennas and Propagation.

AHARON A. KSIENSKI

Education: Ph.D. in Electrical Engineering, 1958; M.Sc.E.E., 1952, University of Southern California; B.E.M.E., 1947, Institute of Mechanical Engineering, London, England.

Professional Experience: Technical Director for Communication and Information Systems, 1967 to present, The Ohio State University ElectroScience Laboratory; Head of Research Staff, 1965-67, Senior Staff Engineer, 1958-65, Hughes Aircraft Company, Antenna Department; Associate Professor, 1964-66, California State College at Long Beach; Lecturer, 1965, University of California at Los Angeles; Research Engineer, 1953-58, Wiancko Engineering Company; Consulting Engineer, 1952-53, Walter Schott Company; Laboratory Instructor, 1951-53, 1955-58, University of Southern California; Commanding Officer (Captain) and Chief Instructor, 1948-51, Israeli Air Force Aircraft Electrical School.

Research Resume: Dr. Ksienski's military experience involved the organization and supervision, at the age of 24, of the Israeli Air Force Electrical School.

While employed by the Walter Schott Company during 1952 and 1953, he designed, built, and tested UHF and VHF antennas.

His duties at Wiancko Engineering Company encompassed the development of new techniques for measuring flight parameters of airplanes and missiles. He also assisted the Chief Engineer in the evaluation of proposed projects, analyzed difficulties of existing measuring systems, and recommended solutions.

From 1958 to 1967, Dr. Ksienski was a Senior Staff Member of the Antenna Department of the Hughes Aircraft Company. There he merged his interests in Electromagnetic Theory and in Information Science in a consideration of antennas as information-handling and decision-making systems.

During 1965, he taught at the University of California an Electrical Engineering course which was focused to antenna processing systems, particularly synthetic arrays, correlation arrays, self-phasing and adaptive arrays, and decision theoretical arrays.

Dr. Ksienski's responsibilities as Head of the Research Staff of the Antenna Department of Hughes Aircraft were to originate and supervise research projects in electromagnetic theory, pattern synthesis, signal-processing antennas, application of information theory and decision theory to antenna systems.

In his present capacity as technical director of communication and information systems, he is responsible for the origination and supervision of various projects involved with the optimum utilization of antenna arrays for communication and radar.

The projects include satellite communication, deep space communication and high resolution radar.

Publications: "Logical Pattern Synthesis," (co-authors, G.C. Comisar, O.R. Price), presented in the 1959 Western Convention of the IRE and published in the Convention Record, Part I: Antennas and Propagation.

"Derivative Control in Shaping Antenna Patterns," IRE National Convention Record, Part I: Antennas and Propagation, March 1960.

"Synthesis of Nonseparable Two Dimensional Patterns by Means of Planar Arrays," IRE Transactions on Antennas and Propagation, Vol. AP-8, No. 2, (Communications), March 1960.

"Maximally Flat and Quasi-Smooth Sector Beams," IRE Transactions on Antennas and Propagation, Vol. AP-8, No. 5, September 1960.

"Equivalence Between Continuous and Discrete Radiating Arrays," Canadian Journal of Physics, Vol. 39, February 1961.

"Signal Processing Antennas," The Microwave Journal, Vol. 4, No. 10, October 1961 (Part I) and Vol. 4, No. 11, November 1961 (Part II).

"Multiple Target Response of Data Processing Antennas," (co-author, M.E. Pedinoff), IRE Transactions on Antennas and Propagation, Vol. AP-10, No. 2, March 1962.

"Signal and Data Processing Antennas," (co-author, G.O. Young), IRE Transactions on Military Electronics, Vol. MIL-5, No. 2, April 1962.

"Spatial Frequency Characteristics of Finite Aperture Antennas," Electromagnetic Theory and Antennas, E.C. Jordan, ed., International Series of Monographs on Electromagnetic Waves (New York: Pergamon Press, 1963); presented at the Symposium on Electromagnetic Theory and Antennas, Copenhagen, Denmark, June 1962.

"Decorrelation of Signals from Double Correlation Arrays," IEEE Transactions on Antennas and Propagation, Vol. AP-11, No. 6, (Communications), November 1963.

"Optimum Multiple Correlation Arrays," IEEE Transactions on Antennas and Propagation, Vol. AP-11, No. 6, (Communications), November 1963.

"Data Processing and Synthetic Aperture Antennas," Progress in Antennas 1960-62, The U.S. National Committee Report for Commission 6 of URSI; published in Radio Science, Vol. 68D, No. 5, May 1964.

"Multiplicative Processing Antennas for Radar Appication," presented at the Symposium on Signal Processing in Radar and Sonar Directional System, University of Birmingham, England, July 1964; published in the Proceedings of the Symposium and in the Radio and Electronic Engineer, Vol. 29, No. 1. January 1965.

"Information Theoretic Optimization and Evaluation of Nonlinear Antenna Systems," (co-author, G.O. Young), Chapter in Recent Advances in Optimization Techniques, Lavi, A. (ed), John Wiley, 1966.

"A Survey of Signal Processing Arrays," presented at the 12th Symposium of the Advisory Group for Aerospace Research and Development, NATO, Dusseldorf, West Germany, July 7-13, 1966, published in the Symposium Proceedings.

"Space Time Correlation Theory for Information Carrying Signals," IEEE Transactions on Antennas and Propagation, Vol. AP-15, (co-author, G.O. Young), January 1967.

"Antenna Processing for High Resolution Mapping," presented at the IEEE International Convention in New York, March 1967, published in the Convention Record, Part 2.

"Radar Signal Processing for Angular Resolution Beyond the Rayleigh Limit," (co-author, R.B. McGhee), The Radio and Electronic Engineer, Vol. 34, No. 3, September 1967.

R.T. COMPTON, JR.

Education: Ph.D. in Electrical Engineering, 1964, M.Sc. in Electrical Engineering, 1961, The Ohio State University; S.B. in Electrical Engineering, M.I.T., 1958.

Professional Experience: Associate Supervisor, The Ohio State University ElectroScience Laboratory, 1968 to present; Associate Professor, The Ohio State University, 1968 to present; National Science Foundation Postdoctoral Fellow, Technische Hochschule, Munich, Germany, 1967-68; Assistant Professor of Engineering, Case Institute of Technology, Cleveland, Ohio, 1965-67; Assistant Professor, The Ohio State University, 1964-65; Assistant Supervisor, The Ohio State University Antenna Laboratory, 1962-65; Battelle Memorial Institute Fellow, 1961-62; Senior Engineer, Battelle Institute, 1959-62; Junior Engineer, DECO Electronics, 1958-59.

Research Resume: Dr. Compton's primary research area has been electromagnetic theory and related fields such as antennas and microwaves. His main research has been on the electrodynamics of moving media and the theory of relativity. He has worked on the properties of slot antennas in lossy media, array antennas, microwave components, radar absorbers, and antenna synthesis. He has also been involved in studies and design problems in communication theory, control systems, and radar.

Publications: "The Time-Dependent Green's Function for Electromagnetic Waves in Moving Conducting Media," J. Math. Phys., 8, 12 (1967), 2445. (Co-author with I.M. Besieris).

"The Time-Dependent Green's Function for Electromagnetic Waves in Moving Simple Media," J. Math. Phys., 7, 12, (1966), 2145.

"One and Two Dimensional Green's Functions for Electromagnetic Waves in Moving Simple Media," accepted for publication in J. Math. Phys.

"Slot Antennas," Chapter 14 of the Antenna Handbook, edited by R.E. Collin and F. Zucker, in press. (co-author with R.E. Collin).

"Open Waveguides and Small Horns," Chapter 15 of the Antenna Handbook, edited by R.E. Collin and F. Zucker, in press. (co-author with R.E. Collin).

"Radiation from Harmonic Sources in a Uniformly Moving Medium," IEEE Trans., AP-13, 4, (July, 1965), 574. (co-author with C.T. Tai).

"Cutoff Phenomena for Guided Waves in Moving Media," IEEE Trans., MTT-14, 8, (August 1966), 358. (co-author with L.J. Du).

"Poynting's Theorem for Radiating Systems in Moving Media," IEEE Trans., AP-12, 3 (March, 1964), 238. (co-author with C.T. Tai).

Reports: "The Dyadic Green's Function for an Infinite Moving Medium" OSU Antenna Laboratory Report 1691-3, January 15, 1965. (co-author with C.T. Tai).

"The Effect of a Pure Time Delay on the Stability of a Phase Lock Loop," OSU Antenna Laboratory Report 1963-6, December 15, 1965.

"A Table of the Integrals $\int_0^x J_0(\rho e^{i\phi})d\rho$, $\int_0^x N_0(\rho e^{i\phi})d\phi$, $\int_0^x H_0^{(1)}(\rho e^{i\phi})d\rho$, $\int_0^x H_0^{(2)}(\rho e^{i\phi})d\rho$, OSU Antenna Laboratory Report 1691-12, July 1, 1965.

"Array Synthesis - A Least Integral Square Error Method," OSU Antenna Laboratory Report 1691-14, August 20, 1965.

"The Admittance of an Infinite Slot Radiating into a Lossy Half-Space," OSU Antenna Laboratory Report 1691-2, October 15, 1963.

"The Aperture Admittance of a Rectangular Waveguide Radiating into a Lossy Half-Space," OSU Antenna Laboratory Report 1691-1, September 30, 1963.

"The Admittance of Aperture Antennas Radiating into Lossy Media," OSU Antenna Laboratory Report 1691-5, March 15, 1964.

"The Surface Roughness of Echo II - A Preliminary Study," OSU Antenna Laboratory Report 1878-7, December 31, 1964.

"The Solution of an Integral Equation for the Lunar Scattering Function," OSU Antenna Laboratory Report 1388-8, April 1, 1963.

"Radar Backscatter from Hollow Dielectric Cylinders," Battelle Memorial Institute, Project No. SD-80, Task 15, August 1962.

"Pulse-Actuated Reed-Switch Relays," Battelle Memorial Institute Report, September 28, 1962.

"The Effect on Radio Telescope Performance of Jack Failures in a Configuration Control System," Battelle Memorial Institute Report, January 18, 1962.

"UHF Mercury-Switch Coaxial Relays," Battelle Memorial Institute Report, July 31, 1961.

"Research on Radar Camouflage Materials and Thickness," Battelle Memorial Institute Report, SR No. 6, July 31, 1960.

"A Computational Procedure for Evaluating Materials as Single- and Double-Layer Absorbers," Battelle Memorial Institute Report, SR No. 5, June 15, 1960.

"The Development of Castable Ceramic Dummy Load Absorbing Materials," Battelle Memorial Institute Report, February, 1960.

"Fresnel Zone Antenna Synthesis," M.Sc. Thesis, The Ohio State University, June, 1961.

III. ACTIVITIES DURING THE PERIOD

During this report period, the research activities which were formerly the results of a cooperative effort between the personnel of the Center of Research (CRES) at the University of Kansas and the ElectroScience Laboratory (ESL) at The Ohio State University were fused together as a single program at the latter research organization. This transfer was made possible by the fact that the principal investigator, Dr. Louis L. Bailin and his graduate student, Mr. C. Don, moved to The Ohio State University in July of 1969. Dr. Bailin has recently been appointed Director of the ElectroScience Laboratory and consequently was able to bring together all the various people involved on this program. Mr. Don was able to pursue his studies for a Ph.D. degree at the University of Kansas by completing his dissertation research at Ohio State University. Thus, all the personnel presently engaged in working on the various portions of this grant were all put together under a single administrative and research activity.

In this period several aspects of the program description (Section II) were pursued. Primarily, these concerned efforts on the adaptive array techniques and to a lesser extent, studies involving aperture blockage among arrays of closely spaced large dish antennas which are to be mechanically scanned. These items are to be summarized briefly in a qualitative manner in this section and reported in detail in the appropriate section of the Technical Summary in Section IV.

1) During this semi-annual period the signal processing equipment for an adaptive array study was completed and tested. This equipment consisted of a two element S-band array to demonstrate the feasibility of automatically generating an antenna pattern null in the direction of an interfering signal. A considerable amount of experimental data including transient response, power density spectra, antenna patterns, etc., was obtained and analyzed.

The experimental work was terminated with the completion of a two element array (rather than with four elements as was the original intention) partly because of financial reasons and partly because the basic objectives could be demonstrated with two elements. Namely, it was experimentally demonstrated that: a) The array could lock-on to an incoming signal from an arbitrary angle and automatically track it thru a full 360^{o} in azimuth; b) The array could automatically produce an antenna pattern null in the direction of an interfering signal, provided the desired and interfering signals did not come from the same direction and were not at precisely the same frequency.

Upon completion of the experimental work, the primary effort was directed at theoretical studies of adaptive arrays. Because the mathematics of the problem is so difficult (systems of coupled differential equations with time varying coefficients), an analog computer was used to help with the analysis. In this program,

computer simulations have been used to study the effect of various feedback transfer functions, loop gain and bandwidth, mean square error, etc.

Currently a noise analysis is being carried out to describe the performance of adaptive arrays operating in the presence of uncorrelated noise. During the next semi-annual period, work will continue on the above fundamental study areas. It is hoped that the results of these studies will provide the information needed to be able to specify the optimum configuration for an adaptive array for use with coded communication systems.

2) A continuing effort is being made to determine quantitatively the performance characteristics of an array of independently steerable paraboloids by mechanical means. Consideration is being given to the proper size and separation of large disk antennas to achieve the requisite high performance characteristics over a $\pm 60^{0}$ angle of scan. A minimum separation distance must be determined in order to utilize a given aperture size most efficiently. However, as the separation is decreased, the interference between adjacent paraboloids becomes important, especially at large scan angles. This interference phenomenon is being investigated by several theoretical approaches in an effort to determine quantitatively the pattern degradation of closely spaced paraboloidal antennas which can be mechanically scanned. As the separation is increased, the formation of grating lobes in a large array of parabolic reflectors presents a problem which requires a detailed study and a quantitative assessment of the results of overall system performance.

A few results regarding the preliminary investigation of the performance of an array of closely spaced paraboloidal antennas have been obtained, such as the minimal element spacing required for no blockage vs. the angle of scan, the blocked aperture and the effective aperture sizes vs. element spacing, and the first grating sidelobe level vs. element spacing. This information is essential to the quantative assessment of the performance of this system. The details will be assessed at the proper sections.

The geometrical theory of diffraction has been very successful to predict radiation patterns of various antenna systems, especially antenna systems with reflector. The employment of the geometrical theory of diffraction to solve the blockage problem associated with an array of closely spaced paraboloidal antennas has been undertaken in complement with several other approaches.

3) During the period, a continuing effort has been made to uncover components and techniques that would provide low loss system for a phased array antenna as described in sub-section IV-C. In addition, an effort has been made to provide for alternative design techniques which permit the problem areas to be circumvented by appropriate new inventions whenever they become available. Thus, in sub-section

IV-C, 5, 6, 7 has been used to discuss various aspects of the need for a low loss system. This discussion considered the individual components, the feeding and distribution systems, as well as the possibilities for combining other scanning techniques with phase shifters or optical devices to achieve optimum system performance. Some of these problem areas and components will require further study and some quantitative improvement before a large phased array can be designed which will satisfy the basic objectives of this program. Certain of the techniques and components discussed are obviously incompatible with the requirements for the desired system. Consequently they are merely presented for completeness in each discussion and summarily rejected because of their inapplicability herein.

There were, in addition, several noteworthy activities somewhat peripheral to the main effort. These involve the Ph.D. candidacy and dissertation research activities of the personnel on this program. Mr. Cheng Don has been accepted as a candidate for the Ph.D. degree at the University of Kansas, and his thesis topic has been approved by his dissertation committee to study an array of large dish antennas with respect to their blocking effect when their spacing is very close. His research activity, of course, was started during the course of this program and has continued to where certain pertinent information are available in this present phase of the program. This work is to be completed during the next period and submitted as Mr. Don's doctoral dissertation. Mr. Robert L. Riegler has been accepted as a doctoral candidate at The Ohio State University with a dissertation topic that will be selected from some aspect of the adaptive array work which is described in subsection IV-D. This effort again was started on this grant and has proceeded through the various phases until it will now become available as a doctoral dissertation by Mr. Riegler.

Dr. R. T. Compton and Mr. R. L. Riegler have presented papers at the following meetings concerning their work on adaptive arrays which were started and continued throughout this grant program.

1) "Adaptive Arrays"
R.T. Compton and R.L. Riegler
USAECOM-AAAA-ION Tech. Symposium on Navigation and Positioning.
Sept. 23-25, 1969, Fort Monmouth, New Jersey.

2) "Adaptive Antennas for Automatic Interference Rejection"
R.T. Compton and R.L. Riegler
19th Annual Illinois Symposium, Oct. 14-16, 1969, University of Illinois, Monticello, Illinois.

3) "Adaptive Antennas for Automatic Interference Rejection"
R.T. Compton and R.L. Riegler
Fall 1969 URSI Meeting, Dec. 8-11, 1969, University of Texas, Austin, Texas

IV. TECHNICAL SUMMARY

The requirement of a constant information rate of the order of 10^6 bit per second with a given probability of error implies a specific system performance in terms of bandwidth and signal-to-noise ratio. In any communications link, the data rate system parameter, R_D, can be given as the product of the following three factors

$$R_D \propto \left[P_t G_t(f)\right] \left[\frac{\lambda^2}{(4\pi R)^2}\right]\left[\frac{G_r(f)}{T_r(f)}\right] \quad ,$$

where the constant of proportionality directly involves such factors as data quality which is determined by the information coding method employed, and inversely the various loss factors in the transmission link. The bracketed terms list the design system and mission parameters as follows: the first bracket contains the transmitter parameters; the second bracket contains the transmission media or free space loss characteristics; the third factor involves the receiver parameters which are the primary concern in this study. Based on Shannon's work, the limiting value of the data rate in terms of signal-to-noise ratio and bandwidth is given by the expression

$$R_D \leq B \log_2(1 + R_o/B)$$

where

$$R_o = \frac{S}{N} \cdot B = \text{information rate parameter}$$

The maximum data rate can be approached with negligible error by a proper choice of coding technique (Ref. IV-1,2,3,4). A simple and fairly efficient technique, for example, is coherent biphase coding. The characteristics of this code in terms of signal-to-noise and bandwidth-to-data-rate ratios, and its relation to the Shannon limit are shown in Figure IV-1. For small error probabilities, the figure indicated that the bandwidth required must be comparable with the data rate ($B/R_D = 1$). Thus an increase in SNR as measured by R_o/R_D is serving to reduce the error probability without appreciable effect on the bandwidth requirements. Tolerable error or probabilities range from 10^{-5} to 10^{-2} depending on the type of data (Ref. IV-5). Thus the practical limit for the product of signal-to-noise and bandwidth, even with a simple code, need not exceed the ideal limit by more than an order of magnitude to provide acceptable performance. The expression $R_o = (S/N)B = 10R_D$ will therefore be taken to represent a practical relationship between signal and bandwidth and the limiting noise level. (The actual relationship for a specific system design will depend on the particular coding scheme adopted as well as on error-rate requirements).

Thus,

$$\frac{S}{N} = 10 \quad \frac{R_D}{B} = 10 = 10 \text{ db}$$

correspond to the requisite error probabilities.

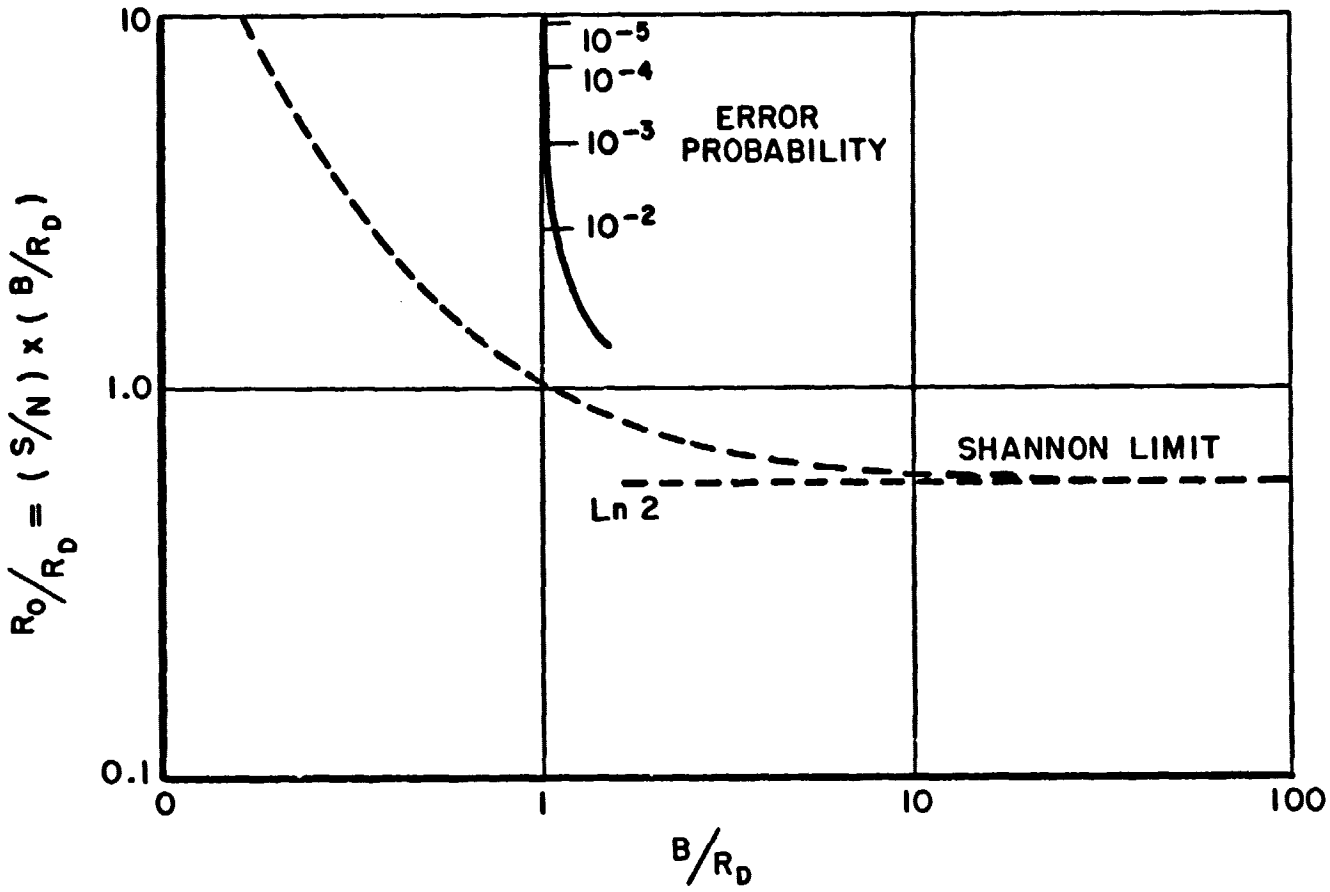

Fig. IV-1. Efficiency of biphase coding.

In view of the background material discussed above, it is possible to make some general assessments of the gain and associated aperture size required to provide nearly continuous communication between the ground and the spacecraft of future mission. It can be anticipated that a gain of 60 to 80 dB will be needed for the ground antenna. The diameters of circular apertures corresponding to these gain values at 2.3 GHz are 200 and 2,000 feet, respectively. This is based on the supposition that the beam formed is always perpendicular to the aperture during the steering processes and that an allowance is made for taper and other losses inherent to the antenna type. The 3-dB beamwidths are on the order of 2.2×10^{-3} and 2.2×10^{-4} radians, respectively. In this section consideration is given to problems associated with satisfying the aperture and gain requirements with various types of ground based antenna systems. Each of the candidate types is discussed on the basis of its suitability to long range communication receiving systems with a generic form as shown in Fig. IV-2. These antenna types are described whether or not their essential components have been developed, are in the experimental form, or are only in the conceptual

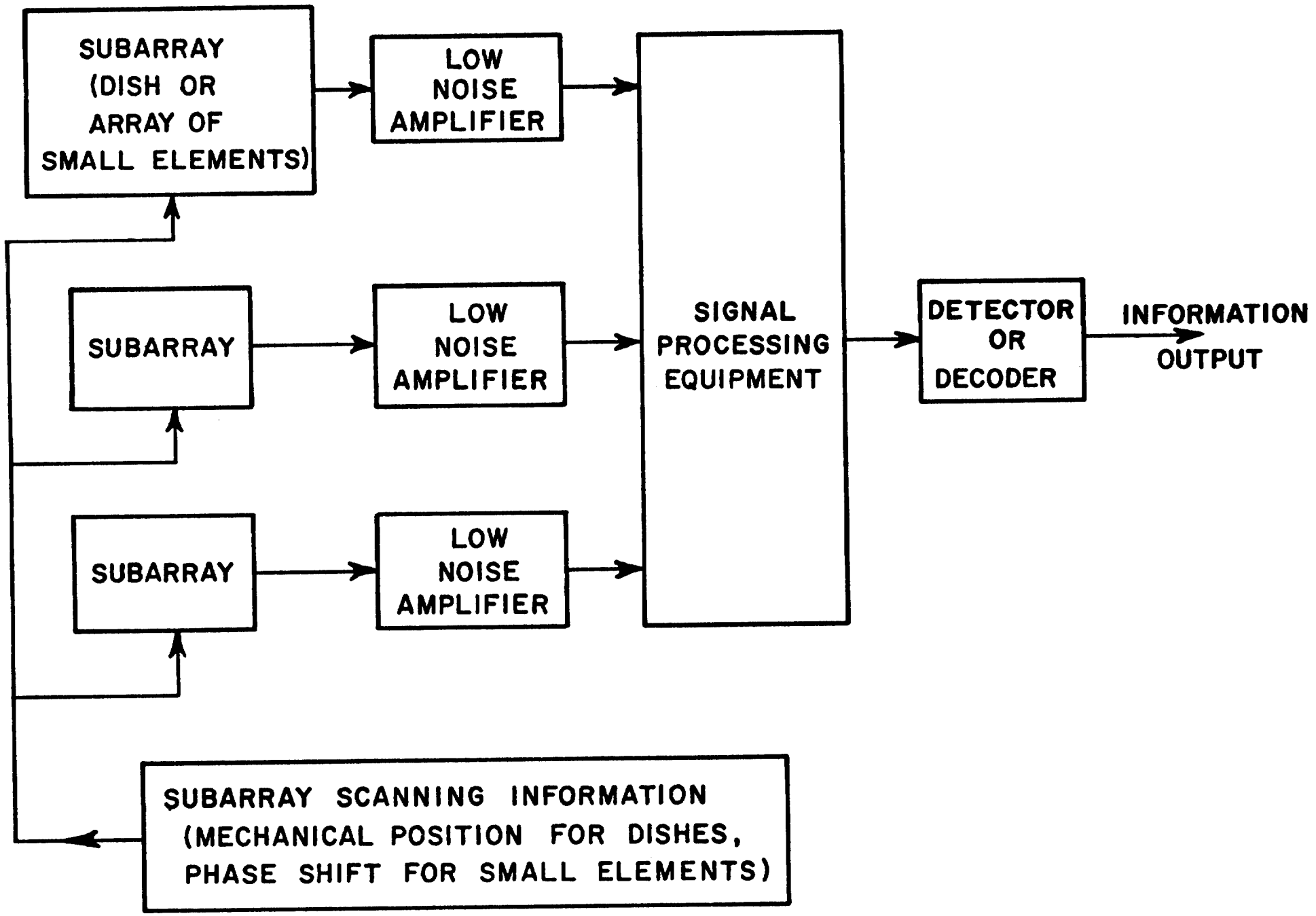

Fig. IV-2. Basic block diagram of receiving system.

or planning stages. Thus, each system is presented in terms of its capabilities and limitations even though some of the crucial component devices and techniques are still being developed. In some cases, the expected ultimate performance must be discussed in terms of a series of competing parameters whose final value is as yet unavailable.

In deep space communication systems requiring high data rates it is necessary to have a very large receiving antenna in order to achieve a SNR which will yield the error rates described above. Ultimately, as the distance or data rate increases, the required aperture may become too large to be constructed as a single antenna element as described in subsection A, and it is necessary to array several smaller apertures as described in subsection B and C. The upper limit on the subaperture size may be imposed by such factors as atmospherically induced wavefront distortion or unobtainable phase tolerances. An additional advantage of subdividing the large aperture into smaller subapertures is the possibility of arraying and processing them in a manner which will give improved performance over that of a single antenna. For example, the weighting factors on the subapertures as elements of the larger array might be adjusted to place a null or region of low sidelobes in the direction of an interfering source, thus reducing the effective array noise temperature. This process, however, requires sophisticated techniques and will be discussed in subsection D.

REFERENCES

IV-1. R.C. Hansen and R.G. Stephenson, "Communications at Megamile Ranges," Micro. Jour. 4, December 1961.

IV-2. R.W. Sanders, "Communication Efficiency Comparison of Several Communication Systems," Proc. IRE 48, April 1960.

IV-3. A.J. Viterbi, "On Coded Phase-Coherent Communications," IRE Trans. SET 7, March 1961.

IV-4. R.C. Hansen and R.G. Stephenson, "Communications at Megamile Ranges," Micro. Jour. 5, January 1962.

IV-5. L.S. Stokes and K.L. Brinkman, "Reference Data for Advanced Space Communication and Tracking Systems," Report P66-135, Contract No. NAS 5-9637, Hughes Aircraft Company ASG, Culver City, California, 1966.

A. A SINGLE LARGE APERTURE

The steerable paraboloidal reflector has been shown to be economically and technically practical for antenna aperture size on the order of a few hundred feet. Such a size will satisfy the lower limit of the above mentioned requirements and is exemplified by the characteristics of the JPL 210-foot paraboloid as given in Table A-1. These characteristics afford a convenient reference list for comparison, since they represent the state-of-the-art at 2.3 GHz. However, for aperture sizes on the order of thousand feet it does not require extensive analysis to show that a single steerable paraboloid is not feasible in the next ten or even twenty years. A parabolic dish of this size is relatively impractical, since it must be assumed to have the same surface tolerance and illumination efficiency as the 210 ft. JPL dish and to maintain the same noise temperature but greater pointing accuracy. For a large single reflector spillover, backscattering and aperture blocking contribute to the noise temperature of the antenna since the radiation from the warm earth couples to the back lobes of the antenna pattern. The effect, of course, varies as a function of scan angle which may be as much as $\pm 60^{o}$. The upper limit in aperture size for a large single steerable paraboloid has probably already been reached and the change of this limit would require the discovery of a new structural material that has a strength to weight ratio several times that of steel.

Paraboloidal antennas are being widely used for deep space communications. The Deep Space Instrumentation Facility is presently equipped at five stations with 85 feet paraboloids having gains of 53 dB at 2.3 GHz. A system noise temperature of $55^{o}K$ is provided at each station. A network of three 210 foot paraboloids is under construction around the world. The first of these antennas has been completed at Goldstone, California. The most recent performance expectations of the 210 ft paraboloid indicate that a noise temperature of $18^{o}K$ can be achieved with a maser front end and some improvements in the feed design. Since the costs of both the 85 ft. and the 210 ft. are now well established, they shall be used as the basic element in Section IV-B, where arrays of dishes are considered. In addition, as indicated by Figure A-1, these structures were designed for optimum performance in the S-band range of frequencies.

Azimuth coverage, deg.	±300 (from SE at Goldstone)
Elevation coverage, deg.	5 to 88 (tracking sidereal target) 4.5 to 90.5 (final limits)
Pointing accuracy, deg.	0.02 pointing 0.01 tracking
Maximum angular rate azimuth, deg/sec	0.5 (wind $\leq$ 30 mph)
Maximum angular elevation, deg/sec	0.5 (wind $\leq$ 30 mph)
Maximum acceleration azimuth, deg/sec	0.2 (wind $\leq$ 30 mph)
Maximum acceleration elevation, deg/sec	0.2 (wind $\leq$ 30 mph)
Servo bandwidth adjustment, hz.	0.01 to 0.2
Gain at 2300 MHz, dB	61
Beamwidth at 2300 MHz, deg.	$\approx$0.13 (2.2×10^{-3} radians)
System temperature, * ^{o}K	18
Antenna temperature, ^{o}K	$\approx$10
Reflector diameter, ft.	210
Reflector f/D ratio	0.4235

*Includes maser amplifier, receiver, transmission line, listening feed, and the antenna pointing at a quiet sky.

Table A-1
Expected performance of 210-foot DSIF
altazimuth antenna.

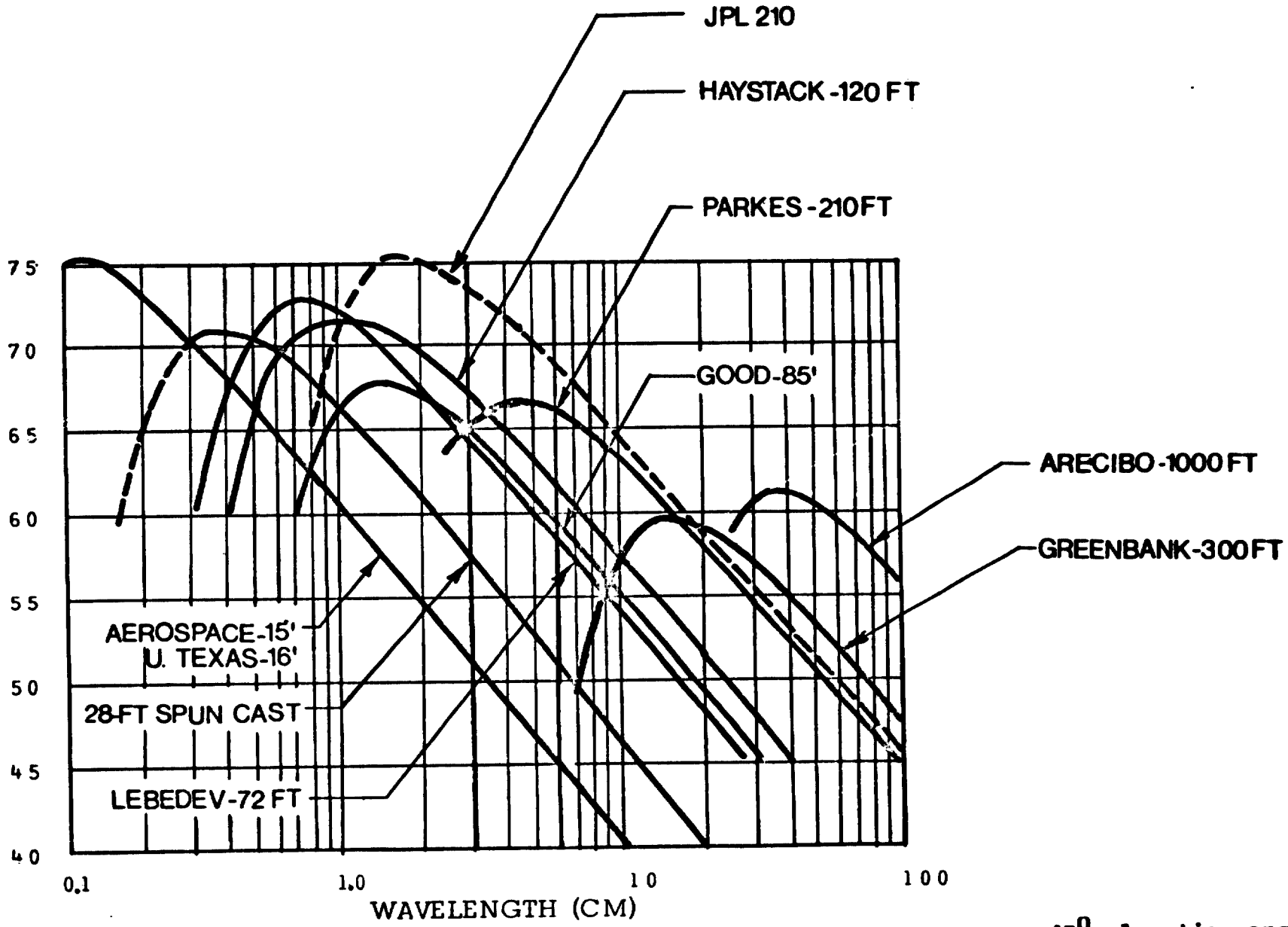

Note: The 210 foot AAS curve is based on uncorrected measurements made at a 45^{o} elevation angle at a wavelength of 3.55 cm with no winds in excess of 20 mph.

Ruze - Proc. of IEEE, 54-4

Fig. A-1. Gain of large parabolids (based on published estimate).

It has been indicated by JPL (Ref. A-1) that apertures which are electrically equivalent, but larger than the 200 ft. in diameter class of paraboloid, are very expensive and are probably not economically warranted for the next ten to fifteen years. Some consideration is being given to a 400 ft. dish for radio astronomy application by the CAMROC group. The CAMROC 400 ft. dish is protected from the environment by a radome which eliminates wind as a parameter in antenna design; therefore new design concepts are possible and they are different from the conventional design requirements (Ref. A-2). Thus, for total apertures less than the aperture of an antenna roughly 250 ft. in diameter, a single paraboloid should be used. For total apertures in excess of this size by an appreciable amount, it will be best realized by arrays paraboloids of optimum size. Several other approaches such as the fixed spherical-reflector approach and multiplate antenna appear to offer a large aperture at low cost. In spite of this apparently attractive feature, they have their respective shortcomings (Ref. A-3, 4 and 5, 6). When used in deep space communications applications, there appears to be little or no economic gain over steerable paraboloids. However, these special forms of optical antennas merit further study in this program.

The requirement of narrow beamwidths, low sidelobe levels and broadband operation for the generation of a pencil-shaped antenna beam has well been achieved by the system of a point source feed and paraboloidal reflector. However, the beam axis coincides with the geometric axis of the paraboloidal surface so that in order to scan the beam, it becomes necessary to move the whole reflector mechanically. A spherical reflector employed in a microwave antenna leads to a system whose beam can be steered without moving the reflector (Ref. A-7). The beam axis coincides with the radius of the sphere upon which the feed happens to lie. Scanning is achieved by a single rotation of the feed about the center of the sphere. Due to the spherical aberration, however, a point source feed cannot be used unless the primary illumination of the reflector is confined to a relatively small zone of the spherical surface (Ref. A-3). Aperture efficiency is then small and total reflector size becomes enormous relative to an equivalent paraboloid. Several proposals exist, however, for correcting the annoying phenomena of spherical aberration. One approach utilizes a secondary reflector to refocus the aberrant rays to a true point focus (Ref. A-8). Another method, analogous to those in present optical use, requires correcting lenses of the Mangan or Maksutov Type. The third approach makes use of the fact that a spherical mirror possesses a line focus. By using a line source, rather than a point source feed, spherical aberration can be eliminated and primary illumination need not be confined to the paraxial region of the sphere (Ref. A-9, 10). The gains of the 10-foot spherical reflectors illuminated either by the square-aperture horn at frequency of 11.2 GHz (Ref. A-3) or a combined line source (Ref. A-10) are in the magnitude of 39 dB. This is equivalent to the gain of a uniformly illuminated circular aperture of 31-inch diameter, or a typical paraboloid of 40-inch diameter. The total useful angle of scan of the former 10-foot spherical reflector antenna is about $\pm 70^{o}$ with approximately 1½ dB loss of gain at 70^{o} from the zenith. A

1000-foot spherical dish was completed in 1962 in Arecibo, Puerto Rico, for radio astronomy applications. The specific designed line source feed corrects for the optical aberrations of the sphere and permits off-axis scanning to 20° with less than 3 dB loss of gain (Ref. A-4). It seems that by use of a fixed spherical reflector to achieve narrow beam of large aperture antenna, high aperture efficiency and wide-angle scan designs are mutually exclusive.

A multiplate reflector system is another distinct approach to steer antenna beams without moving a huge reflector. A multiplate antenna consists of a large number of independently adjustable reflecting plates with optimum sizes, which could be used with a fixed feed to form a steerable beam. For a feed located above the plates which are distributed over an area, energy radiated from the feed impinges upon the identical plates which are individually tilted and tipped to redirect the energy in the desired direction. However, the gaps between plates, the diffraction around plate edges and the double reflection due to the openings of the gaps are the kind of problems which the antenna system with a continuous reflector surface does not encounter. The multiplate antenna tested by Air Force Cambridge Research Lab. suffers from low efficiency and coverage problems, compounded by high antenna noise temperature (Ref. A-5, 6).

REFERENCES

A-1. Potter, Merrick, Ludwing, "Large Antenna Apertures and Arrays for Deep Space Communications," JPL Technical Report No. 32-848, Jet Propulsion Laboratory, California Institute of Technology, Pasadena, California, November 1965.

A-2. "A Large Radio-Radar Telescope: CAMROC Design Concepts," Vol. 1, Sec. 3, January 15, 1967, CAMROC Report 1967-1, The Cambridge Radio Observatory Committee, Lincoln Laboratory, Massachusetts Institute of Technology.

A-3. Li, Tingye, "A Study of Spherical Reflectors as Wide Angle Scanning Antennas," IRE Transactions on Antennas and Propagation, vol. AP-7, No. 3, pp. 223-226, July 1959.

A-4. Kay, A.F., "Design of Line Feed for World's Largest Aperture Antenna," Electronics vol. 34, pp. 46-47, July, 1961.

A-5. Schell, A.C., "An Analysis of the Effects Caused by Interstices on a Multiplate Plate Antenna; AFCRL Technical Memo CRRD-81, February, 1963.

A-6. Schell, A.C., "A Multiplate Radio Astronomy Antenna," Nerem Record, pp. 196-197, 1963.

A-7. Ashmead, J. and Pipard, A.B., "The Use of Spherical Reflectors as Microwave Scanning Aerials," J. IEE, vol. 93, pt. IIIA, p. 627, July, 1946.

A-8. Head, A.K., "A New Form for a Giant Radio Telescope," Nature, vol. 170, pp. 692-693, April, 1957.

A-9. Spencer, R.C., Sleten, C.J., and Walsh, J.E., "Correction of Spherical Aberration by a Phase Line Source," Proc. N.E.C., vol. 5, pp. 320-333, 1959.

A-10. Shell, A.C., "The Diffraction Theory of Large-Aperture Spherical Reflector Antenna," IEEE Trans. on Antennas and Propagation, vol. AP-11, pp. 428-432, July 1963.

B. AN ARRAY OF LARGE DISH ANTENNAS

1) Introduction

As it has been mentioned before, an array of independently mechanically steerable paraboloids with proper size and separation may be one of several workable approaches capable of achieving the high gain requirement for the DSCS. To provide the requisite scanning angle of $\pm 60^{o}$ without interference between adjacent paraboloids, the spacing between reflectors must be kept at a reasonable distance which is larger than the diameter of the paraboloids. Thus, a minimum separation distance must be determined which utilizes a given aperture size most efficiently. As the separation is increased, the formation of grating lobes in a large array of parabolic reflectors constitutes a serious difficulty for which no generally satisfactory solution has yet been developed. The problem can be visualized if the array pattern is considered as the product of an element pattern and an array factor. The element pattern consists of the radiation pattern produced by a parabolic reflector, while the array factor is the pattern of an array of isotropic radiators which is a two-dimensional grating lobe pattern. The array factor can be steered electronically by shifting the phase between elements while the element pattern is directed by the mechanical movement of the individual dishes. In the ideal case, the element pattern and a single lobe of the array factor will both point in the desired direction. Multiple beams appear, however, when more than one grating lobe falls within the main beam of the element factor; this condition occurs when the array spacing is substantially greater than the diameter of the subapertures.

It can be easily shown that the spacing of the grating lobes from the main beam can be increased by a decrease in the separation of the parabolic reflector antenna elements. However, if this spacing is decreased, the diameter of the reflectors must also be decreased so that the effective scan range can be maintained, while at the same time more array elements must be added to meet the gain requirement. The end result will be a broader element pattern which in turn will ensure that the grating lobes will have essentially the same amplitude relative to the main beam. The beamwidth of both the main beam and the grating lobes will, for all practical purposes, remain the same as long as the overall array dimensions remain unaltered. The fine grain structure around the various lobes will change, however, as more elements are added. Similarly, if the spacing between the elements is increased, and the diameter of the reflectors is increased correspondingly, the grating lobes will be moved in closer to the principal beam. Once again the relative amplitude and beamwidth of all the grating lobes should remain essentially constant.

There are some esoteric techniques available to suppress the size of the grating lobes. A possibility exists that the grating lobes adjacent to the principal beam may be reduced in amplitude by the use of random spacing among the array elements. However, it is anticipated that the selection of such a design will prove to be an extremely difficult

problem. Another means of suppressing the grating lobes might involve the use of an auxiliary array that could be steered and phased to cancel out any given lobe. A major difficulty that might be anticipated from such a scheme would be the obtaining of sufficient gain from the auxiliary array.

The juxtaposition of spacing and reflector size discussed above is predicted on little or no interaction between the elements as a function of scan angle. When this interaction effect is taken into account an entirely different solution may be obtained for the competing parameters. Thus, it shall be the purpose of this section to study the problems associated with being able to analytically determine a spacing and antenna size which is optimum between the interference effects at minimum separation, and the grating lobe effects at a maximum distance commensurate with high aperture efficiency. Since the theory and manipulation of the array factor and element pattern is available elsewhere, the effort herein shall be concerned with methods and techniques for analyzing the interaction effects between large parabolic reflectors in a relatively closely spaced array.

An analysis of the blocking effect of a closely spaced array obtained by the consideration of the geometric optics only has been done in paragraph (3). First, the field in Franhofer region for an antenna system of two closely neighboring paraboloids has been formulated; then the field for a linear array of N-paraboloid is obtained. In these expressions, they show clear evidence of the interaction between neighboring paraboloids due to the close separation between them.

2) Theoretical consideration of the interaction between neighboring paraboloid antennas

a) Introduction - It has been learned that some mutual coupling measurements on neighboring paraboloid antennas has been done by Andrews (Ref. B-1) for Collins Radio Co. and a similar measurement also has been done recently by Reiche (Ref. B-2) at the Hughes Aircraft Co. It seems, however, that there is no literature concerning theoretical analysis available. Therefore, it is desirable to develop the analytical form which governs the fields of a paraboloid antenna as a function of scan angle in the presence of neighboring array elements of an identical kind.

The far field transmitting and receiving patterns of the neighboring paraboloidal antennas with their vertices far apart will be the vector sum of individual contributions at the field point and the vector sum of the receiving fields at individual feeds respectively. In fact, the transmitting and receiving patterns of the paraboloidal antennas system in Fraunhofer region are the same in this case. As the positions of the vertices of the paraboloidal antennas get near enough, the interaction between them can no longer be negligible. The interaction between the paraboloidal antennas for which the system being used for transmitting function and that for which the system being used for receiving function

will constitute different problems which merit separate investigations. In this report, however, the following paragraphs are devoted to the interaction between the paraboloidal antennas for transmitting function. The case for receiving function will be included in a future report.

For transmitting function, the interaction may be approximately solved by considering the second paraboloid as a disklike obstacle in the near field of the first paraboloid. The surface current distribution on the disk due to the first paraboloid can be calculated; this current distribution on the disk then sets up a secondary surface current distribution on the surface of the first paraboloid. This secondary current distribution then becomes a modification factor on the primary current distribution due to the feed of the first paraboloid and thus modifies its far-field pattern.

The surface current density $\bar{K}$ on the disk due to the primary current distribution of the first paraboloid and the secondary current density $\bar{K}'$ on the first paraboloid due to the current density $\bar{K}$ on the disk have been formulated in paragraph (b) and paragraph (c) respectively. In paragraph (d), the electric field $\bar{E}'_{p_1}$ due to the secondary current density $\bar{K}'$ on the first paraboloid has been found. Also, the electric field $\bar{E}_{p_1}$ due to the primary current distribution of the first paraboloid and the electric field $\bar{E}_{p_2}$ due to the primary current distribution of the second paraboloid have been found in paragraph (e). The total electric field $\bar{E}_p$ in the far-zone region of these neighboring paraboloidal antennas is the vector sum of $\bar{E}_{p_1}$, $\bar{E}'_{p_1}$, and $\bar{E}_{p_2}$.

b) The surface current distribution on the disk The coordinate of the current distribution on the disk is $P'(u,\alpha,\theta)$ in the spherical coordinate with the origin at the focus, F_1, of the first paraboloid and also is $P'(R',\theta',\phi')$ in the fixed spherical coordinate with the origin at point O. The source point Q on the surface of the first paraboloid is $Q(\rho,\xi,\psi)$ with the origin at the focus F_1; the axes of the paraboloids are in $(\theta_1;\phi_1)$ direction as shown in Fig. 1 and Fig. 2.

Considering the case where the disk being in the far-zone region of the first paraboloid, the electric field at point P' on the disk is

$$\text{(B-1)} \qquad \bar{E}_{p'} = -\frac{j\omega\mu}{4\pi}\,\frac{e^{-jku}}{u}\left[8\left(\frac{\varepsilon}{\mu}\right)^{\frac{1}{2}}\,\frac{P_T}{4\pi}\right]^{\frac{1}{2}} \cdot \int_{S_1}[G_f(\xi,\psi)]^{\frac{1}{2}}\,\frac{e^{-jk\rho[1-\bar{a}_u\cdot\bar{a}_\rho]}}{\rho} \cdot \left[-\cos\frac{\psi}{2}\,\bar{e}_1 + (\bar{n}\cdot\bar{e}_1)\bar{S}_1\right]dS'$$

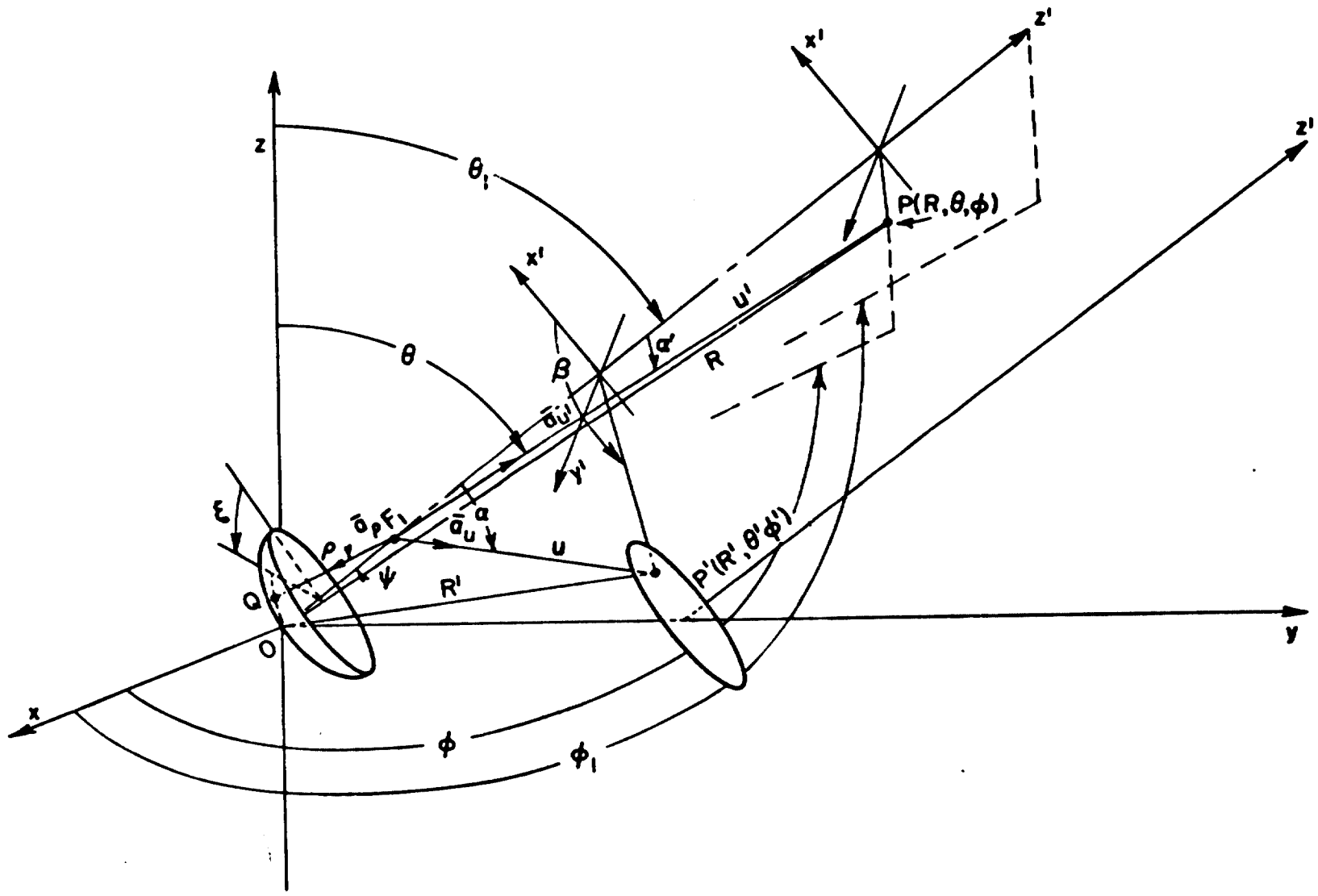

Fig. B-1. The parameters for calculating the current density at $P(R',\theta',\phi')$ on the conducting disk.

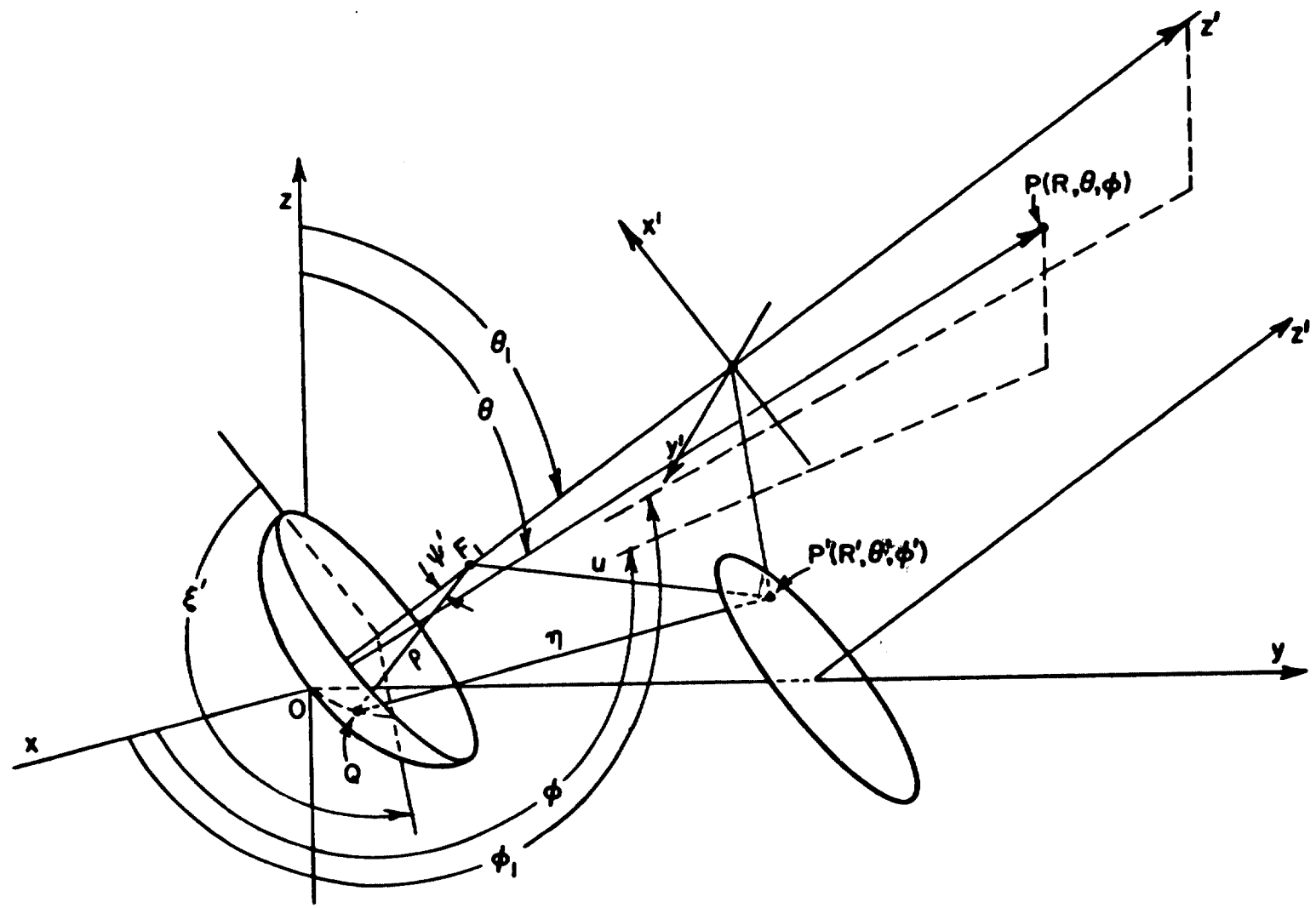

Fig. B-2. The parameters for calculating the secondary current density at $Q'(P',\psi',\xi')$ on the first paraboloid.

where

(B-2)

$$\bar{a}_u = \sin\alpha\cos\beta\,\bar{a}_{x'} + \sin\alpha\sin\beta\,\bar{a}_{y'} + \cos\alpha\,\bar{a}_{z'}$$

$$\bar{a}_\rho = \sin\psi\cos\xi\,\bar{a}_{x'} + \sin\psi\sin\beta\,\bar{a}_{y'} - \cos\psi\,\bar{a}_{z'}$$

$$\bar{a}_u,\bar{a}_\rho = -\cos\alpha\cos\psi + \sin\alpha\sin\psi\cos(\beta-\xi)$$

and

ϵ permittivity of the medium

μ permeability of the medium

P_T the total power transmitted by the feeds of the paraboloids

$G_f(\xi,\psi)$ the directivity of the feeds of the paraboloids

$\bar{n}$ the unit normal vector to the surface of the paraboloids, which is $n_x\bar{a}_x + n_y\bar{a}_y + n_z\bar{a}_z$

$\bar{e}_1$ the polarization of the reflected wave from the paraboloids, which is $e_{1x}\bar{a}_x + e_{1y}\bar{a}_y + e_{1z}\bar{a}_z$

$\bar{S}_1$ the propagation direction of the reflected wave for the present case,
$\bar{S}_1 = \bar{a}_{z'} = \sin\theta_1\cos\phi_1\,\bar{a}_x + \sin\theta_1\sin\phi_1\,\bar{a}_y + \cos\theta_1\,\bar{a}_z$

dS' the element of the surface of the paraboloids, which is $\rho^2\sin\psi\sec\psi/2\,d\psi\,d\xi$

F the focal length of the paraboloids

To the first approximation, the electric field at P' on the disk becomes

(B-3)
$$\bar{E}_{p'} = -\frac{j\omega\mu}{4\pi}\left[8\left(\frac{\epsilon}{\mu}\right)^{\frac{1}{2}}\frac{P_T}{4\pi}\right]^{\frac{1}{2}}\frac{e^{-jkR'}}{R'}\,e^{jkF\cos(\phi_1-\phi')}$$

$$\cdot\{\bar{I}_1 + \bar{I}_2\}$$

where

(B-3a)
$$\bar{I}_1 = \int_{\xi=0}^{2\pi}\int_{\psi=0}^{\Psi}[G_f(\xi,\psi)]^{\frac{1}{2}}\frac{e^{-jk\rho[1-\bar{a}_u\cdot\bar{a}_\rho]}}{\rho}\,[-\cos\tfrac{\psi}{2}\,\bar{e}_1]$$

$$\cdot\,\rho^2\sin\psi\sec\tfrac{\psi}{2}\,d\psi\,d\xi$$

(B-3b)

$$\bar{I}_2 = \int_{\xi=0}^{2\pi} \int_{\psi=0}^{\Psi} [G_f(\xi,\psi)]^{\frac{1}{2}} \frac{e^{-jk\rho\,[1-\bar{a}_u\cdot\bar{a}_\rho]}}{\rho} [(\bar{n}\cdot\bar{e}_1)\bar{a}_{z'}] \cdot \rho^2 \sin\psi \sec\tfrac{\psi}{2}\, d\psi\, d\xi$$

Thus, the magnetic field at point p' on the disk becomes

(B-4)

$$\bar{H}_{p'} = -\frac{j\omega\mu}{4\pi}\left(\frac{\varepsilon}{\mu}\right)^{\frac{1}{2}}\left[8\left(\frac{\varepsilon}{\mu}\right)^{\frac{1}{2}}\frac{P_T}{4\pi}\right]^{\frac{1}{2}} \frac{e^{-jkR'}}{R'} e^{jkF\cos(\phi_1-\phi')}$$

$$\cdot \int_{\xi=0}^{2\pi}\int_{\psi=0}^{\Psi} [G_f(\xi,\psi)]^{\frac{1}{2}} \frac{e^{-jk\rho\,[1-\bar{a}_u\cdot\bar{a}_\rho]}}{\rho} \cos\tfrac{\psi}{2}$$

$$\cdot [\bar{e}_1 x \bar{a}_{z'}] \cdot \rho^2 \sin\psi \sec\tfrac{\psi}{2}\, d\psi\, d\xi$$

Then, the surface distributed current density $\bar{K}$ on the conducting disk is

(B-5)

$$\bar{K} = (-2)\left\{-\frac{j\omega\mu}{4}\left(\frac{\varepsilon}{\mu}\right)^{\frac{1}{2}}\left[8\left(\frac{\varepsilon}{\mu}\right)^{\frac{1}{2}}\frac{P_T}{4\pi}\right]^{\frac{1}{2}}\right\} \frac{e^{-jkR'}}{R'} e^{jkF\cos(\phi_1-\phi')}$$

$$\cdot \int_{\xi=0}^{2\pi}\int_{\psi=0}^{\Psi} [G_f(\xi,\psi)]^{\frac{1}{2}} \frac{e^{-jk\rho\,[1-\bar{a}_u\cdot\bar{a}_\rho]}}{\rho} \cos\tfrac{\psi}{2}\, [\bar{a}_{z'} x (\bar{e}_1 x \bar{a}_{z'})]$$

$$\cdot \rho^2 \sin\psi \sec\tfrac{\psi}{2}\, d\psi\, d\xi$$

Let

(B-6) $$[\bar{a}_{z'} x (\bar{e}_1 x \bar{a}_{z'})] = A_x\bar{a}_x + A_y\bar{a}_y + A_z\bar{a}_z$$

where

(B-6a) $$A_x = \sin\theta_1 \sin\phi_1 (e_{1x}\sin\theta_1\sin\phi_1 - e_{1y}\sin\theta_1\cos\phi_1) - \cos\theta_1(e_{1z}\sin\theta_1\cos\phi_1 - e_{1x}\cos\phi_1)$$

(B-6b) $$A_y = \cos\theta_1 (e_{1y}\cos\theta_1 - e_{1z}\sin\theta_1\sin\phi_1) - \sin\theta_1\sin\phi_1 (e_{1x}\sin\theta_1\sin\phi_1 - e_{1y}\sin\theta_1\cos\phi_1)$$

(B-6c) $$A_z = \sin\theta_1\cos\phi_1 (e_{1z}\sin\theta_1\cos\phi_1 - e_{1x}\cos\theta_1) - \sin\theta_1\sin\phi_1 (e_{1y}\cos\theta_1 - e_{1z}\sin\theta_1\sin\phi_1)$$

Finally, the surface current density $\bar{K}$ on the conducting disk becomes

(B-7) $$\bar{K} = \frac{Ae^{-jkR'}}{R'} e^{jkF\cos(\phi_1-\phi')} [I_x\bar{a}_x + I_y\bar{a}_y + I_z\bar{a}_z]$$

where

(B-7a) $$A = (-2)\left\{ -\frac{j\omega\mu}{4\pi}\left(\frac{\varepsilon}{\mu}\right)^{\frac{1}{2}}\left[8\left(\frac{\varepsilon}{\mu}\right)^{\frac{1}{2}}\frac{P_T}{4\pi}\right]^{\frac{1}{2}}\right\}$$

(B-7b) $$I_x = \int_{\xi=0}^{2\pi}\int_{\psi=0}^{\Psi} [G_f(\xi,\psi)]^{\frac{1}{2}} \frac{e^{-jk\rho[1-\bar{a}_u\cdot\bar{a}_\rho]}}{\rho} A_x\cos\frac{\psi}{2} \cdot \rho^2\sin\psi\sec\frac{\psi}{2}\, d\psi\, d\xi$$

(B-7c) $$I_y = \int_{\xi=0}^{2\pi}\int_{\psi=0}^{\Psi} [G_f(\xi,\psi)]^{\frac{1}{2}} \frac{e^{-jk\rho[1-\bar{a}_u\cdot\bar{a}_\rho]}}{\rho} A_y\cos\frac{\psi}{2} \cdot \rho^2\sin\psi\sec\frac{\psi}{2}\, d\psi\, d\xi$$

(B-7d) $$I_z = \int_{\xi=0}^{2\pi}\int_{\psi=0}^{\Psi} [G_f(\xi,\psi)]^{\frac{1}{2}} \frac{e^{-jk\rho[1-\bar{a}_u\cdot\bar{a}_\rho]}}{\rho} A_z\cos\frac{\psi}{2} \cdot \rho^2\sin\psi\sec\frac{\psi}{2}\, d\psi\, d\xi$$

c) The Secondary Surface Current Distribution on the First Paraboloid The surface distributed current density K at point P' on the conducting disk will again set up a secondary current density $\bar{K}'$ on the surface of the first paraboloid. This secondary surface current density will become a modification factor to the far-field pattern of these neighboring paraboloid antennas system.

The magnetic field at Q' on the first paraboloid due to the current density $\bar{K}$ at P' on the disk is

$$(B\text{-}8) \qquad \bar{H}_{Q'} = \frac{jkA}{4\pi} \left[L_x \bar{a}_x + L_y \bar{a}_y + L_z \bar{a}_z\right]$$

where

$$(B\text{-}8a) \qquad L_x = \int_{\xi'=0}^{2\pi} \int_{\psi'=0}^{\Psi} \frac{e^{-j2kR'}}{(R')^2} e^{jkF\cos(\phi_1-\phi')}$$

$$\cdot \left[\sin\theta' \sin\phi' I_z - \cos\theta' I_y\right]$$

$$\cdot e^{jkB_1}$$

$$\cdot e^{jkB_2}$$

$$\cdot e^{jkB_3}$$

$$\cdot (\rho')^2 \sin\psi' \sec\frac{\psi'}{2}\, d\psi'\, d\xi'$$

$$(B\text{-}8b) \qquad L_y = \int_{\xi'=0}^{2\pi} \int_{\psi'=0}^{\psi} \frac{e^{-j2kR'}}{(R')^2} e^{jkF\cos(\phi_1-\phi')} \left[\cos\theta' I_x - \sin\theta' \cos\phi' I_z\right]$$

$$\cdot e^{jkB_1}$$

$$\cdot e^{jkB_2}$$

$$\cdot e^{jkB_3}$$

$$\cdot (\rho')^2 \sin\psi' \sec\frac{\psi'}{2}\, d\psi'\, d\xi'$$

$$(B\text{-}8c)\qquad L_z = \int_{\xi'=0}^{2\pi}\int_{\psi'=0}^{\Psi} \frac{e^{-j2kR'}}{(R')^2}\, e^{jkF\cos(\phi_1-\phi')}\,[\cos\theta' I_x - \sin\theta'\cos\theta' I_z]$$
$$\cdot e^{jkB_1}$$
$$\cdot e^{jkB_2}$$
$$\cdot e^{jkB_3}$$
$$\cdot (\rho')^2 \sin\psi' \sec\frac{\psi'}{2}\, d\psi'\, d\xi'$$

with

(B-8d)

$$B_1 = \sin\theta'\cos\phi'[F\sin\theta_1\cos\phi_1 + \rho'(A_1\sin\psi'\cos\xi' + A_2\sin\psi'\sin\xi' - A_z\cos\psi')]$$

$$B_2 = \sin\theta'\sin\phi'[F\sin\theta_1\sin\phi_1 + \rho'(A_4\sin\psi'\cos\xi' + A_5\sin\psi'\sin\xi' - A_6\cos\psi')]$$

$$B_3 = \cos\theta'[F\cos\theta_1 + \rho'(A_7\sin\psi'\cos\xi' + A_8\sin\psi'\sin\xi' - A_9\cos\psi')]$$

(B-8e)

$$A_1 = \sin\theta_2\cos\phi_2$$

$$A_2 = \sin\theta_1\sin\phi_1\cos\theta_2 - \sin\theta_2\sin\phi_2\cos\theta_1$$

$$A_3 = \sin\theta_1\sin\phi_1$$

$$A_4 = \sin\theta_2\sin\phi_2$$

$$A_5 = \sin\theta_2\cos\phi_2\cos\theta_1 - \sin\theta_1\cos\phi_1\cos\theta_2$$

$$A_6 = \sin\theta_1\sin\phi_1$$

$$A_7 = \cos\theta_2$$

$$A_8 = \sin\theta_1\sin\theta_2$$

$$A_9 = \cos\theta_1$$

The angles θ_1, ϕ_1; θ_2, ϕ_2 are defined as follows:

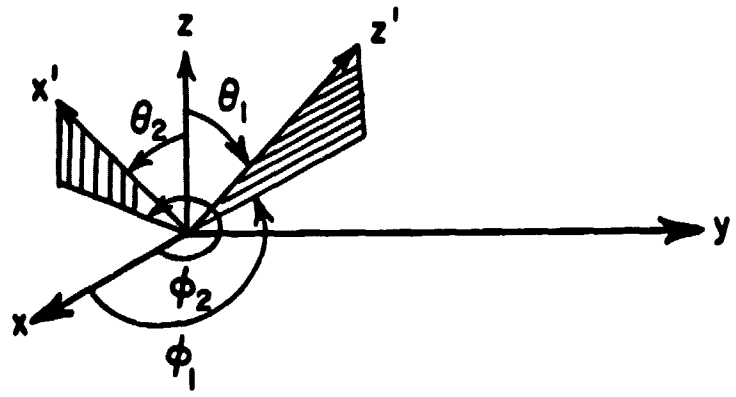

$$\bar{a}_{x'} = \sin\theta_2 \cos\phi_2\, \bar{a}_x + \sin\theta_2 \sin\phi_2\, \bar{a}_y + \cos\theta_2\, \bar{a}_z$$

$$\bar{a}_{z'} = \sin\theta_1 \cos\phi_1\, \bar{a}_x + \sin\theta_1 \sin\phi_1\, \bar{a}_y + \cos\theta_1\, \bar{a}_z$$

$$\bar{a}_{y'} = \bar{a}_{z'} \times \bar{a}_{x'}$$

Thus, the secondary current density $\bar{K}'$ on the first paraboloid due to the current density $\bar{K}$ on the conducting disk becomes

$$\text{(B-9)} \qquad \bar{K}' = 2\,\frac{jkA}{4\pi}\,[\,\bar{a}_x(n_yL_z - n_zL_y) + \bar{a}_y(n_zL_x - n_xL_z) + \bar{a}_z(n_xL_y - n_yL_x)]$$

d) The Electric Field in Fraunhofer Region due to the Secondary Surface Current Distribution The electric field at observation point $P(R,\theta,\phi)$ in the far-field zone due to the secondary current density $\bar{K}'$ on the surface of the first paraboloid is

(B-10)

$$\bar{E}'_{p_1} = -\frac{jk^2}{4\pi\omega\varepsilon}\,\frac{j2kA}{4\pi}\,\frac{e^{-jkR}}{R} \cdot \left[\bar{a}_x \int_{\xi'=0}^{2\pi}\int_{\psi'=0}^{\Psi} [(n_yL_z - n_zL_y) - C\sin\theta\cos\phi]\, e^{jk\,\overline{OQ'}\cdot\bar{a}_R} \cdot (\rho')^2 \sin\psi' \sec\frac{\psi'}{2}\, d\psi'\, d\xi'\right.$$

$$+ \bar{a}_y \int_{\xi'=0}^{2\pi} \int_{\psi'=0}^{\Psi} [(n_z L_x - n_x L_z) - C \sin\theta \sin\phi] e^{jk\,\overline{OQ'} \cdot \bar{a}_R} \cdot (\rho')^2 \sin\psi' \sec\frac{\psi'}{2}\, d\psi'\, d\xi'$$

$$+ \bar{a}_z \int_{\xi'=0}^{2\pi} \int_{\psi'=0}^{\Psi} [(n_x L_y - n_y L_x) - C \cos\theta]\, e^{jk\,\overline{OQ'} \cdot \bar{a}_R} \cdot (\rho')^2 \sin\psi' \sec\frac{\psi'}{2}\, d\psi'\, d\xi'$$

where

(B-11a)

$$C = \sin\theta \cos\phi\,(n_y L_z - n_z L_y) + \sin\theta \sin\phi\,(n_z L_x - n_x L_z) + \cos\theta\,(n_x L_y - n_y L_x)$$

(B-11b)

$$\bar{a}_R = \sin\theta \cos\phi\, \bar{a}_x + \sin\theta \sin\phi\, \bar{a}_y + \cos\theta\, \bar{a}_z$$

(B-11c)

$$\overline{OQ'} = F\, \bar{a}_{z'} + \rho'\, \bar{a}_{\rho'}$$

$$= \bar{a}_x [F \sin\theta_1 \cos\phi_1 + \rho'(A_1 \sin\psi' \cos\xi' + A_2 \sin\psi' \sin\xi' - A_3 \cos\psi')]$$

$$+ \bar{a}_y [F \sin\theta_1 \sin\phi_1 + \rho'(A_4 \sin\psi' \cos\xi' + A_5 \sin\psi' \sin\xi' - A_6 \cos\psi')]$$

$$+ \bar{a}_z [F \cos\theta_1 + \rho'(A_7 \sin\psi' \cos\xi' + A_8 \sin\psi' \sin\xi' - A_9 \cos\psi')]$$

Notice that the equation for $\bar{E}'_{p_1}$ involves three surface integrals.

e) The Electric Field of Neighboring Paraboloid Antennas in Fraunhofer Region The electric field at observation point P due to the primary current density of the first paraboloid is

(B-12)

$$\bar{E}_{p_1} = -\frac{j\omega\mu}{4\pi}\left[8\left(\frac{\epsilon}{\mu}\right)^{\frac{1}{2}}\ \frac{P_T}{4\pi}\right]^{\frac{1}{2}}\ \frac{e^{-jkR}}{R}\ e^{jkF\cos(\phi_1-\phi)}$$

$$\cdot \int_{\xi=0}^{2\pi}\int_{\psi=0}^{\Psi} [G_f(\xi,\psi)]^{\frac{1}{2}}\ \frac{e^{-jk\rho[1-\bar{a}_{u'}\cdot\bar{a}_\rho]}}{\rho}$$

$$\cdot [-\cos\tfrac{\psi}{2}\ \bar{e}_1 + (\bar{n}\cdot\bar{e}_1)\bar{a}_{z'}]\cdot\rho^2\sin\psi\sec\tfrac{\psi}{2}\,d\psi\,d\xi$$

where

(B-13)

$$\bar{a}_{u'} = \sin\alpha'\cos\beta'\,\bar{a}_{x'} + \sin\alpha'\sin\beta'\,\bar{a}_{y'} + \cos\alpha'\,\bar{a}_{z'}$$

$$\bar{a}_\rho = \sin\psi\cos\xi\,\bar{a}_{x'} + \sin\psi\sin\xi\,\bar{a}_{y'} - \cos\psi\,\bar{a}_{z'}$$

$$\bar{a}_{u'}\cdot\bar{a}_\rho = -\cos\alpha'\cos\psi + \sin\alpha'\sin\psi\cos(\beta'-\xi).$$

The electric field, for the first approximation, at observation point P due to the primary current distribution of the second paraboloid is

(B-14)

$$\bar{E}_{p_2} = -\frac{j\omega\mu}{4\pi}\left[8\left(\frac{\epsilon}{\mu}\right)^{\frac{1}{2}}\ \frac{P_T}{4\pi}\right]^{\frac{1}{2}}\ \frac{e^{-jkR}}{R}$$

$$\cdot e^{jkL\sin\theta\sin\phi}$$

$$\cdot e^{jkF[\cos\theta\cos\theta_1 + \sin\theta\sin\theta_1\cos(\phi-\phi_1)]}$$

$$\cdot e^{-jk\frac{LF}{R}\sin\theta_1\sin\phi_1}$$

$$\cdot \int_{\xi_2=0}^{2\pi}\int_{\psi_2=0}^{\Psi} G_f(\xi_2,\psi_2)^{\frac{1}{2}}\ \frac{e^{-jk\rho_2[1-\bar{a}_{u2}\cdot\bar{a}_{\rho 2}]}}{\rho_2}$$

$$\cdot [-\cos\tfrac{\psi_2}{2}\ \bar{e}_1 + (\bar{n}\cdot\bar{e}_1)\bar{a}_{z'}]\cdot\rho_2^2\sin\psi_2\sec\tfrac{\psi_2}{2}\ d\psi_2\,d\xi_2$$

where

(B-15)

$$\bar{a}_{u_2} = \sin\alpha_2 \cos\beta_2\, \bar{a}_{x'} + \sin\alpha_2 \sin\beta_2\, \bar{a}_{y'} + \cos\alpha_2\, \bar{a}_{z'}$$

$$\bar{a}_{\rho_2} = \sin\psi_2 \cos\xi_2\, \bar{a}_{x'} + \sin\psi_2 \sin\xi_2\, \bar{a}_{y'} - \cos\psi_2\, \bar{a}_{z'}$$

$$\bar{a}_{u_2} \cdot \bar{a}_{\rho_2} = -\cos\alpha_2 \cos\psi_2 + \sin\alpha_2 \sin\psi_2 \cos(\beta_2 - \xi_2)$$

The parameters for calculating the electric field at $P(R,\theta,\phi)$ due to the contribution of second paraboloid is shown in Fig. 3. The separation between vertices of the paraboloids is L.

The total electric field at observation point P, $\bar{E}_p$, is the vector sum of the following components which are found in the previous paragraphs:

$\bar{E}_{p_1}$ The electric field at P due to the primary current distribution of the first paraboloid.

$\bar{E}'_{p_1}$ The electric field at P due to the secondary current distribution of the first paraboloid.

$\bar{E}_{p_2}$ The electric field at P due to the prmimary current distribution of the second paraboloid.

Thus

(B-16)
$$\bar{E}_p = \bar{E}_{p_1} + \bar{E}'_{p_1} + \bar{E}_{p_2}$$

$$= \bar{a}_x(\bar{E}_p)_x + \bar{a}_y(\bar{E}_p)_y + \bar{a}_z(\bar{E}_p)_z$$

where $(\bar{E}_p)_x$, $(\bar{E}_p)_y$ and $(\bar{E}_p)_z$ are defined in the following pages.

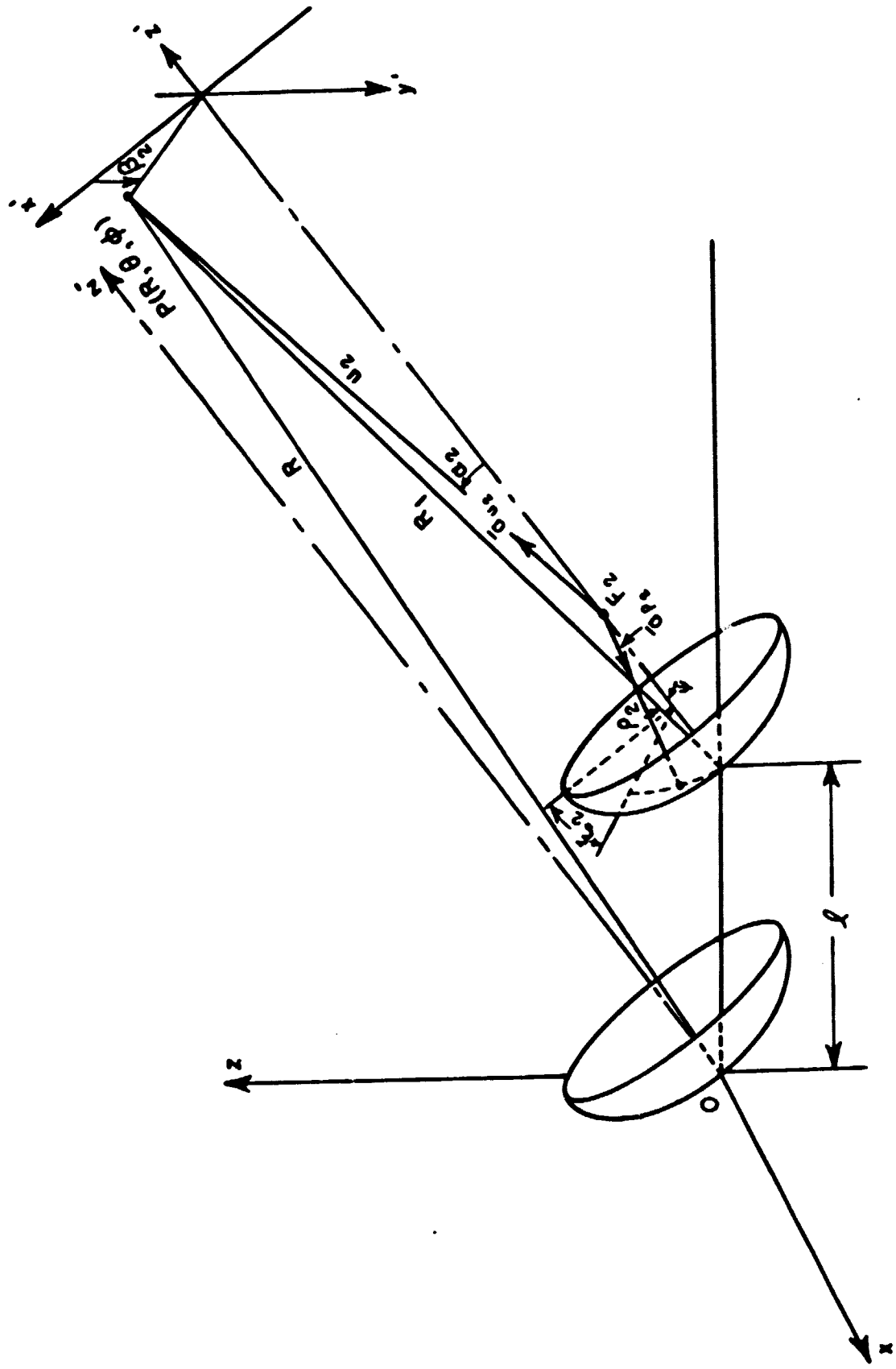

Fig. B-3. The parameters for calculating the electric field at P(R,θ,φ) due to the contribution of second paraboloid.

(B-16a)

$$(\bar{E}_p)_x = -\frac{j\omega\mu}{4\pi}\left[8\left(\frac{\varepsilon}{\mu}\right)^{\frac{1}{2}}\frac{P_T}{4\pi}\right]^{\frac{1}{2}}\frac{e^{-jkR}}{R}\; e^{jkF\cos(\phi_1-\phi)}$$

$$\cdot \int_{\xi=0}^{2\pi}\int_{\psi=0}^{\Psi}[G_f(\xi,\psi)]^{\frac{1}{2}}\frac{e^{-jk\rho[1+\cos\alpha'\cos\psi-\sin\alpha'\sin\psi\cos(\beta'-\xi)]}}{\rho}$$

$$\cdot [-\cos\tfrac{\psi}{2}\; e_{1x} + (n_x e_{1x} + n_y e_{1y} + e_z e_{1z})\sin\theta_1\cos\phi_1]$$

$$\cdot \rho^2 \sin\psi \sec\tfrac{\psi}{2}\; d\psi\, d\xi$$

$$-\frac{jk^2}{4\pi\omega\varepsilon}\;\frac{j2kA}{4\pi}\;\frac{e^{-jkR}}{R}$$

$$\cdot \int_{\xi'=0}^{2\pi}\int_{\psi'=0}^{\Psi}[(n_y L_z - n_z L_y) - C\sin\theta\cos\phi]e^{jk\,\overline{OQ'}\cdot\bar{a}_R}$$

$$\cdot (\rho')^2 \sin\psi' \sec\tfrac{\psi'}{2}\; d\psi'\, d\xi'$$

$$-\frac{j\omega\mu}{4\pi}\left[8\left(\frac{\varepsilon}{\mu}\right)^{\frac{1}{2}}\frac{P_T}{4\pi}\right]^{\frac{1}{2}}\frac{e^{-jkR}}{R}$$

$$\cdot e^{jkL\sin\theta\sin\phi}$$

$$\cdot e^{jkF[\cos\theta\cos\theta_1 + \sin\theta\sin\theta_1\cos(\theta-\phi_1)]}$$

$$\cdot e^{-jk\frac{LF}{R}\sin\theta_1\sin\phi_1}$$

$$\cdot \int_{\xi_2=0}^{2\pi}\int_{\psi_2=0}^{\Psi}[G_f(\xi_2,\psi_2)]^{\frac{1}{2}}\frac{e^{-jk\rho_2[1+\cos\alpha_2\cos\psi_2-\sin\alpha_2\sin\psi_2\cos(\beta_2-\xi_2)]}}{\rho^2}$$

$$\cdot [-\cos\tfrac{\psi_2}{2}\; e_{1x} + (n_x e_{1x}+n_y e_{1y}+n_z e_{1z})\sin\theta_1\cos\phi_1]$$

$$\cdot \rho_2^2 \sin\psi_2 \sec\tfrac{\psi_2}{2}\; d\psi_2\, d\xi_2$$

(B-16b)

$$(E_p)_y = -\frac{j\omega\mu}{4\pi}\left[8\left(\frac{\varepsilon}{\mu}\right)^{\frac{1}{2}}\frac{P_T}{4\pi}\right]^{\frac{1}{2}}\frac{e^{-jkR}}{R}\; e^{jkF\cos(\phi_1-\phi)}$$

$$\cdot \int_{\xi=0}^{2\pi}\int_{\psi=0}^{\Psi}[G_f(\xi,\psi)]^{\frac{1}{2}}\frac{e^{-jk\rho[1+\cos\alpha'\cos\psi-\sin\alpha'\sin\psi\cos(\beta'-\xi)]}}{\rho}$$

$$\cdot [-\cos\tfrac{\psi}{2}\, e_{1y} + (n_x e_{1x}+n_y e_{1y}+n_z e_{1z})\sin\theta_1\sin\phi_1]$$

$$\cdot \rho^2\sin\psi\sec\tfrac{\psi}{2}\, d\psi\, d\xi$$

$$-\frac{jk^2}{4\pi\omega\varepsilon}\;\frac{j2kA}{4\pi}\;\frac{e^{-jkR}}{R}$$

$$\cdot \int_{\xi'=0}^{2\pi}\int_{\psi'=0}^{\Psi}[(n_z L_x-n_x L_z)-C\sin\theta\sin\phi]\, e^{jk\,\overline{OQ'}\cdot\bar{a}_R}$$

$$\cdot (\rho')^2\sin\psi'\sec\tfrac{\psi'}{2}\; d\psi'\, d\xi'$$

$$-\frac{j\omega\mu}{4\pi}\left[8\left(\frac{\varepsilon}{\mu}\right)^{\frac{1}{2}}\frac{P_T}{4\pi}\right]^{\frac{1}{2}}\frac{e^{-jkR}}{R}$$

$$\cdot e^{jkL\sin\theta\cos\phi}$$

$$\cdot e^{jkF[\cos\theta\cos\theta_1+\sin\theta\sin\theta_1\cos(\phi-\phi_1)]}$$

$$\cdot e^{-jk(FL/R)\sin\theta_1\sin\phi_1}$$

$$\cdot \int_{\xi_2=0}^{2\pi}\int_{\psi_2=0}^{\Psi}[G_f(\xi_2,\psi_2)]^{\frac{1}{2}}\frac{e^{-jk\rho_2[1+\cos\alpha_2\cos\psi_2-\sin\alpha_2\sin\psi_2\cos(\beta_2-\xi_2)]}}{\rho_2}$$

$$\cdot [-\cos\tfrac{\psi_2}{2}\; e_{1y} + (n_x e_{1x}+n_y e_{1y}+n_z e_{1z})\sin\theta\sin\phi_1]$$

$$\cdot \rho_2^2\sin\psi_2\sec\tfrac{\psi_2}{2}\; d\psi_2\, d\xi_2$$

(B-16c)

$$(\bar{E}_p)_z = -\frac{j\omega\mu}{4\pi}\left[8\left(\frac{\varepsilon}{\mu}\right)^{\frac{1}{2}}\frac{P_T}{4\pi}\right]\frac{e^{-jkR}}{R}\; e^{jkF\cos(\phi_1-\phi)}$$

$$\cdot\int_{\xi=0}^{2\pi}\int_{\psi=0}^{\Psi}[G_f(\xi,\psi)]^{\frac{1}{2}}\;\frac{e^{-jk\rho[1+\cos\alpha'\cos\psi-\sin\alpha'\sin\psi\cos(\beta'-\xi)]}}{\rho}$$

$$\cdot[-\cos\tfrac{\psi}{2}\,e_{1z}+(n_x e_{1x}+n_y e_{1y}+n_z e_{1z})\cos\theta_1]$$

$$\cdot\rho^2\sin\psi\sec\tfrac{\psi}{2}\,d\psi\,d\xi$$

$$-\frac{jk^2}{4\pi\omega\varepsilon}\;\frac{j2kA}{4\pi}\;\frac{e^{-jkR}}{R}$$

$$\cdot\int_{\xi'=0}^{2\pi}\int_{\psi'=0}^{\Psi}[(n_xL_y-n_yL_x)-C\cos\theta]\;e^{jk\,\overline{OQ'}\cdot\bar{a}_R}$$

$$\cdot(\rho')^2\sin\psi'\sec\tfrac{\psi'}{2}\,d\psi'\,d\xi'$$

$$-\frac{j\omega\mu}{4\pi}\left[8\left(\frac{\varepsilon}{\mu}\right)^{\frac{1}{2}}\frac{P_T}{4\pi}\right]^{\frac{1}{2}}\frac{e^{-jkR}}{R}$$

$$\cdot e^{jkL\sin\theta\sin\phi}$$

$$\cdot e^{jkF[\cos\theta\cos\theta_1+\sin\theta\sin\theta_1\cos(\phi-\phi_1)]}$$

$$\cdot e^{-jk(FL/R)\sin\theta_1\sin\phi_1}$$

$$\cdot \int_{\xi_2=0}^{2\pi} \int_{\psi=0}^{\Psi} [G_f(\xi_2,\psi_2)]^{\frac{1}{2}} \frac{e^{-jk\rho_2[1+\cos\alpha_2\cos\psi_2-\sin\alpha_2\sin\psi_2\cos(\beta_2-\xi_2)]}}{\rho_2}$$

$$\cdot[-\cos\frac{\psi_2}{2}\ e_{1z} + (n_x e_{1x} + n_y e_{1y} + n_z e_{1z})\cos\theta_1]$$

$$\cdot\ \rho_2^2 \sin\psi_2 \sec\frac{\psi_2}{2}\ d\psi_2\ d\xi_2$$

3) The Blocking Effect of a Closely Spaced Array

(a) Consideration of the Coordinate Systems - The fixed coordinate system (x,y,z) with origin at point 0 will be used to define the observation point in space. The paraboloid coordinate system (x',y',z') with origins at the vertex of each paraboloid will be used to define the source points in space. The condition of the paraboloid coordinate system is specified in such a way that when the axis of the paraboloid (z'-axis) points in its zenith direction (in the direction of z-axis) the remaining x' and y' axes coincide with the fixed x and y axes respectively. That is, when paraboloid is at its zenith direction, the coordinates x', y' and z' coincide with the fixed coordinates x, y and z respectively. In order to define uniquely the pointing direction of the paraboloid in the direction (θ',ϕ') in the fixed coordinate, the axes of the paraboloid are being rotated as follows: first, x'-axis is rotated by an angle ϕ' in azimuth direction with z-axis as the axis of rotation. Hence, the angle between axes y' and y is ϕ'. Next, z'-axis is rotated by an angle θ' with y'-axis as the axis of rotation. Thus, the angle between axes z' and z is θ' and the angle between x-axis and the projection of x'-axis on the xy plane is ϕ'.

Let the direction of the projection of x'-axis on the xy plane be ξ, then

$$\bar{a}_y,\bar{a}_{y'} = \phi'$$

$$\bar{a}_x,\bar{a}_\xi = \phi'$$

$$\bar{a}_z,\bar{a}_{z'} = \theta'$$

$$\bar{a}_{x'},\bar{a}_\xi = \theta'$$

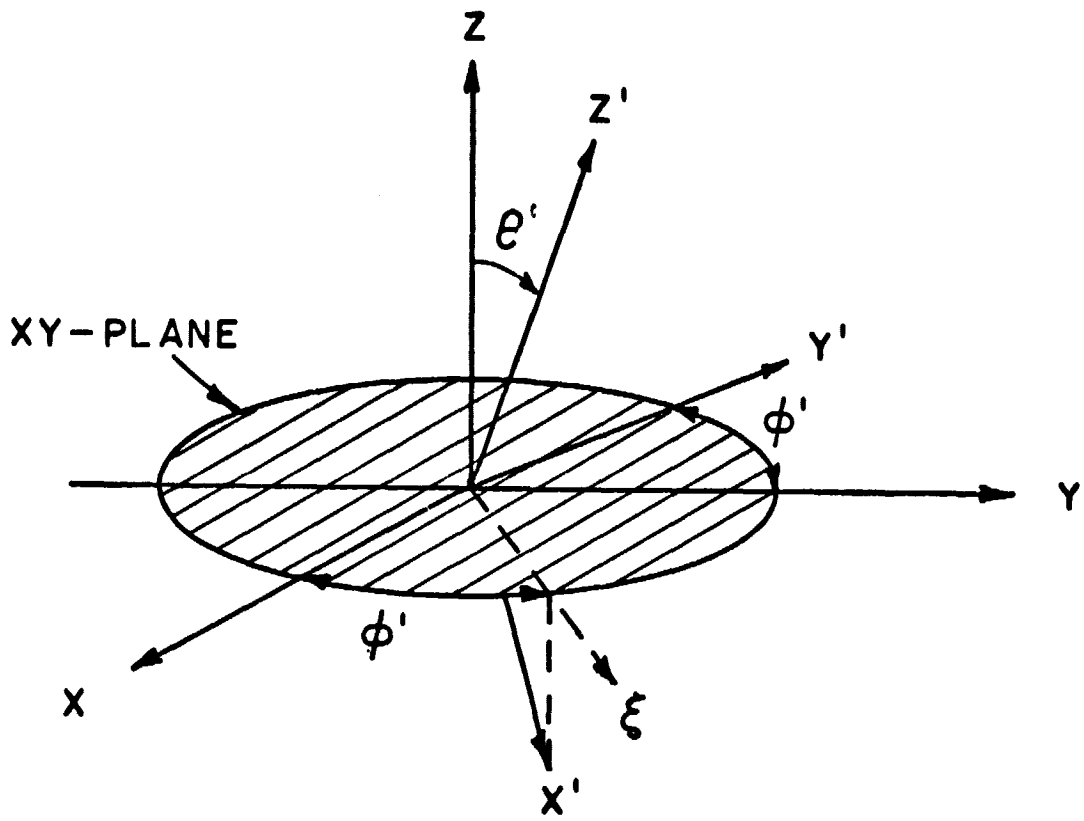

By these two rotations, the paraboloid coordinates have been uniquely defined in the fixed coordinate system. Hence,

(B-17)

$$\bar{a}_{x'} = \bar{a}_x \cos\theta' \cos\phi' + \bar{a}_y \cos\theta' \sin\phi' + \bar{a}_z(-\sin\theta')$$

$$\bar{a}_{y'} = \bar{a}_x(-\sin\phi') + \bar{a}_y \cos\phi' + \bar{a}_z\, 0$$

$$\bar{a}_{z'} = \bar{a}_x \sin\theta' \cos\phi' + \bar{a}_y \sin\theta' \sin\phi' + \bar{a}_z \cos\theta'$$

b) Fields in Fraunhofer Region for an Antenna System of Two Neighboring Paraboloids

A Two Neighboring Paraboloidal Antenna System is shown in Fig. B-4, where $\bar{a}_{v_1}$, $\bar{a}_{v_2}$ and $\bar{a}_R$ are unit vectors in the direction of v_1, v_2 and R respectively. Both paraboloids point in the direction of z'-axis. Let the field distribution over the circular aperture be designated by

(B-18) $$F(\rho,\psi) = A(\rho,\psi)\, e^{jk\Psi(\rho,\psi)}$$

with amplitude distribution $A(\rho,\psi)$ and phase distribution $\Psi(\rho,\psi)$; where ρ and ψ are the variables for the polar coordinates on the aperture.

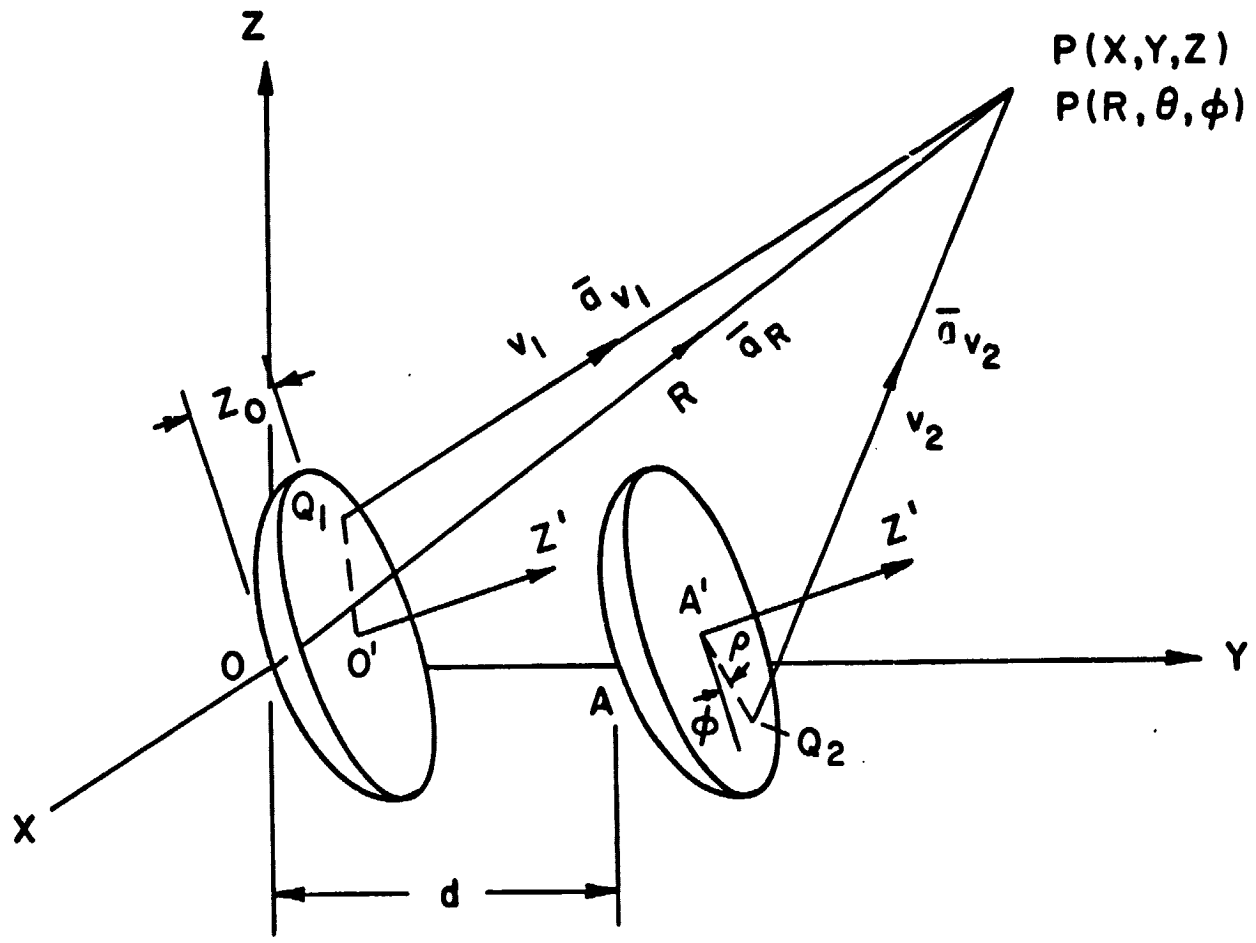

Fig. B-4.

For the far-zone region, the field due to a single aperture is given by

(B-19)

$$U_p = \frac{j}{2\lambda} \frac{e^{-jkR}}{R} (1 + \gamma) e^{jkz_0\gamma} \cdot \int_{\psi=0}^{2\pi} \int_{\rho=0}^{a} F(\rho,\psi) e^{jk\rho[\alpha \cos \psi + \beta \sin \psi]} \rho d\rho \, d\psi$$

where

$$\gamma = \sin\theta \sin\theta' \cos(\phi-\phi') + \cos\theta \cos\theta'$$

$$\alpha = \sin\theta \cos\theta' \cos(\phi-\phi') - \cos\theta \sin\theta'$$

$$\beta = \sin\theta \sin(\phi-\phi')$$

For the configuration in Fig. B-4, the total field at observation point due to the identical aperture distribution $F(\rho,\psi)$ on apertures No. 1 and No. 2 is

(B-21)

$$U_p = U_{p_1} + U_{p_2}$$

$$= \frac{j}{2\lambda} \frac{e^{-jkR}}{R} (1+\gamma) e^{jkz_o\gamma}$$

$$\cdot \int_0^{2\pi} \int_0^a F(\rho,\phi) e^{jk\rho[\alpha \cos\phi + \beta \sin\phi]} \rho d\rho \, d\phi$$

$$+ \frac{j}{2\lambda} \frac{e^{-jkR}}{R} (1+\gamma) e^{jkz_o\gamma} e^{jkd \sin\theta \sin\phi}$$

$$\cdot \int_0^{2\pi} \int_0^a F(\rho,\phi) e^{jk\rho[\alpha \cos\phi + \beta \sin\phi]} \rho d\rho \, d\phi$$

Equation (B-21) is the total field at observation point without considering the blocking effect. In the case that the separation between the neighboring paraboloids is not large enough, the blocking effect due to the geometric optics obstacles has to be taken into account when the system scans away from its zenith direction. In the latter case, the first aperture of the paraboloid with vertex at origin is partially blocked by the presence of the second aperture of the second paraboloid with vertex at A in Fig. B-4.

If it is assumed that the beam diameter equals the element aperture diameter, the separation between two adjacent elements required for no blockage is given by

(B-22) $$d = \frac{2a}{\cos\theta_m}$$

where

d = separation between elements (parabolic antennas)
a = radius of element apertures
θ_m = maximum polar angle coverage for which no aperture blockage occurs when scanning.

Theoretically, for an angle coverage up to 90 degrees, the separation d has to be infinity in order to have no blockage. The normalized minimal separation with respect to the diameter of element apertures vs the maximum polar angle coverage is shown in Fig. B-5. It is seen that for an aperture diameter of 30 ft with maximum angle coverage θ_m of 60 degrees, the minimal separation required for no blockage is 60 ft (twice the size of the aperture); however, for θ_m of 87 degrees (i.e., for an elevation angle of 3 degrees above horizon), the separation increases up to approximately 600 ft (20 times the size of the aperture).

On the other hand, with a given aperture radius "a", the blockage will not occur until the array pointing direction θ' reaches certain value for a given element separation d = pa in terms of the aperture radius by a constant p. Let this "certain value" of array direction θ' for a given d = pa be θ_b'. Then θ_b' can be obtained as

$$\text{(B-23)} \qquad \theta_b' = \cos^{-1}\left(\frac{2a}{d}\right) = \cos^{-1}\left(\frac{2}{p}\right)$$

For the scan angles less than or equal to θ_b', there exists no blockage in a geometrical optics sense; for scan angles larger than θ_b', blockage occurs. The dependence of θ_b' on the element separation d is shown in Fig. B-6.

Considering the blocking effect due to the geometrical optics obstacles, the field in far-zone region can be taken care of as follows: looking back along z'-axis toward the vertices, the overlap portion of the adjacent apertures due to scanning away from its zenith direction is shown in Fig. B-7. The distance d' can be found as

$$\text{(B-24a)} \qquad d' = d\sqrt{1 - \sin^2\theta' \sin^2\phi'}$$

and

$$\text{(B-24b)} \qquad d_\ell = 2a - d' = 2a - d\sqrt{1 - \sin^2\theta' \sin^2\phi'}$$

where d' is the distance between the axes, which is the projection of the separation d of the vertices of the paraboloids on the plane perpendicular to z'-axis, when the axes point at (θ',ϕ') direction and d_ℓ is the overlap distance along this projection. It is noted that if d' is larger than or equal to the aperture diameter, there is no blockage.

The blockage occurs when the corresponding d' for an arbitrary array pointing direction (θ', ϕ') is less than the aperture diameter. For the latter case, the overlap angle ξ is given by

$$\xi = \cos^{-1}\left(1 - \frac{d_\ell}{2a}\right) \tag{B-25}$$

The blocked area A_b which is the shaded area in Fig. (B-7) can be found as

$$A_b = 2\left[a^2\xi - \left(a - \frac{d_\ell}{2}\right) \; a \sin \xi\right] \tag{B-26}$$

Hence, the blocking effect can be taken care of by subtracting the part of contribution due to the blocked aperture; thus

$$U_{p1} = \frac{j}{2\lambda} \frac{e^{-jkR}}{R} (1+\gamma) e^{jkz_o\gamma} \cdot \left\{ \int_0^{2\pi} \int_0^{a} F(\rho,\psi)\, e^{jk\rho[\alpha \cos\psi + \beta \sin\psi]}\, \rho \, d\rho d\psi - \int_{-\xi}^{+\xi} \int_{a-d_\ell}^{a} F(\rho,\psi) e^{jk\rho[\alpha \cos\psi + \beta \sin\psi]}\, \rho \, d\rho d\psi \right\} \tag{B-27}$$

Therefore, the total field at observation point due to apertures No. 1 and No. 2 with blocking effect is

$$\begin{aligned} U_p &= U_{p1} \text{ (partially blocked)} + U_{p2} \text{ (unblocked)} \\ &= \frac{j}{2\lambda} \frac{e^{-jkR}}{R} (1+\gamma) e^{jkz_o\gamma} \cdot \left\{ \int_0^{2\pi} \int_0^{a} F(\rho,\psi) e^{jk\rho[\alpha \cos\psi + \beta \sin\psi]}\, \rho \, d\rho d\psi - \int_{-\xi}^{+\xi} \int_{a-d_\ell}^{a} F(\rho,\psi) e^{jk\rho[\alpha \cos\psi + \beta \sin\psi]}\, \rho \, d\rho d\psi \right\} \\ &\quad + \frac{j}{2\lambda} \frac{e^{-jkR}}{R} (1+\gamma) e^{jkz_o\gamma} e^{jkd \sin\theta} \cdot \int_0^{2\pi} \int_0^{a} F(\rho,\psi) e^{jk\rho[\alpha \cos\psi + \beta \sin\phi]}\, \rho \, d\rho d\psi \end{aligned} \tag{B-28}$$

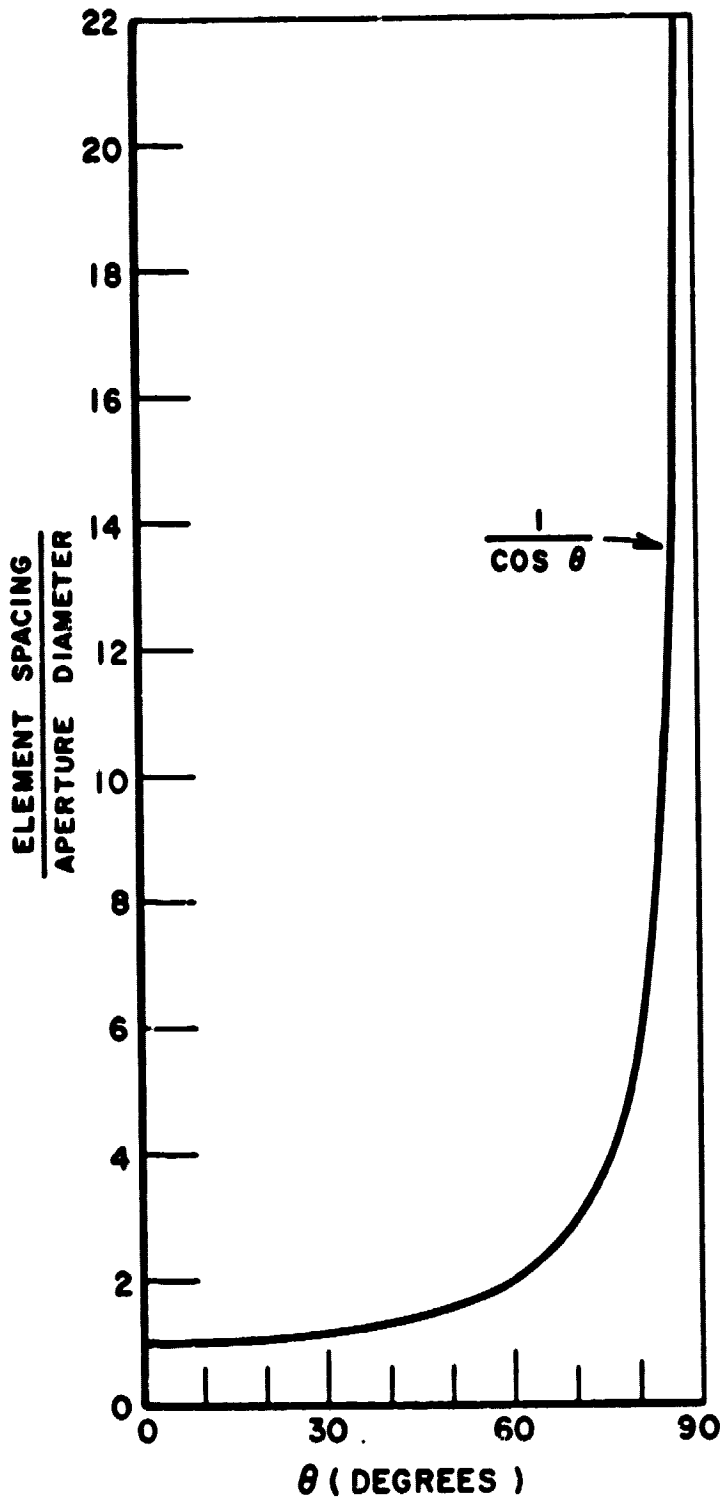

Fig. B-5. Minimum element separation vs angle of coverage.

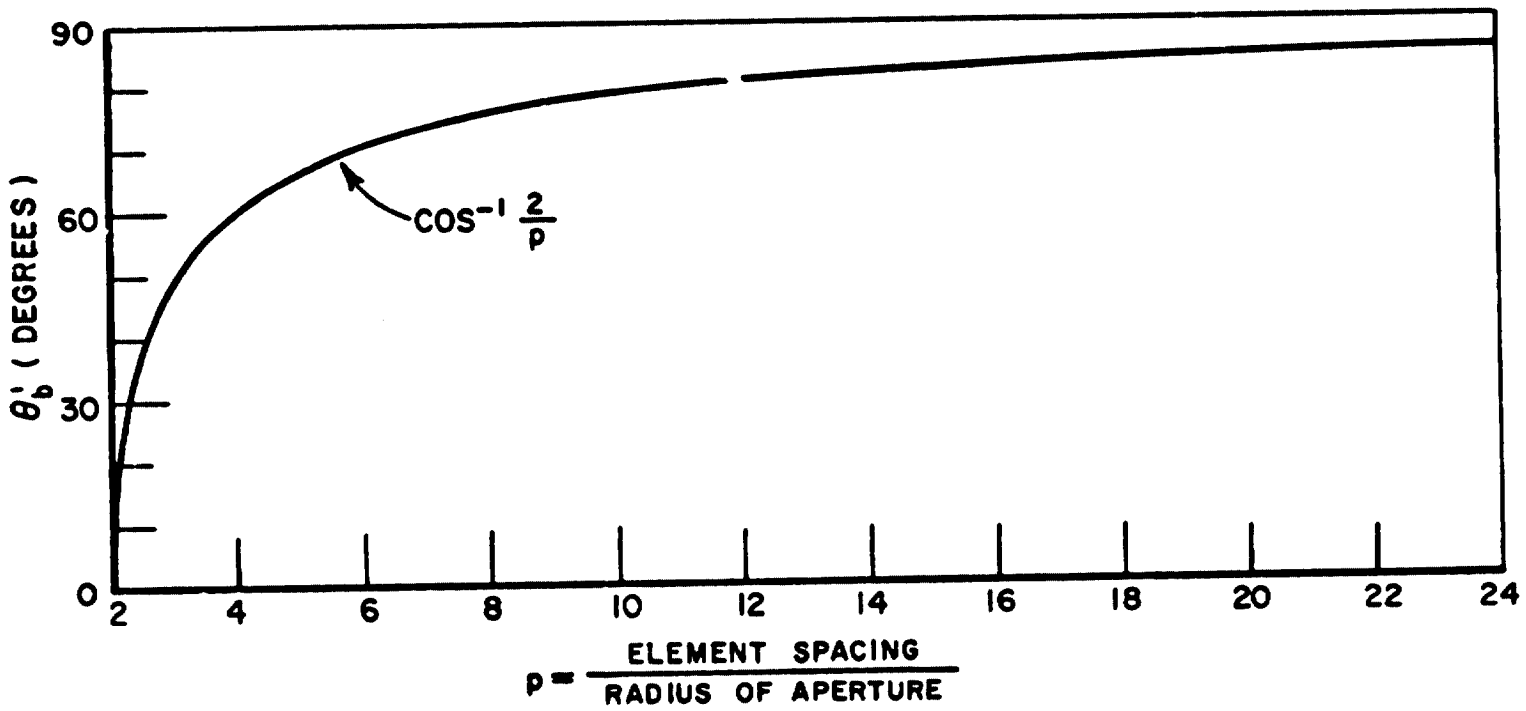

Fig. B-6. θ_b' vs element separation.

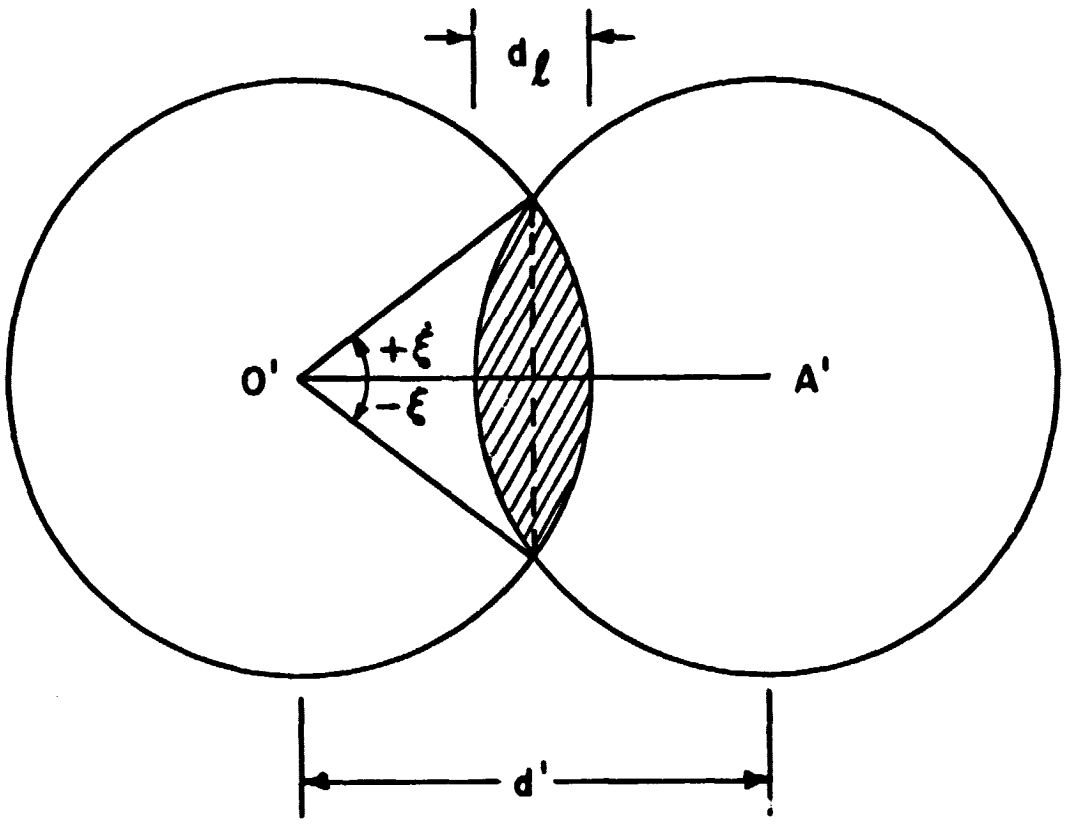

Fig. B-7.

c) Fields in Fraunhofer Region for a Linear Array of N-Paraboloid

The array is composed of N identical paraboloids and it is assumed that they point in the same direction simultaneously without delay.

The total blocked area A_b for a linear array of N identical paraboloidal antennas is the sum of the first (N-1) blocked area for the system of two-element array given in Equation (B-26). Hence, A_b becomes

$$(B\text{-}29) \qquad A_b = (N-1) \cdot 2a^2 \left[\xi - \frac{p}{2} \cos\theta' \left(1 - \frac{p^2}{4} \cos^2\theta'\right)^{\frac{1}{2}}\right]$$

The total aperture A of an array of N-element with no blockage is given by

$$(B\text{-}30) \qquad A = N(\pi a^2)$$

The total effective aperture A_u of an array of N-element with blockage thus becomes

$$(B\text{-}31) \qquad A_u = a^2 \left\{N\pi - 2\left[\xi - \frac{p}{2} \cos\theta' \left(1 - \frac{p^2}{4} \cos^2\theta'\right)^{\frac{1}{2}}\right]\right\}$$

where

N = number of elements in an array
a = radius of individual aperture
ξ = angle of overlap defined in Equation (B-25)
p = a constant defined by the relationship given as d = pa, where d is the separation between adjacent elements
θ' = angle of scan or the pointing direction of an array.

It is desirable to know the percentages of the blocked and the effective apertures over the total aperture A with no blockage. Let r_b and r_u be the ratios of A_b/A and A_u/A respectively, then they are given as

$$(B\text{-}32a) \quad r_b = \frac{N-1}{N} \cdot \frac{2}{\pi} \left[\xi - \frac{p}{2} \cos\theta' \left(1 - \frac{p^2}{4}\cos^2\theta'\right)^{\frac{1}{2}}\right]$$

$$(B\text{-}32b) \quad r_u = 1 - r_b$$

It is noted that the ratio r_b and r_u are functions of parameters N, p (or d, the element separation), and the array pointing direction θ'. They are independent of the aperture size.

The ratios r_b and r_u vs the element separation for a given array direction θ' have the same significance of the curve θ_b' vs the element separation as given in Fig. B-6. It has shown that for the scan angles less than or equal to the corresponding angle θ_b' given in Equation (B-23), there exists no blockage, $r_b = 0$ and $r_u = 1$. For the scan angle larger than θ_b', the blockage occurs. On the other hand, for the case of the smallest element separation of which the element separation is equal to the diameter of the aperture and it corresponds to the best case of the grating-lobe-problem, the ratio r_b vs the scan angle is shown in Fig. B-8 for the array elements of 2, 10, 20, and 200. The percentage of the effective aperture of an array r_u is equal to $(1-r_b)$ as shown in Equation (B-32b). It is, therefore, obtained that r_u is 100% for any number of elements in an array when the array is pointed at zenith. However, when the array is pointed horizontally, r_u becomes 50% for two-element arrays, 10% for ten-element arrays, 5% for twenty-element arrays, and 0.5% for two-hundred-element arrays. The dependence of r_u on parameters N and θ' is tabulated in Table B-1.

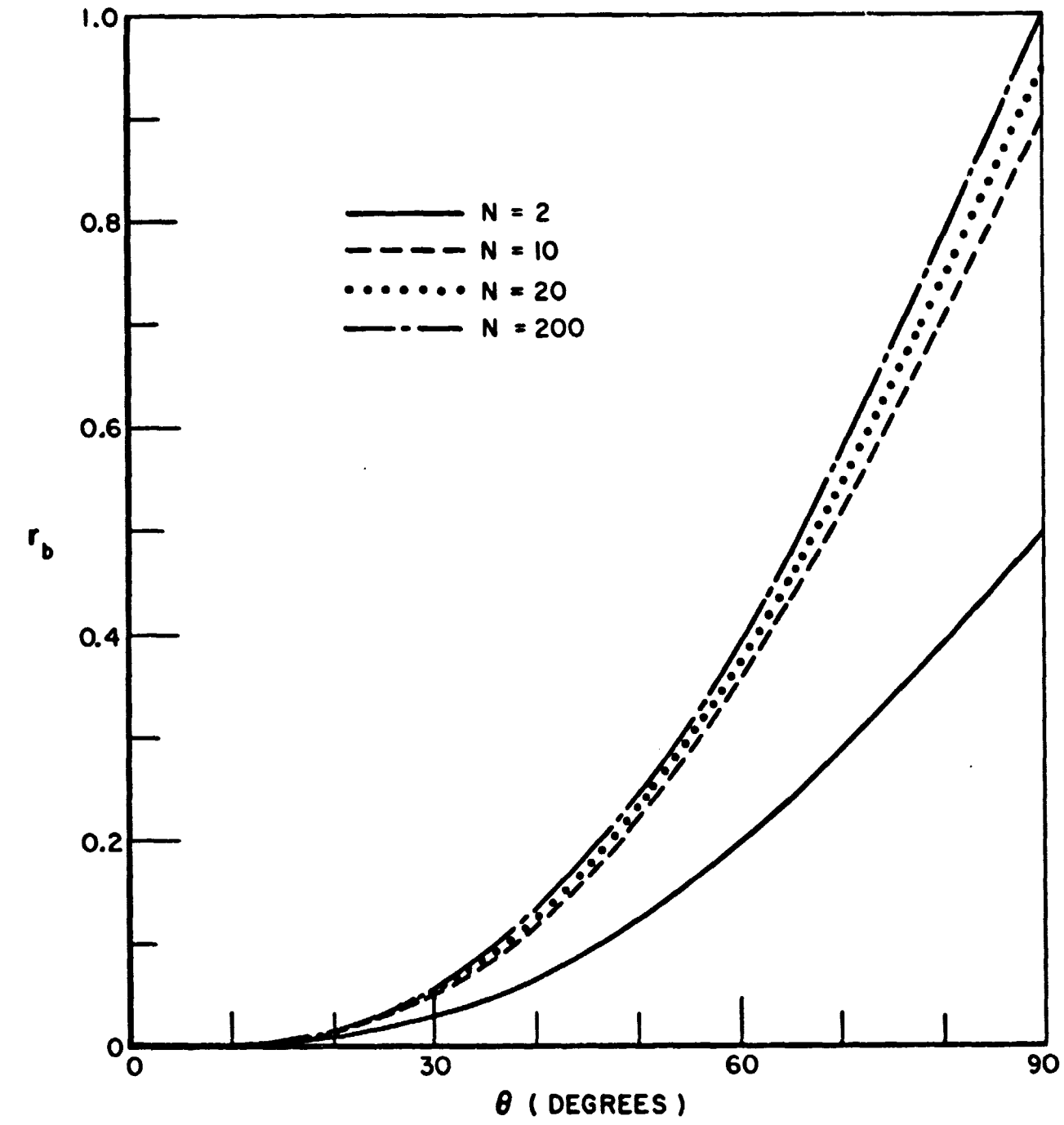

Fig. B-8. The ratio r_b vs angle θ for d = 2a case.

Pointing Direction θ' \ Number of Elements N		2	10	20	200	2000
r_u%	0^c	100	100	100	100	100
	40^o	93.45	88.21	87.56	86.97	86.91
	60^o	80.45	64.81	62.86	61.10	60.92
	80^o	60.99	29.80	25.90	22.39	22.04
	90^o	50	10	5	0.5	0.05

TABLE B-1.
The effective aperture r_u in percentage for various array elements and array pointing directions

The total field at observation point due to a linear array of N-aperture with the arrangement in Fig. B-9 will be the sum of the contribution of the first (N-1) partially blocked apertures and the last unblocked aperture, thus

(B-33)

$$U_p = \sum_{j=0}^{N-2} U_{p_j} \text{ (partially blocked)} + U_{p_{N-1}} \text{ (unblocked)}$$

$$= \frac{j}{2\lambda} \frac{e^{-jkR}}{R} (1+\gamma) e^{jkz_o\gamma} \left[\sum_{n=0}^{N-2} e^{jknd \sin\theta} \right]$$

$$\cdot \left\{ \int_0^{2\pi} \int_0^a F(\rho,\phi) e^{jk\rho[\alpha \cos\phi + \beta \sin\phi]} \rho d\rho \, d\phi \right.$$

$$\left. - \int_{-\xi}^{\xi} \int_{a-d_\ell}^{a} F(\rho,\phi) e^{jk\rho[\alpha \cos\phi + \beta \sin\phi]} \rho d\rho \, d\phi \right\}$$

$$+ \frac{j}{2\lambda} \frac{e^{-jkR}}{R} (1+\gamma) e^{jkz_o\gamma} e^{jk(N-1)d \sin\theta}$$

$$\cdot \int_0^{2\pi} \int_0^a F(\rho,\phi) e^{jk\rho[\alpha \cos\phi + \beta \sin\phi]} \rho d\rho \, d\phi$$

or

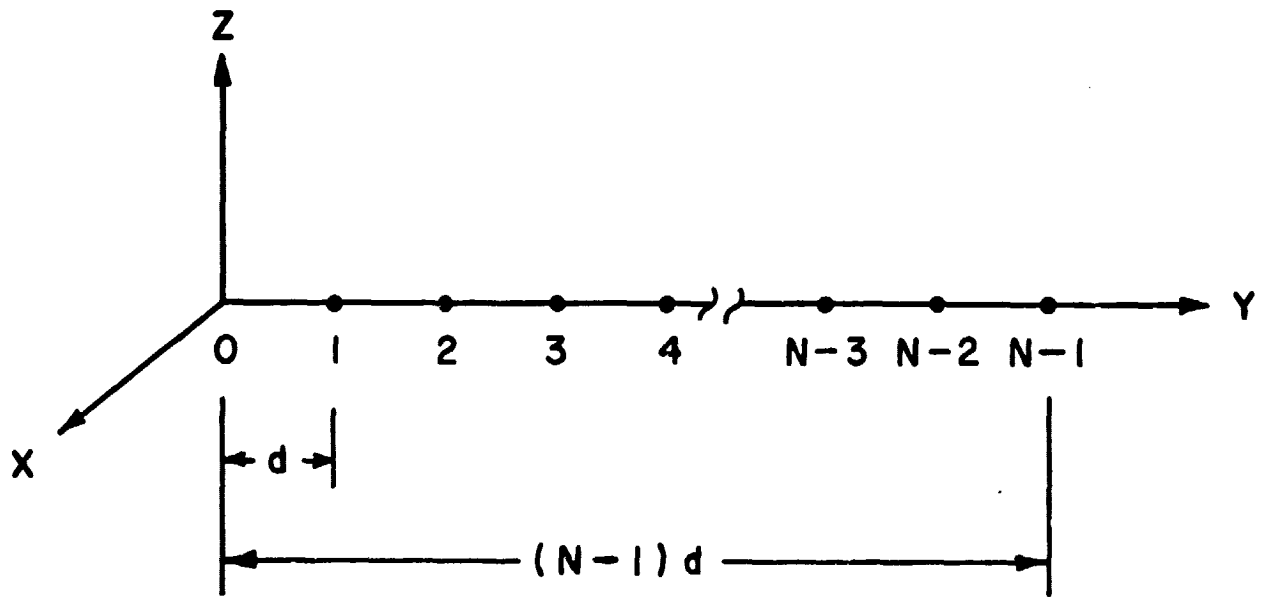

Fig. B-9.

(B-34)

$$U_p = \frac{j}{2\lambda} \frac{e^{-jkR}}{R} (1+\gamma) e^{jkz_o\gamma} \left[\sum_{n=0}^{N-1} e^{jknd \sin\theta} \right] \cdot \int_0^{2\pi} \int_0^{a} F(\rho,\phi) e^{jk\rho[\alpha \cos\phi + \beta \sin\phi]} \rho d\rho \, d\phi - \frac{j}{2\lambda} \frac{e^{-jkR}}{R} (1+\gamma) e^{jkz_o\gamma} \left[\sum_{n=0}^{N-2} e^{jknd \sin\theta} \right] \cdot \int_{-\xi}^{+\xi} \int_{a-d_\ell}^{a} F(\rho,\phi) e^{jk\rho[\alpha \cos\phi + \beta \sin\phi]} \rho d\rho \, d\phi$$

Let

(B-35a)

$$I = \int_0^{2\pi} \int_0^{a} F(\rho,\phi) e^{jk\rho[\alpha \cos\phi + \beta \sin\phi]} \rho d\rho \, d\phi$$

(B-35b)

$$I_b = \int_{-\xi}^{+\xi} \int_{a-d_\ell}^{a} F(\rho,\phi) e^{jk\rho[\alpha \cos \phi + \beta \sin \phi]} \rho d\rho \, d\phi$$

Hence,

(B-36)

$$U_p = \frac{j}{2\lambda} \frac{e^{-jkR}}{R} (1+\gamma) e^{jkz_o\gamma} I \left[\sum_{n=0}^{N-1} e^{jknd \sin \theta} \right]$$

$$- \frac{j}{2} \frac{e^{-jkR}}{R} (1+\gamma) e^{jkz_o\gamma} I_b \left[\sum_{n=0}^{N-2} e^{jknd \sin \theta} \right]$$

where the factors I and $\sum_{n=0}^{N-1} e^{jkmd \sin \theta}$ are the element factor and the array factor respectively for a linear array of N-paraboloid without blocking effect; the factors I_b and $\sum_{n=0}^{N-2} e^{jkmd \sin \theta}$ are the element factor and the array factor respectively for taking into account the blocking effect; where α, β, γ, are given in Eq. (B-20).

d) Consideration of a Simple Case

In order to observe the pattern of the system in Fraunhofer region, first we consider a simple case in which the array lies along the y-axis and the scanning will perform in the right corner sector of the yz-plane. For this given condition, ϕ is $\pi/2$, and ϕ' is $\pi/2$. Thus from Eq. (B-20)

$$\gamma = \cos(\theta - \theta')$$
$$\alpha = \sin(\theta - \theta')$$
$$\beta = 0.$$

Hence from Eqs. (B-35a) and (B-35b) we have

(B-37) $$I = \int_0^{2\pi} \int_0^{a} F(\rho,\phi) e^{jk\rho \sin(\theta-\theta')\cos \phi} \rho d\rho \, d\phi$$

(B-38) $$I_b = \int_{-\xi}^{+\xi} \int_{a-d_\ell}^{a} F(\rho,\phi) e^{jk\rho \sin(\theta-\theta')\cos \phi} \rho d\rho \, d\phi$$

For the aperture distribution $F(\rho,\psi)$, it is assumed that the feeds are normally designed to illuminate the paraboloidal reflectors with an

intensity at the reflector edges that is approximately 10 dB below that at center. Thus

$$F(\rho,\psi) = 1 - (1-\delta)\frac{\rho^2}{a^2} \quad \text{for } \rho \leq a \tag{B-39}$$

For this 10 dB tapered illumination, the value of δ has to be equal to 0.1.

To obtain the desired aperture distribution, in the present case, the 10 dB tapered aperture illumination, is itself an attractive problem namely aperture synthesis. For the purpose of analyzing the blocking effect of the closely spaced linear array of N-dish, it is assumed that the desired aperture distribution has been achieved without worrying about the actual technique to obtain it. The effect of tapering the illumination down toward the edge is: reduction in gain, increasing beamwidth, and reduction in side lobes as compared with the uniform aperture distribution, and reduction of the energy spilled over the edge.

To perform the integrations in Eq. (B-37) and (B-38), a change of variables is done as follows: Let

$$r = \frac{\rho}{a} \tag{B-40}$$

$$u = ka \sin(\theta-\theta')$$

Then the aperture distribution becomes

$$F(r,\psi) = 1 - (1-\delta)r^2 \tag{B-41}$$

with $\delta = 0.1$ for 10 dB tapered illumination and the factor

$$e^{jk\rho \sin(\theta-\theta')\cos\psi} = e^{jur\cos\psi} \tag{B-42}$$

Thus, Eqs. (B-37) and (B-38), respectively, become

(B-43)

$$I = a^2 \int_0^{2\pi}\int_0^1 e^{jur\cos\psi} r\,dr\,d\psi - a^2(1-\delta)\int_0^{2\pi}\int_0^1 r^2 e^{jur\cos\psi}\, r\,dr\,d\psi$$

$$= 2a^2\delta\frac{J_1(u)}{u} + 4\pi a^2(1-\delta)\frac{J_2(u)}{u}$$

(B-44)

$$I_b = \frac{a^2}{u^2} \int_{-\xi}^{+\xi} \int_{z_1}^{z_2} z e^{jz \cos \psi} \, dz \, d\psi$$

$$- \frac{a^2(1-\delta)}{u^4} \int_{-\xi}^{+\xi} \int_{z_1}^{z_2} z^3 \, e^{jz \cos \psi} \, dz \, d\psi$$

When integration is performed, I_b will be a complex number, hence I_b may be denoted by its real part I_{br} and imaginary part I_{bi}; thus

(B-45) $$I_b = I_{br} + j \, I_{bi}$$

with

(B-45a)

$$I_{br} = \frac{a^2}{u^2} \int_{-\xi}^{+\xi} \int_{z_1}^{z_2} z \cos(z \cos \psi) dz \, d\psi$$

$$- \frac{a^2(1-\delta)}{u^4} \int_{-\xi}^{+\xi} z^3 \cos(z \cos \psi) dz \, d\psi$$

(B-45b)

$$I_{bi} = \frac{a^2}{u^2} \int_{-\xi}^{+\xi} \int z \sin(z \cos \psi) dz \, d\psi$$

$$- \frac{a^2(1-\delta)}{u^4} \int_{-\xi}^{+\xi} z^3 \sin(z \cos \psi) dz \, d\psi$$

where

$$u = ka \sin(\theta - \theta')$$

$$z = ur = k\rho \sin(\theta - \theta')$$

$$z_1 = u\left(1 - \frac{d_\ell}{a}\right)$$

$$z_2 = u$$

$$d_\ell = 2a - d \cos \theta'$$

$$\xi = \tan^{-1} \frac{\sqrt{a^2 - \left(a - \frac{d_\ell}{2}\right)^2}}{a - \frac{d_\ell}{2}}$$

a = radius of the circular aperture

d = separation between the adjacent paraboloids

$k = \frac{2\pi}{\lambda}$

The array factors in Eq. (B-36) are

$$\sum_{n=0}^{N-1} e^{jknd \sin\theta} = \frac{\sin \frac{kNd \sin\theta}{2}}{\sin \frac{kd \sin\theta}{2}} e^{j \frac{k(N-1)d \sin\theta}{2}}$$

$$\sum_{n=0}^{N-2} e^{jknd \sin\theta} = \frac{\sin \frac{k(N-1)d \sin\theta}{2}}{\sin \frac{kd \sin\theta}{2}} e^{j \frac{k(N-2)d \sin\theta}{2}}$$

Let

(B-46a) $$F_1(\theta) = \frac{\sin \frac{kNd \sin\theta}{2}}{\sin \frac{kd \sin\theta}{2}}$$

$$F_2(\theta) = \frac{\sin \frac{k(N-1)\sin\theta}{2}}{\sin \frac{kd \sin\theta}{2}}$$

Therefore, the total field U_p at observation point in Eq. (B-36) becomes

(B-47)

$$U_p = \frac{j}{2} \frac{e^{-jkR}}{R} (1+\gamma) e^{jkz_o\gamma} \cdot \left\{ F_1(\theta)\, I\, e^{j \frac{k(N-1)d \sin\theta}{2}} - F_2(\theta)\, I_b\, e^{j \frac{jk(N-2)d \sin\theta}{2}} \right\}$$

The angular distribution $g(\theta,\phi)$ of U_p is

(B-48)

$$g(\theta,\phi) = (1+\gamma)\left\{\left[F_1(\theta)I - F_2(\theta)\left(I_{br}\cos\frac{kd\sin\theta}{2} + I_{bi}\sin\frac{kd\sin\theta}{2}\right)\right]^2 + \left[F_2(\theta)\left(I_{br}\sin\frac{kd\sin\theta}{2} - I_{bi}\frac{\cos kd\sin\theta}{2}\right)\right]^2\right\}^{\frac{1}{2}} \cdot e^{jkz_0\gamma + j\frac{k(N-1)d\sin\theta}{2}} \cdot e^{j\tan^{-1}\frac{F_2(\theta)\left[I_{br}\sin\frac{kd2\sin\theta}{2} - I_{bi}\cos\frac{kd\sin\theta}{2}\right]}{F_1(\theta)I - F_2(\theta)\left[I_{br}\cos\frac{kd\sin\theta}{2} + I_{bi}\sin\frac{kd\sin\theta}{2}\right]}}$$

Let the amplitude and phase distributions of $g(\theta,\phi)$ be denoted by $A(\theta,\phi)$ and $\Psi(\theta,\phi)$ respectively, then

(B-49) $$g(\theta,\phi) = A(\theta,\phi)\, e^{j\Psi(\theta,\phi)}$$

with

(B-49a)

$$A(\theta,\phi) = (1+\gamma)\left\{\left[F_1(\theta)I - F_2(\theta)\left(I_{br}\cos\frac{kd\sin\theta}{2} + I_{bi}\sin\frac{kd\sin\theta}{2}\right)\right]^2 + \left[F_2(\theta)\left(I_{br}\sin\frac{kd\sin\theta}{2} - I_{bi}\cos\frac{kd\sin\theta}{2}\right)\right]^2\right\}^{\frac{1}{2}}$$

(B-49b)

$$\Psi(\theta,\phi) = kz_0\gamma + \frac{k(N-1)d\sin\theta}{2} + \tan^{-1}\frac{F_2(\theta)\left[I_{br}\sin\frac{kd\sin\theta}{2} - I_{bi}\cos\frac{kd\sin\theta}{2}\right]}{F_1(\theta)I - F_2(\theta)\left[I_{br}\cos\frac{kd\sin\theta}{2} + I_{bi}\sin\frac{kd\sin\theta}{2}\right]}$$

where $F_1(\theta)$ and $F_2(\theta)$ are defined in Eqs. (B-46a) and (B-46b) respectively; I_{br} and I_{bi} are defined in Eqs. (B-45a) and (B-45b) respectively and I is defined in Eq. (B-43).

With the help of IBM 7094 digital computer, some preliminary results have been obtained. Several main beam patterns for parabolic antenna of aperture diameter D = 14, 30, 60, and 100 ft are shown in Fig. B-10. These patterns are obtained for frequency of 3 GHz and 10 dB tapered illumination (δ = 0.1) with the parabolic antenna pointing at zenith. It is seen that the larger the aperture size, the narrower the main beam. Also, the main beam patterns of various tapered illuminations, 10 dB (δ = 0.1), 3 dB (δ = 0.5 approximately) and uniform (δ = 1.0), are shown in Fig. B-11 for frequency of 3 GHz and both aperture sizes D = 14 and 60 ft. The reason for choosing these two particular paraboloid antenna sizes is that they are currently used to support satellite missions at various tracking stations throughout the world by United States Air Force. It is noted that the half-power beam widths for two extreme cases, uniform illumination (δ = 1.0) and 10 dB tapered illumination (δ = 0.1) are 0.7 degrees and 0.82 degrees approximately. The difference is 0.12 degrees. For larger aperture sizes, however, the half-power beam width difference for the extreme cases mentioned above is less than 0.12 degrees. With aperture size of 60 ft, the difference is less than 0.05 degrees. More numerical results for this simple case will be included in the next report.

The following steps are going to be taken in the course of this study:

1) A continuing effort will be devoted to the theoretical study of this problem. The current-distribution and aperture-distribution methods, and the geometrical theory of diffraction will be applied to solve the proposed problem.

2) A comparison between the results obtained by using different methods will be made in order to observe any discrepency and hopefully it may be interpreted.

3) During the above investigations, it may be necessary to look into the possibility to apply a combination of the aforementioned methods at different stages along the course of solving the proposed problem in order to obtain better results.

4) While the theoretical study being performed, an experimental array of two dishes with a diameter of a few feet will be designed and tested in S-band (or in X-band depending upon the availability of equipment) in order to compare the measured data with theoretical results predicted by the above methods.

5) An experimental array of more elements, four or six dishes (again, depending upon the availability of equipment) may be tested in order to observe any unusual behaviors which are not predictable by a two-dish array.

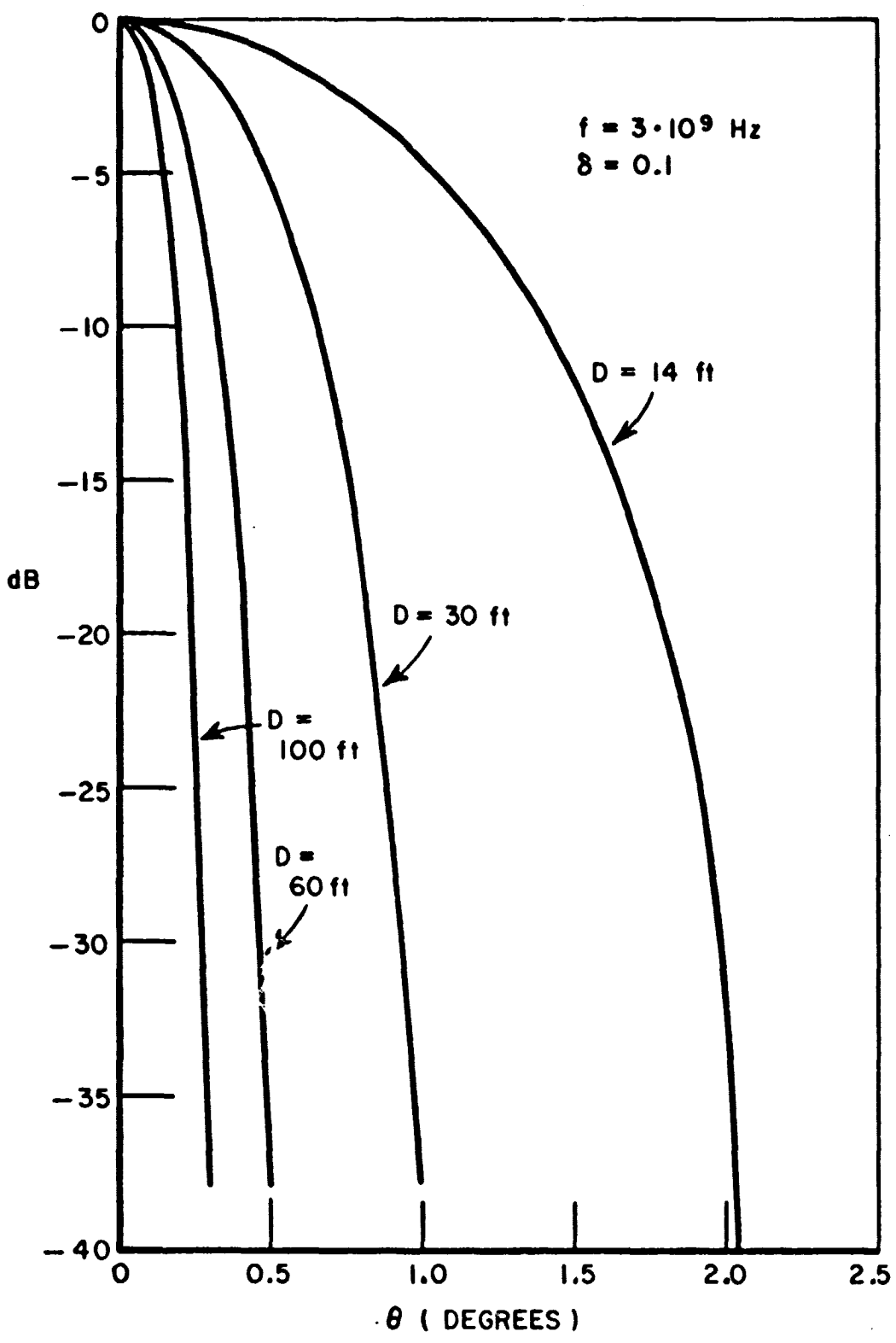

Fig. B-10. Parabolic antenna pattern vs angle θ for various aperture size D.

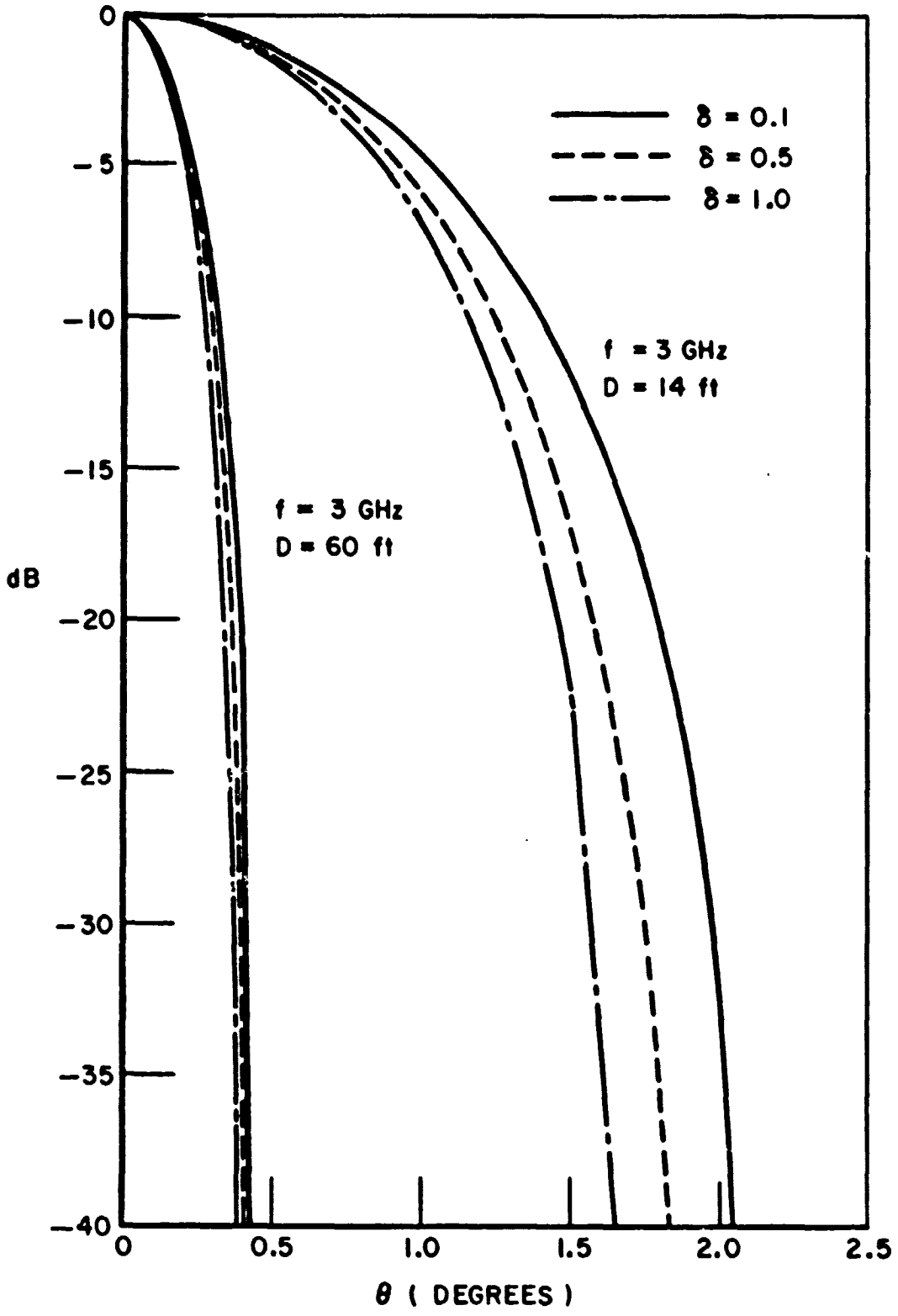

Fig. B-11. Parabolic antenna pattern vs angle θ for various aperture size D and tapered illumination factor δ.

It is hoped that through this study it may draw some criterion which governs the optimum performance of a closely spaced linear array of antennas of reflector type with element spacing, element aperture size, and scanning angle as parameter. The techniques thus established in this study may also be extended to treat a linear planar array of reflector antennas.

REFERENCES

B-1 Private Communication of work done by the Andrews Corporation, Chicago, Illinois for the Collins Radio Corporation.

B-2. Private Communication from J. Reiche, Hughes Aircraft Company, Culver City, California as an Inderdepartmental Correspondence.

C. A PHASED ARRAY OF SMALL CLOSELY SPACED ELEMENTS ORGANIZED INTO SUBAPERTURES

1) Introduction

Although the present state-of-the-art in extremely large phased arrays, especially at S-band, is behind that for large dishes, there is no fundamental reason that limits the size of an array except the questions of signal to noise ratio, availability of low loss transmission line, and the basic cost of the individual components. At present these questions concerned with the fundamentals of organization versus economics is one of the problems to which this program has been addressed during its entirety. There will be more discussion of this point at a later date after some of the results obtained in the section can be analyzed and compared with the corresponding results from the other types of antenna systems. These problems coupled with the practical problems of distribution and feeding techniques, element type, and scanning techniques require some special consideration when the array is divided into an appropriate number of subapertures. It is the purpose of this report to delineate some of the studies and to present the information that has been uncovered in the area of phase array technology which must be advanced to make such an array feasible for the DSCS program. An additional purpose is to relate the problem areas of various phased array techniques and to establish avenues for the solution in each of the problem areas to have the highest probability of success.

An important consideration in the design of such a large array is how the system should be organized; i.e., how the individual elements should be combined, phase shifted and detected to obtain the required specifications at the minimum cost. In order to quantitatively study this problem and obtain some numerical results, a dense array of dipoles over a ground plane was chosen as a receiving antenna model; this choice of a model was made partly because it could be analyzed rather easily and partly because it represents a practical high gain element which could be economically mass produced by depositing or photoetching techniques. All the calculations reported here were made for uniform distribution broadside condition (equal amplitude and constant phase) and linear polarization. Phase shifters were included in the models, however, so that the results could validly be extended to the beam steering mode of operation and used for problems in adaptive systems.

It was assumed that for large arrays or subarrays with fixed interelement spacing the effective collecting aperture is proportional to the number of elements and, in fact, is equal to the physical array size. This assumption is verified in Appendix I. Thus an interelement spacing was fixed at $\lambda/2$ (center to center) in both directions and elevated $\lambda/4$ over a ground plane; this choice was made because it represents a model commonly used in practice, and because it avoids any spurious or grating lobes.

In order to make some quantitative evaluation of the merits of the different organization schemes some numerical values were established for the communication link. These are

Frequency	2.3 GHz
Transmitted power	50 watts
Transmitter antenna gain (30' parabolic dish with 55% aper. eff.)	44 dB
Data rate	10^6 bits/sec
Maximum bit error probability	10^{-5}
Modulation	Biphase modulation 70^o

During the course of this program, an economic analysis was developed for the array of dipoles. A computer program was written that calculates the required system cost as a function of component cost using the subarray size as a parameter. Several choices and values for each component can be analyzed simultaneously; the program determines how to construct the array with the minimum total cost and also tabulates the cost and size of the remaining possible system configurations. Of course, the results are highly dependent upon component characteristics and costs which require frequent review and update. However, the technique for this economic analysis can be easily applied at any time to new date points since the computer program is listed in its entirety in Appendix II.

2) Theoretical SNR Considerations

a) Received Signal Power - The total signal power received at the output of an antenna system is given by the one-way transmission equation:

$$(C\text{-}1) \qquad S_R = \frac{G_T P_T}{L}\left(\frac{\lambda}{4\pi R}\right)^2 G_R$$

where

S_R = signal power received G_T = transmitter antenna gain

G_R = receiver antenna gain P_T = transmitter power

λ = signal wavelength R = transmission pathlength

L = transmission losses (greater than unity)

The factor $\left(\frac{\lambda}{4\pi R}\right)^2$ is commonly called the free space loss and has a value of -264 dB at 2.3 GHz for 1 Au. The signal losses, L, included in the transmission equation comprise small losses due to inefficiency of transmitting and receiving antennas, feeds, etc., and transmission losses due to the fundamental propagation characteristics of the earth's atmosphere. The signal losses due to atmospheric attenuation, as well as those due to plasma effects during atmospheric entry and exit by high velocity vehicle are discussed elsewhere. The effective gains, G_T and G_R, of transmitter and receiver antennas, respectively, may be limited by atmospheric propagation effects as well as by practical limitations on achievable fabrication tolerances. Wavefront distortions due to atmospheric inhomogeneities across the aperture will have an effect similar to that caused by deviations in the antenna surface. The problem of illumination errors across large apertures is discussed by Bailin and Hanren (Ref. C-1).

The division of power between the carrier and the spectrum which carries useful information depends on the particular type of modulation used. For example, the biphase modulation scheme considered here yields about 10% residual carrier when the modulation swing is $\pm 70^{o}$; this represents a loss in useful signal power of only 0.5 dB. The residual carrier is used by the phase lock system to coherently combine the subarrays to produce a single array output. There are techniques available in which no carrier is required, for example the squaring loop (Ref. C-2); but since an improvement in SNR would be 0.5 dB maximum, it was felt that the more commonly used technique of locking to a carrier could be used without significantly effecting the result.

b) Received Noise Power - The signal power required at the receiver, however, is determined by the required data accuracy and by the total noise present, due both to external sources and to the receiver itself. Almost all of the noise power is contributed by three general sources; antenna noise, noise produced by lossy components, and excess noise generated in the receiver mostly by the first amplifier. Thus noise presents a fundamental limitation on system performance and can be accounted for in terms of the ideal noise limit (Ref. C-3)

$$(C\text{-}2) \qquad N_R = hf\,[1 + (e^{hf/kT} - 1)^{-1}]\,B$$

where

h = Planck's constant
f = c/λ = signal frequency
k = Boltzmann's constant
T = effective absolute temperature of the receiver
B = receiver bandwidth.

In the microwave region where kT >> hf, this expression converges to the familiar quantity kTB. For non-ideal systems detection efficiency and the additional noise contribution due both to external and internal noise sources can be included by taking T as the equivalent system noise input temperature of the receiver. This temperature is the sum of various contributions as discussed below.

b1) Antenna Temperature - The antenna noise temperature in the direction θ_o is given by (Ref. C-4)

$$(C\text{-}3) \qquad T_{ant}(\theta_o) = \frac{\sum_{i=1}^{2} \int_0^{2\pi} \int_0^{\pi} T_i(\theta')f_i(\theta',\phi')\sin\theta'\,d\theta'\,d\phi'}{\sum_{i=1}^{2} \int_0^{2\pi} \int_0^{\pi} f_i(\theta',\phi')\sin\theta'\,d\theta'\,d\phi'}$$

where $f_1(\theta',\phi')$ is the normalized antenna power pattern measured with the design polarization and $T_1(\theta)$ is the temperature of radiation impinging on the antenna with that polarization; $f_2(\theta',\phi')$ is the antenna pattern for polarization orthogonal to the design polarization and $T_2(\theta)$ is the incident radiation of the corresponding polarization. For a well designed antenna the cross polarized component contributes only a degree or two. This equation assumes that the pattern does not change significantly over the frequency band of interest; if this assumption is not valid the integration must be carried out over the frequency domain as well as the spatial domain. For an array of elements the above expression is still valid and the appropriate power pattern to be integrated is the product of the element pattern and the sub-array factor.

It is interesting to note that the effective array temperature is quite insensitive to array size when the array is looking in the zenith direction with no interference from the sun. This is due to the slowly varying form of the radiometric sky absorption temperature distribution. An expression for this distribution which has been shown to agree quite well with measurements is given by (Ref. C-5)

$$(C\text{-}4) \qquad T_{sky}(\theta) = (1 - t_o^{\sec\theta})\, T_m$$

where

t_o is the fractional transmission of atmosphere at zenith ($\theta = 0$)

T_m is the mean absorption temperature

At S-band the normal zenith temperature is about 3^oK; at 60^o from zenith it has increased to only 6^oK. Thus, the component of antenna temperature due to this type of noise for a large array is not much different than from a single dipole element. This excludes the contribution from other sources such as the sun.

b) Noise Produced by Lossy Components - The total output noise contribution from any matched network of reciprocal lossy elements is given by (Ref. C-6)

$$(C\text{-}5) \qquad T_{eff} = \sum_{i=1}^{N} T_i P_i$$

where

N = number of elements in the network

T_i = temperature in the i-th element

P_i = fraction of power received by the i-th element when unit power is sent back in the system from the output terminals

$$\left(\sum_{i=1}^{N} P_i = 1 \right)$$

Thus the effective output temperature is the sum of the contributions from each of the elements weighted by the amount of power absorbed when unit power is delivered to the network. For a single lossy element this reduces to the well known expression

$$(C\text{-}6) \qquad T_{out} = \alpha\, T_{in} + (1 - \alpha)\, T_o$$

where $(1 - \alpha)$ is the fraction of power absorbed by the element at T_o and T_{in} is the effective input temperature to the element. The loss factors for several types of transmission lines and their effects on performance are discussed in the subsection on distribution networks.

b3) Excess Noise Produced by Amplifiers - The excess noise produced by several commonly used amplifiers is shown in Table C-1 (Ref. C-7).

TABLE C-1

Ampl. type	Physical temp.	Noise temp. T_e
TWT	290^oK	400^oK
TDA	290^o	380^o
Transistor	290^o	625^o
Paramp	290^o	80^o
Paramp	20^o	20^o
Maser	5^o	$10\text{-}15^o$

The amplifier's noise figure F is related to its excess noise temperature T_e by

(C-7) $\quad T_e = (F - 1)\, T_o \quad$ where $\quad T_o = 290^ok$

c) Relationship Between SNR and Bit Error Probability - One of the most important considerations for evaluating a communication link is the bit error probability. For a given modulation and detection scheme this parameter can be related to the SNR, which is a more convenient parameter to work with. Figure C-1 shows this relationship for several coherent and noncoherent binary systems (Ref. C-8). It can be seen that for large SNR the bit error probability decreases quite rapidly. For a system utilizing binary phase shift keying (PSK), a SNR of 10 dB is adequate to assure an error probability of approximately 10^{-5}. This SNR is sufficient for both coherent and differentially coherent PSK, but not for either of the frequency shift keying (FSK) systems. Therefore, a nominal value of SNR = 10 dB was chosen for the analysis and comparison of the systems examined below.

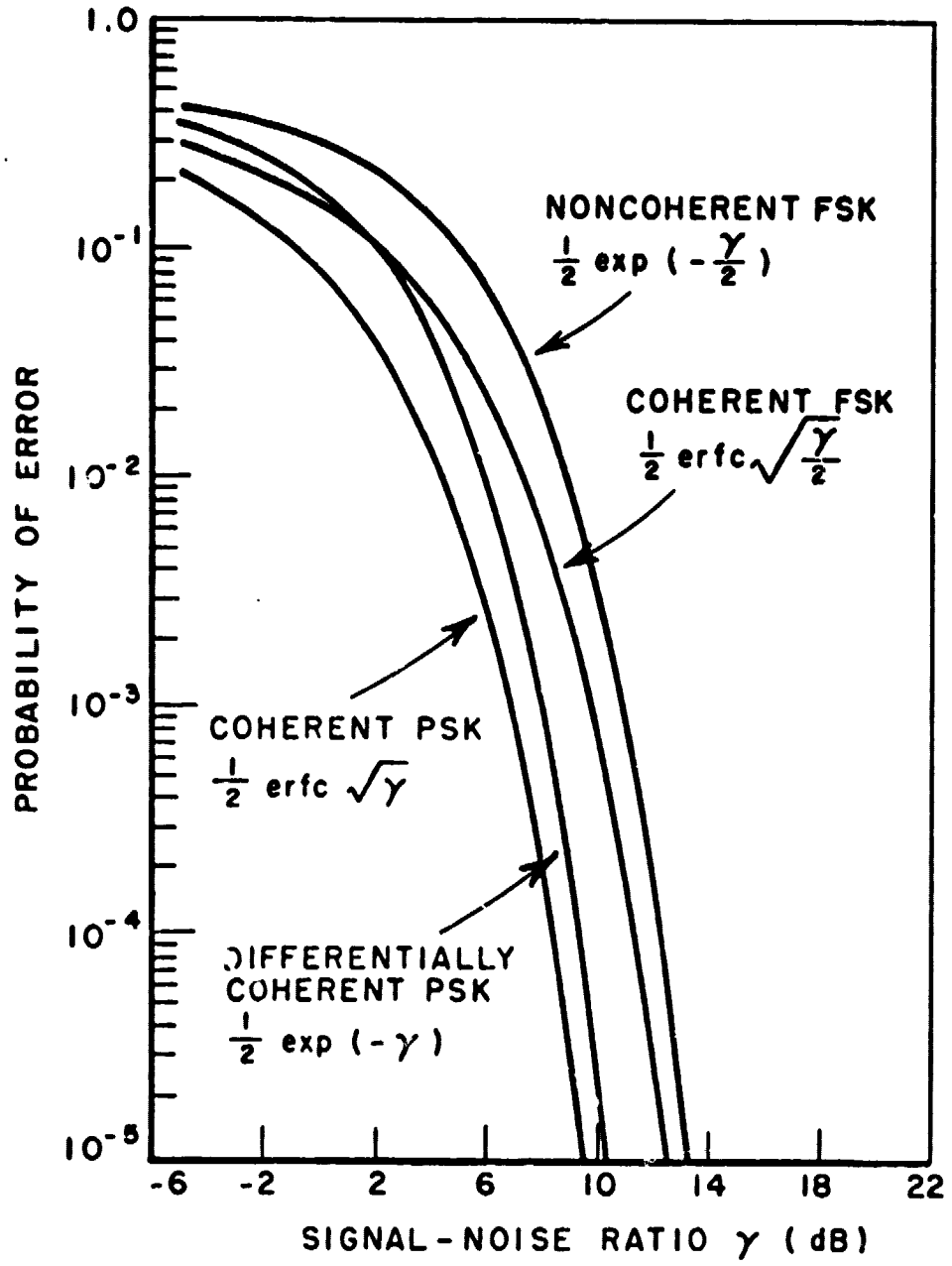

Fig. C-1. Error rates for several binary systems. (Reference C-8).

3) Predetection vs. Postdetection Combining

There are two basic ways in which the detection process can be performed. The first, as shown in Fig. C-2, consists of summing the properly adjusted IF outputs from each subarray and then detecting the resultant to obtain a series of ones and zeros at the modulation rate. The second scheme, as shown in Fig. C-3, consists of detecting the output of each subarray at the IF level and then using a majority count to make the final decision as to whether a one or a zero occurred. The first, the coherent addition scheme, will obviously be more efficient than the second, but the latter system has several advantages which merit closer

consideration; for example, the time delay can be a digital device such as a shift register. The summation is also done digitally at the base band frequency rate, rather than at IF.

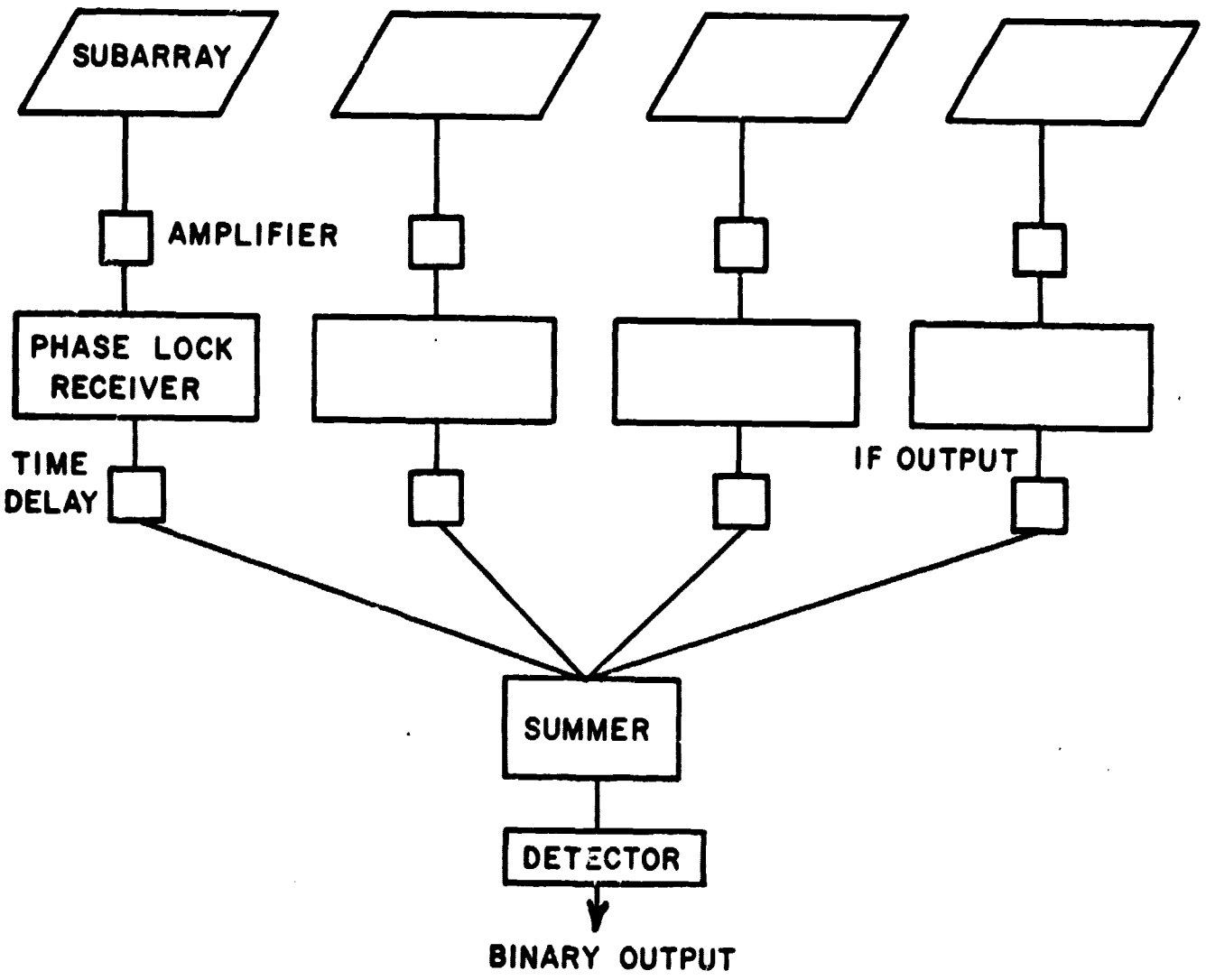

Fig. C-2. Predetection combining program.

An analysis has been done on these two schemes (Ref. C-5) which showed that for the limiting case where the SNR of each subarray is very small, but the SNR of the combined subarrays is large, the post-detection summing requires a total SNR $\pi/2$ (2 dB) greater than the predetection combining in order to produce the same bit error probability. Since this establishes the relationship between the two processes the remainder of this report will be concerned with coherent predetection combining system.

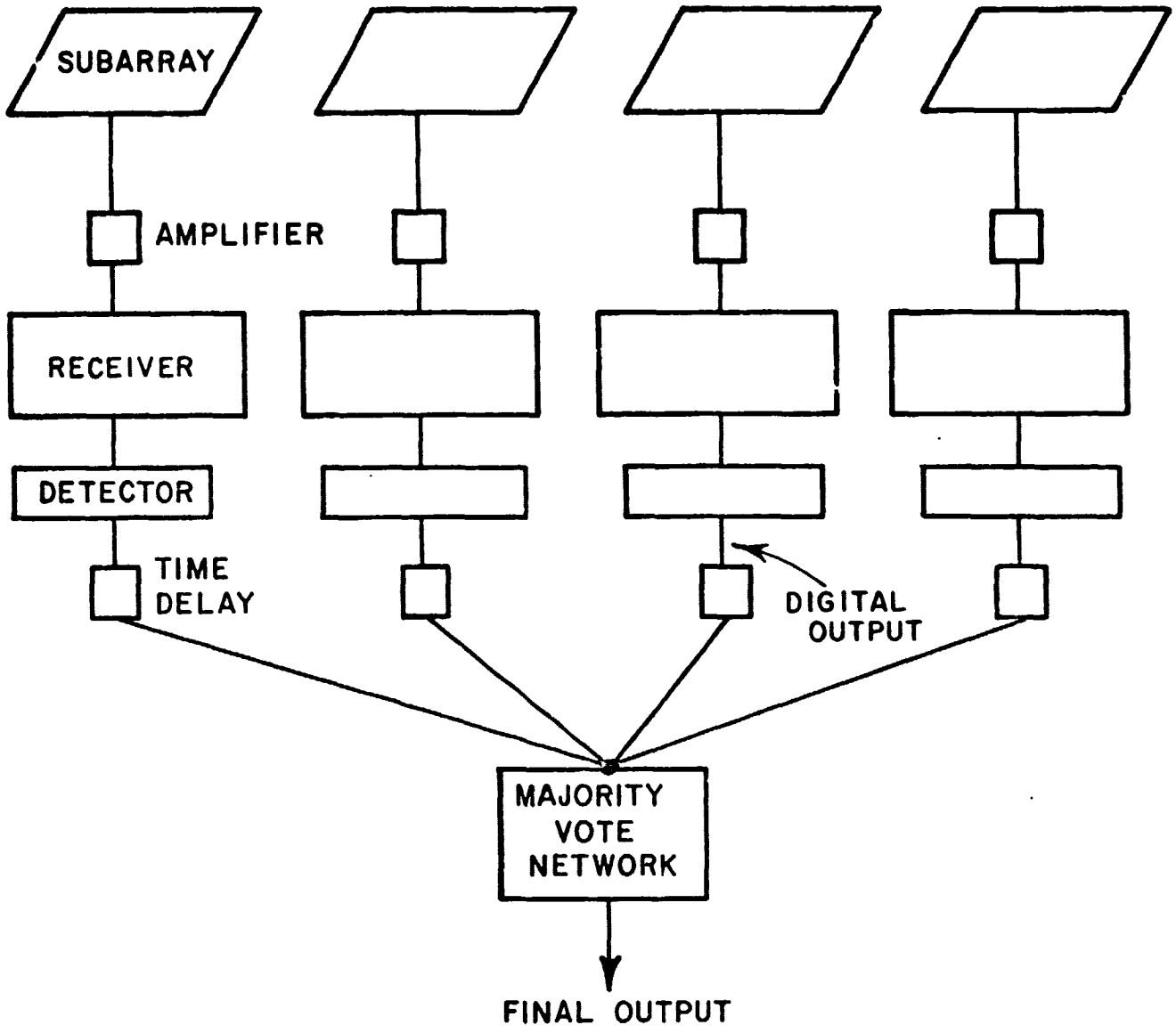

Fig. C-3. Postdetection combining diagram.

4) Array-Subarray Organization

The subarray model consists of dipole elements which are phase shifted and combined to form a single output at the RF frequency. Due to the relatively large beamwidth of a single subarray, it is expected that the proper phase adjustment can be performed with a special purpose computer using a priori knowledge of the source location.

The number of elements required to achieve the specified 10 dB SNR will, in general, be a function of the phase shifter loss and temperature, feed line losses, amplifier noise temperature, and subarray size.

a) Maximum Subarray Size If phase control is used for combining, rather than time delay compensation, the total time delay across the subarray must be less than the modulation period in order that each element simultaneously receives the same information bit. For an information rate of 10^6 bits per second this time delay must be much less than 1μ sec, which limits the maximum subarray size to about 30 meters (1μ sec has spatial length of 300 meters) if the system is required to operate at low elevation angles. This does not represent a stringent limitation; for the antenna model considered here a subarrray of this size would contain about 200,000 elements.

b) Minimum Subarray Size For any adaptive scheme each subarray must produce a SNR which is sufficient to lock on the signal during the acquisition mode and maintain lock during the information transfer mode. For a typical phase lock system using coherent addition the following equations can be used to obtain a comparison between different organizational parameters:

$$(C\text{-}8) \qquad SNR_{TOT} = N \cdot SNR_{SA} = 10$$

$$(C\text{-}9) \qquad CNR_{PLL} = K \cdot SNR_{SA} \frac{B_{IF}}{B_{PLL}}$$

where

SNR_{TOT} = total numeric signal-to-noise power ratio taken to be 10 in order to produce a bit error probability of 10^{-5}

N = number of subarrays

CNR_{PLL} = carrier to noise ratio in the phase lock loop of each subarray receiver

K = fraction of power transmitted at the carrier frequency

B_{IF} = bandwidth of the IF, taken to be 0.5×10^6 Hz to receive 10^6 bits/sec using matched integrate and dump detection

B_{PLL} = bandwidth of phase lock loop, taken to be 10 Hz.

During the acquisition time all the power can be transmitted at the carrier frequency ($K = 1$) so that

$$(C\text{-}10) \qquad CNR_{PLL} = SNR_{SA} \frac{B_{IF}}{B_{PLL}} = \frac{10^6}{2N}$$

From experience (Ref. C-9,10), it has been shown that about 6-7 dB CNR_{PLL} is required for acquisition; using this criteria and the above constants yields the minimum SNR_{SA} = -40 dB to obtain lock. However, during normal operation of this subarray, when most of the power is contained in the modulation components, the CNR_{PLL} would drop to -3 dB which is not sufficient to maintain phase lock. Hence the actual minimum SNR_{SA} is not set by the acquisitior requirement but rather by having to maintain lock during the signaling. Requiring a 3 dB SNR_{SA} during normal operation constrains the minimum SNR_{SA} to be -34 dB.

c) Feeding Techniques Two types of feed systems were considered; the commonly used modified series-series shown in Fig. C-4 and the equal length corporate feed shown in Fig. C-5. The effective noise temperature and SNR at the subarray output are now calculated for both feeding systems.

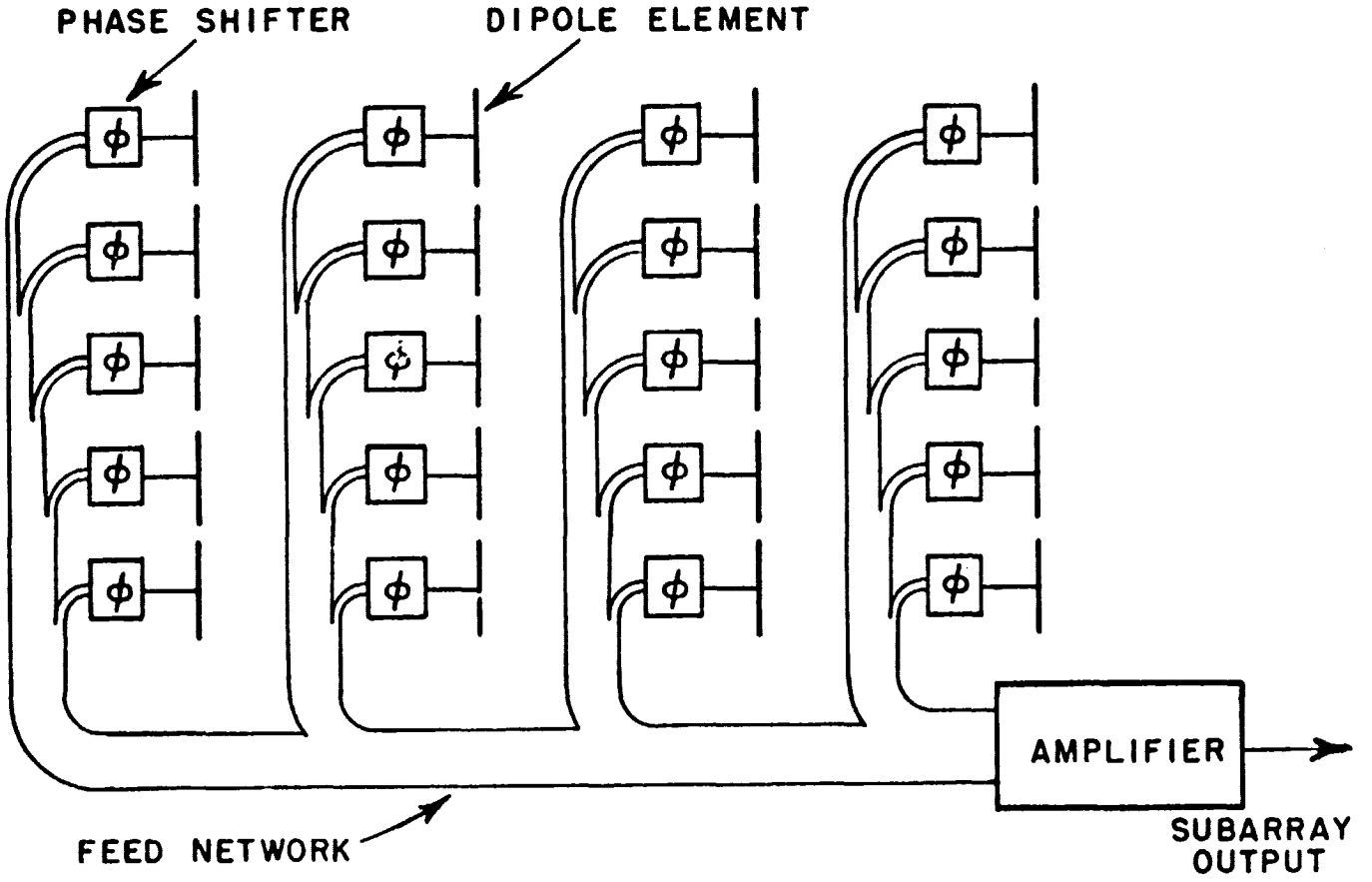

Fig. C-4. Series-series feed system.

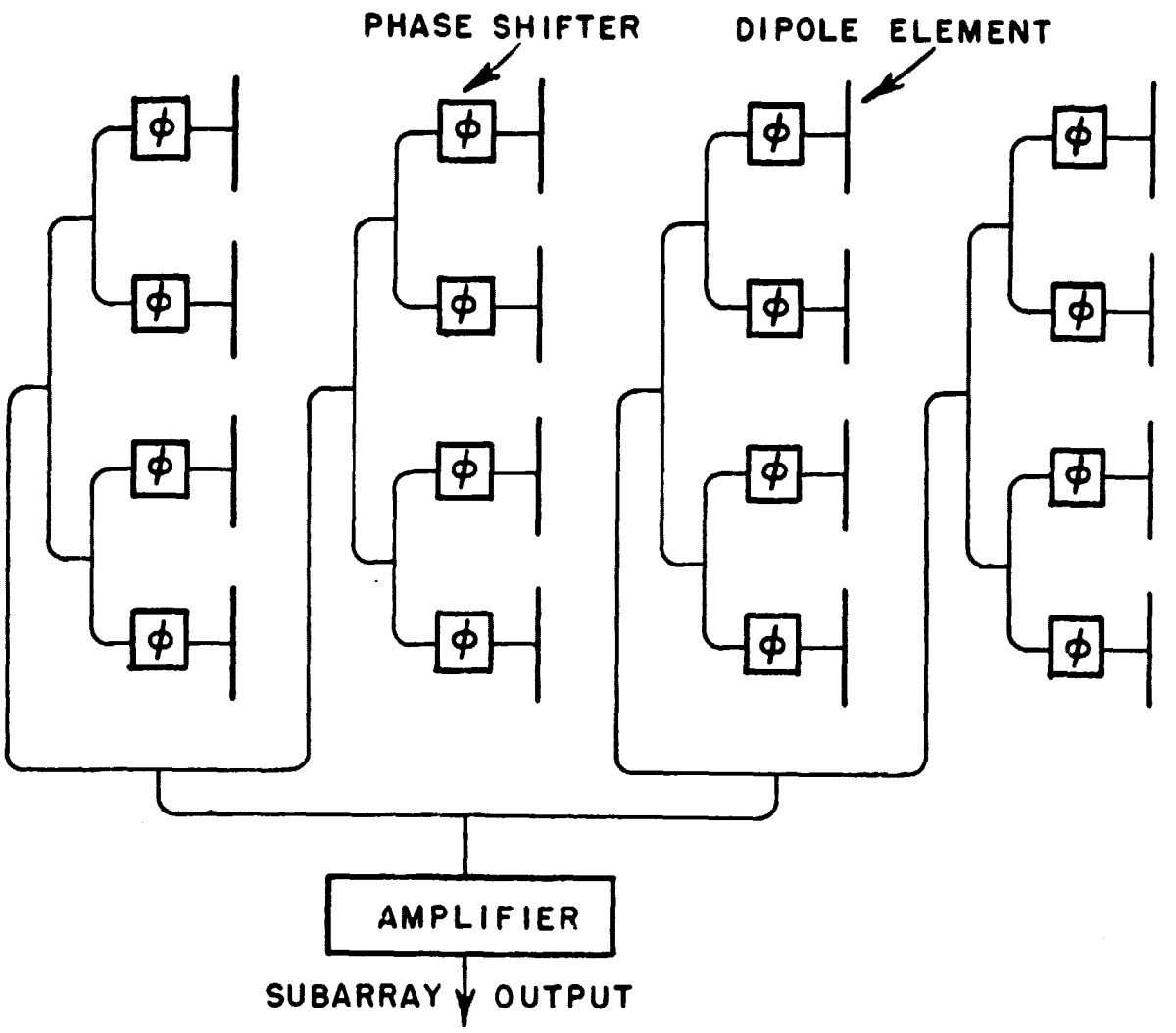

Fig. C-5. Equal length corporate feed system.

Series-series model - Consider an arbitrary unit of power delivered to this subarray (Fig. C-4). The fraction of power delivered to the phase shifters is

$$\Gamma = \frac{\alpha}{N^2}\left(\sum_{n=1}^{N} \alpha^{n-1}\right)^2 \qquad \text{(C-11)}$$

where

N^2 = number of elements in the subarray

α = transmission coefficient for a $\lambda/2$ section of the feed line.

Hence the fraction of power absorbed by the feed system is $1 - \Gamma$. The fraction absorbed by the phase shifters is $(1 - \alpha_\phi)\Gamma$, where α_ϕ is the transmission coefficient of the phase shifters, and the fraction of power which is delivered to the dipole antennas is $\alpha_\phi \Gamma$.

Finally, the expression for the total effective noise temperature of the subarray is

$$(C\text{-}12) \qquad T_{eff} = [1 - \Gamma]\, T_o + T_\phi\, [1 - \alpha_\phi]\Gamma + T_a\, \alpha_\phi \Gamma + T_{amp}$$

where

T_o = physical temperature of the feed structure assumed constant at 290^oK

T_ϕ = physical temperature of the phase shifters

T_a = antenna temperature = 9^oK for the dipole model

T_{amp} = effective amplifier noise temperature.

For a transmitted power of 50 watts and a thirty-foot transmit antenna two Au from the array the resulting expresion for the subarray SNR in dB is

$$(C\text{-}13) \qquad SNR_{SA} = -144 - PSLDB + 10 \log_{10} N^2 - 10 \log_{10} \frac{1}{\Gamma}$$

$$-10 \log_{10}(k\, T_{eff}\, B)$$

where

PSLDB = phase shifter loss in dB

k = Boltzmann constant

B = bandwidth = 0.5×10^6 Hz

Equal length corporate model A similar analysis yields the effective temperature for this subarray model:

$$(C\text{-}14) \qquad T_{eff} = LT_\phi + L_\phi\, [T_a - T_\phi] + [1\text{-}L]\, T_o + T_{amp}$$

where

$$L = \exp[-2.3LDB/10]$$

$$LDB = LPF(\lambda/2)\left[2\log_2 N + \sum_{i=0}^{\log_2(N-1)} 2^i\right]$$

LPF = Attenuation of the feed in dB per foot

The resulting SNR in dB at the subarray is:

$$(C\text{-}15) \qquad SNR = -144 - LDB - PSLDB + 10\log_{10}N^2 - 10\log_{10}[k\,T_{eff}B]$$

As shown in the numerical results the equal length system is slightly less efficient than the series-series system; it has the advantage of not requiring any phase shifting devices if the subarray panels are to be mechanically pointed.

5) Numerical Results of System Analyses

This subsection contains some typical results obtained for various subarray organizational models of a large aperture. These numerical results were obtained from a system analysis of previous subsections using typical values for the key parameters and a computer program of the appropriate equations.

Figures C-6 and C-7 present the subarray performance for the two feeding models utilizing stripline and waveguide and lossless feeds. The important range of subarray SNR loss is between -20 and -30 dB which corresponds to 10^3 and 10^4 subarrays in order to satisfy the 10 dB SNR for the communication link. It can be noted in Fig. C-7 presenting the performance for 4 Au, that an increase in the number of elements will not improve SNR beyond a certain point if stripline is used. In contrast the waveguide fed subarray improved its SNR proportionally to the number of elements almost as well as a lossless feeding system.

Figures C-8 and C-9 describe the effect of phase shifter loss for various feed loss parameters. Note that the use of phase shifters incurring 0.5 dB of loss may require twice as many elements as would be needed for lossless phase shifters. For the case of stripline feeds that are quite lossy the increase in required number of elements is not as sensitive to phase shifter loss.

Figures C-10 and C-11 present the array performance as a function of amplifier temperature. Note the linear variation of SNR with the number of elements. This linearity is due to the lack of build up with increased number of elements which occurs with feed lines. For large values of amplifier temperature where its effect is dominant the SNR declined, as expected, linearly with amplifier temperature.

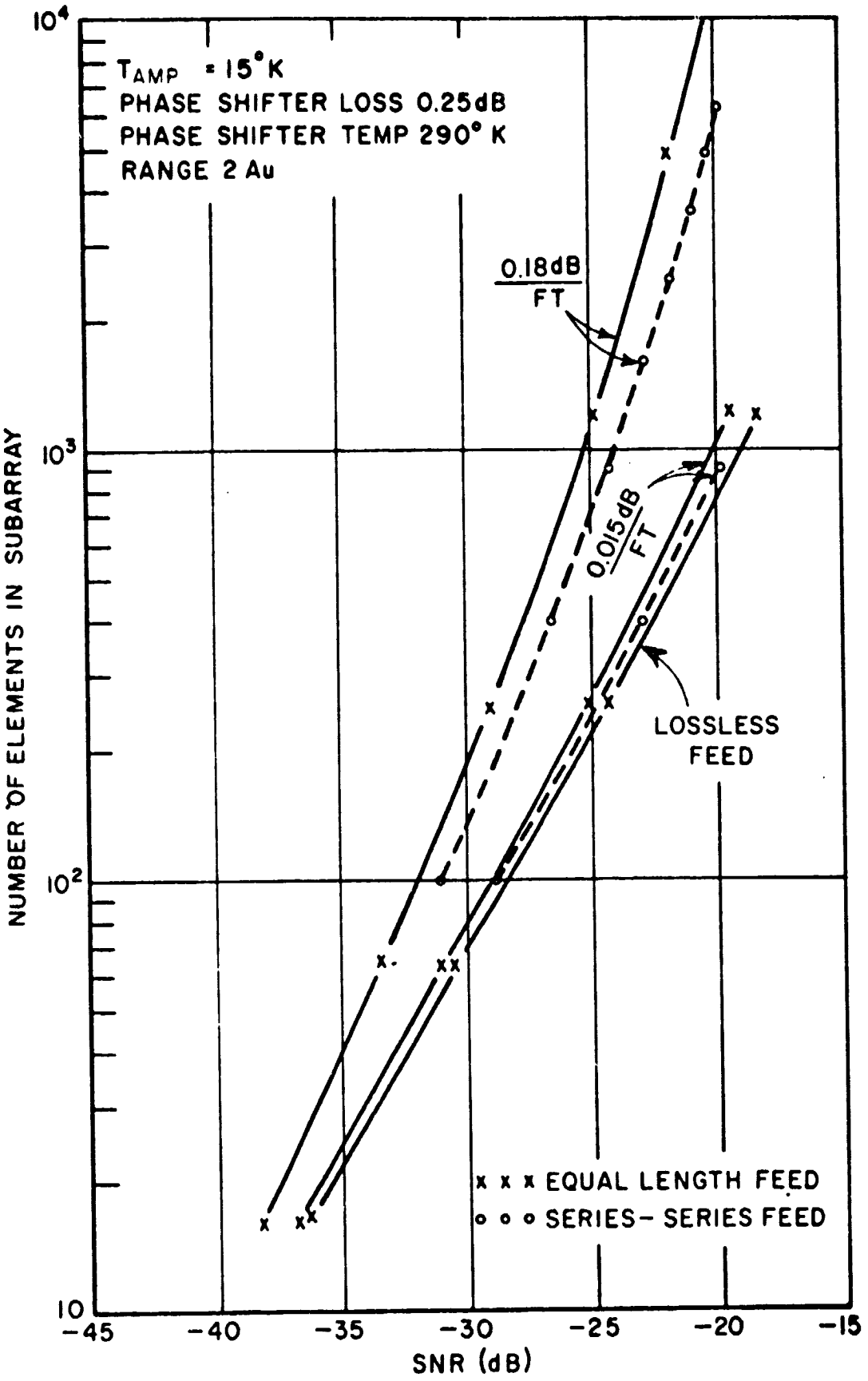

Fig. C-6. Subarray size vs SNR as a function of feeding model and loss.

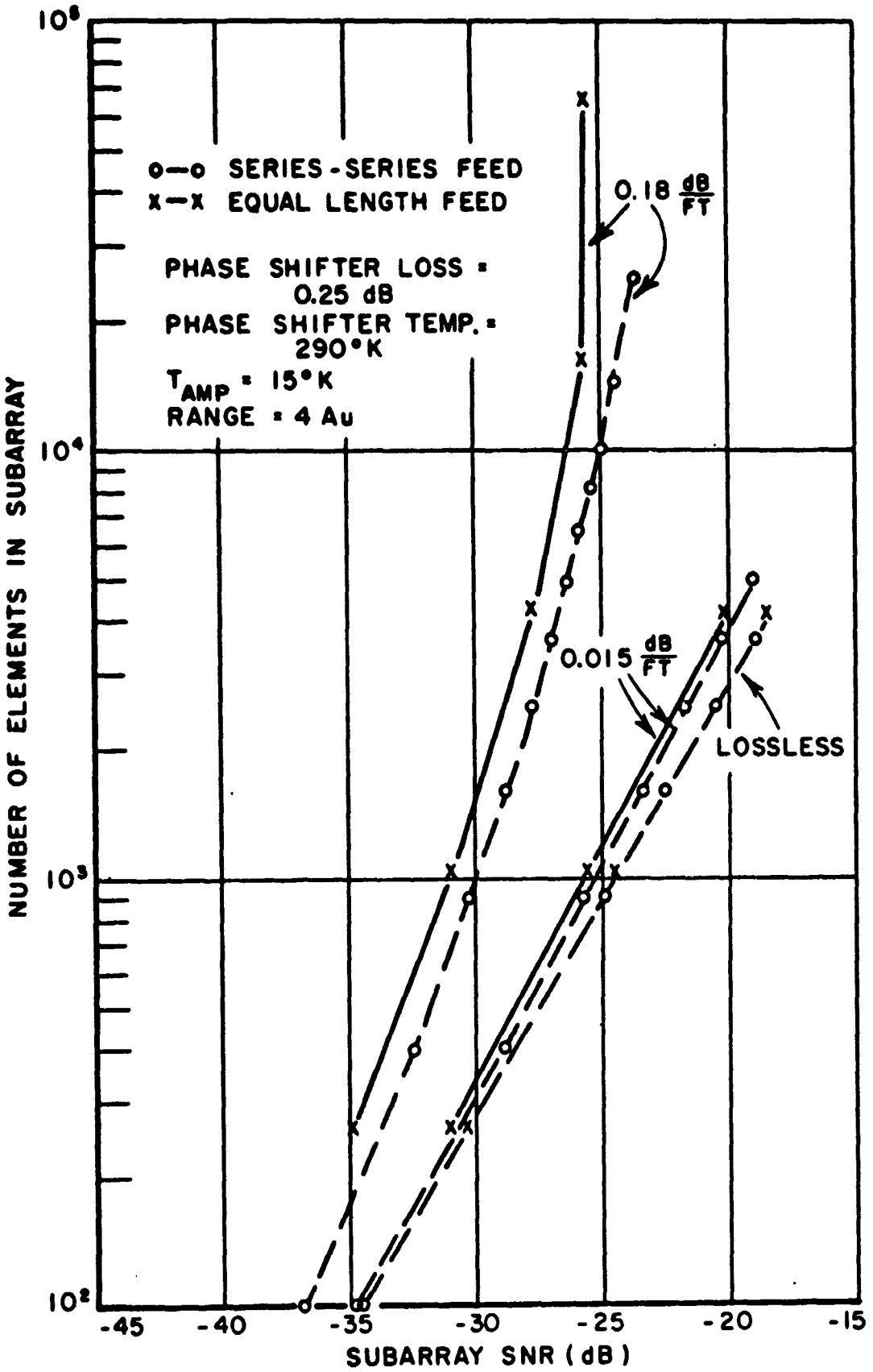

Fig. C-7. Subarray size vs. SNR as a function of feeding model and loss.

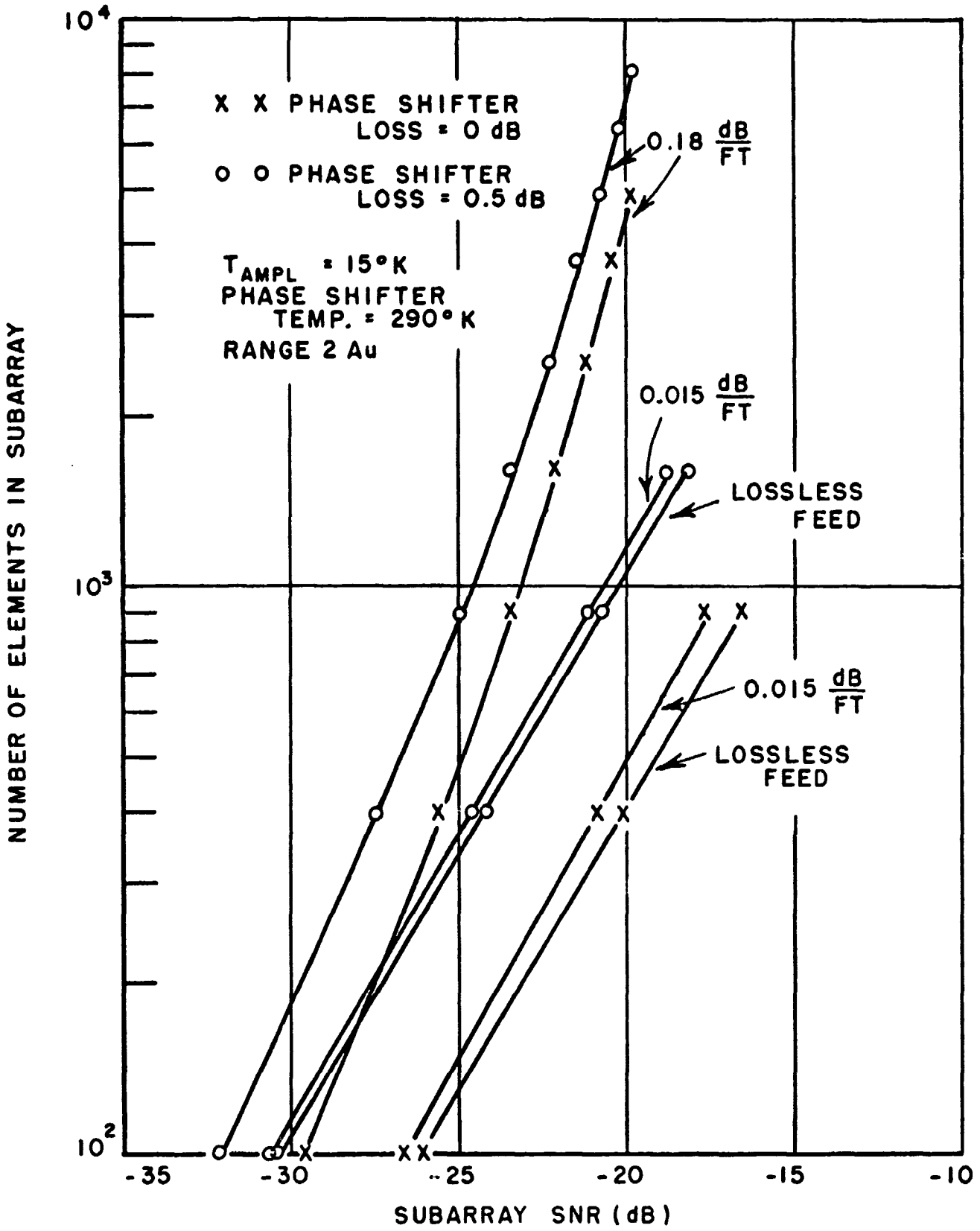

Fig. C-8. Subarray size vs SNR as a function of phase shifter loss.

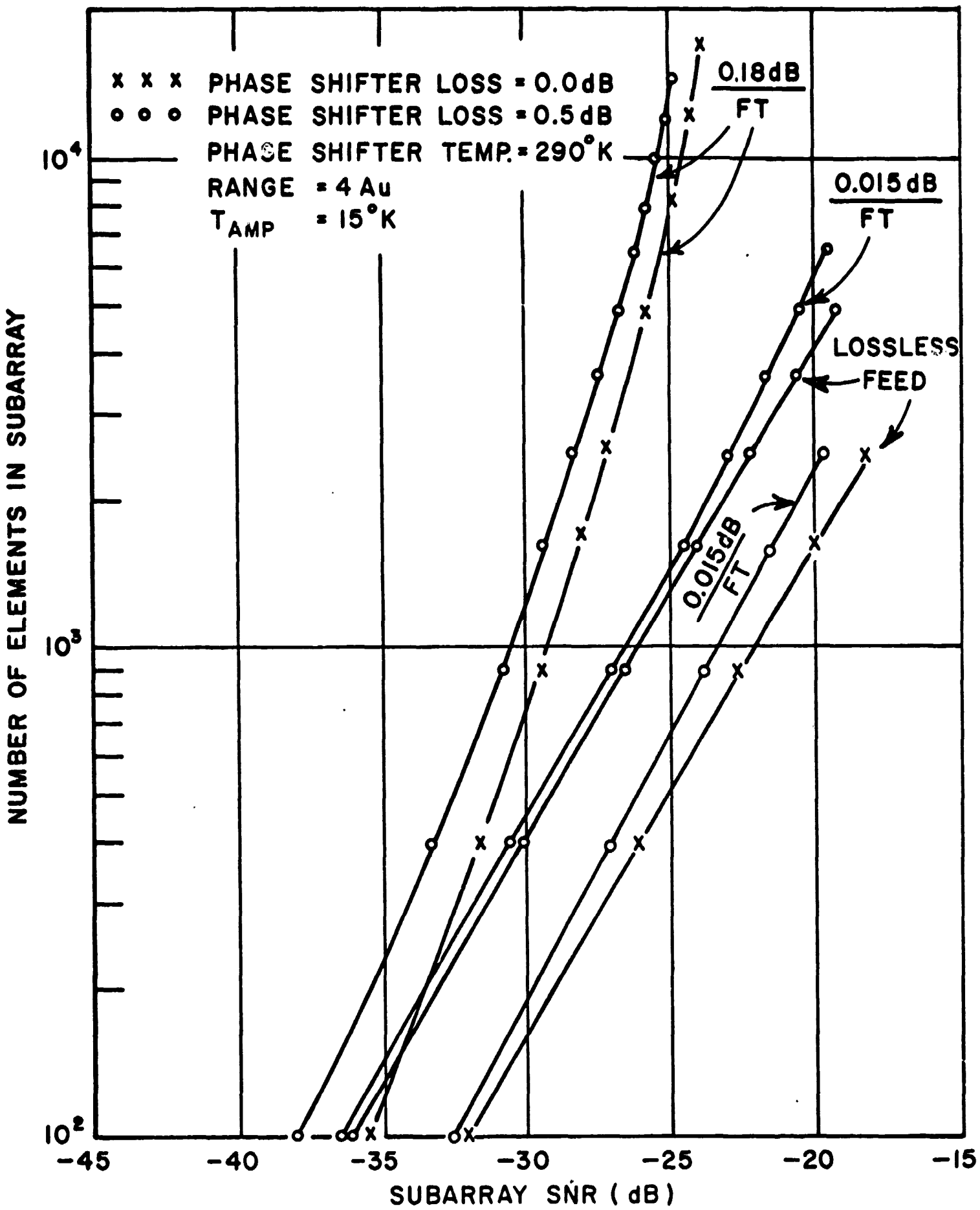

Fig. C-9. Subarray size vs SNR as a function of phase shifter loss.

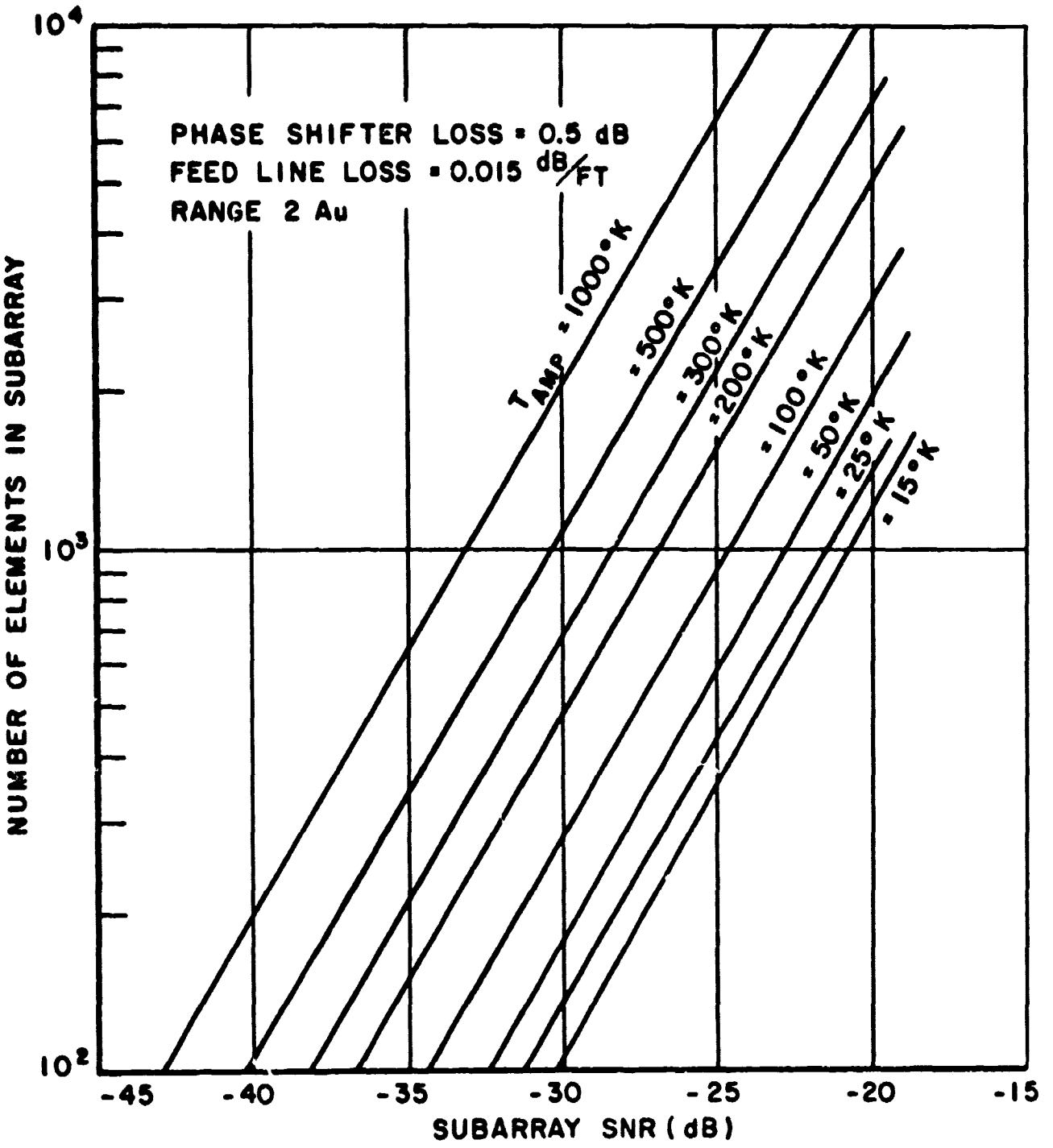

Fig. C-10. Subarray size vs SNR for various values of amplifier noise temperature.

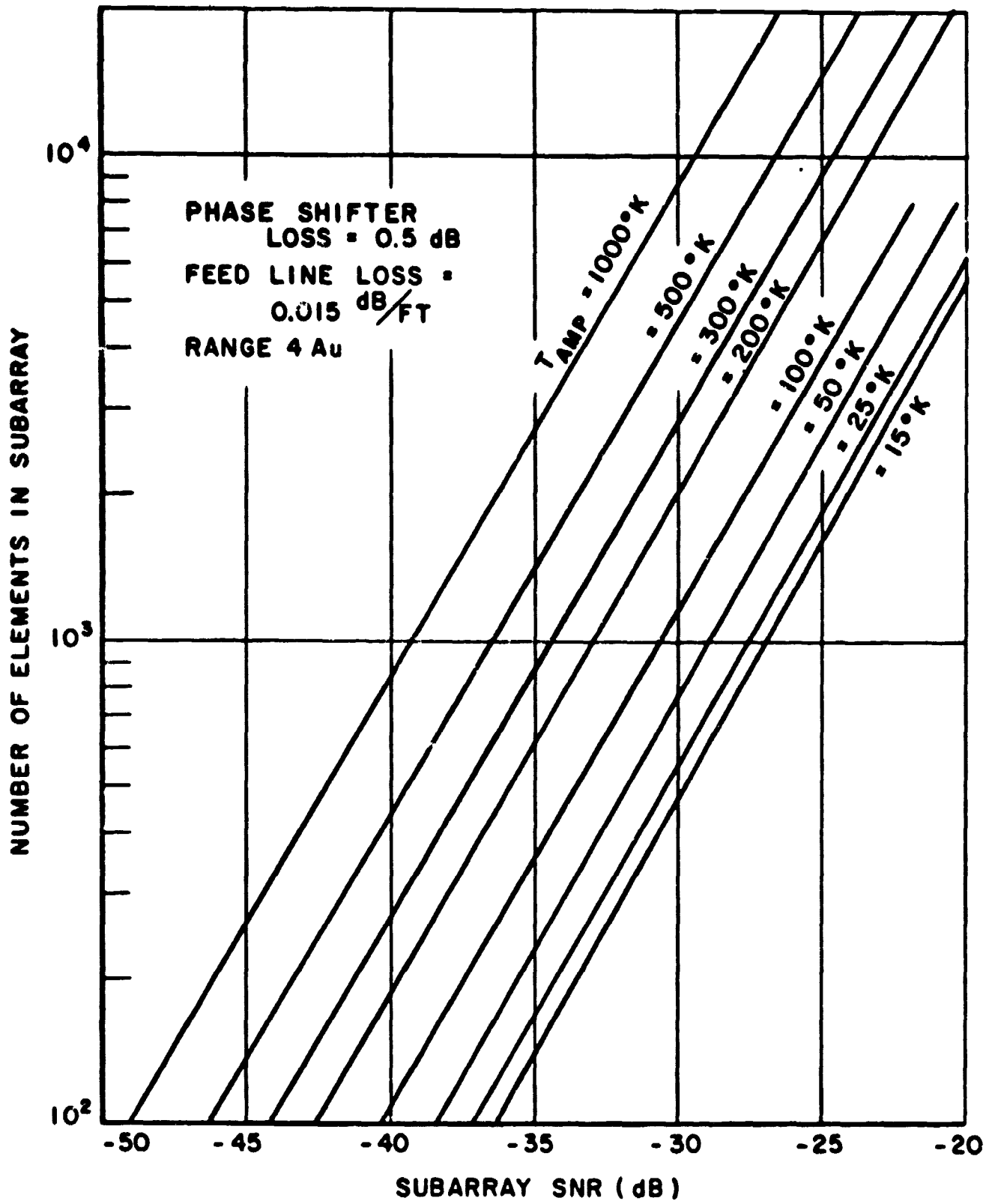

Fig. C-11. Subarray size vs SNR for various values of amplifier noise temperature.

Figure C-12 presents the functional relationship between the number of subarrays and subarray SNR required to satisfy a 10^{-5} bit error probability for the communication system.

Some of the graphical results in this section have been condensed in Table II. This shows some of the tradeoffs involved in selecting the system parameters. For example it is not possible to use a stripline feed system at 4 Au for 0.25 dB phase shifter loss using 1000 subarrays, even with the best maser amplifiers; however this system will be possible if 10,000 subarrays are permitted, in fact the maser may be replaced by an amplifier which has 4 times more noise. Using the larger number of subarrays means the size of a single subarray can be smaller and the cumulative effect of feed loss is not as great as with a larger subarray.

6) System Cost Analysis

The cost analysis of this receiving array model is quite difficult due to the large number of parameters involved; moreover these parameters interact in a non-linear manner. For example as the aperture size is doubled the SNR does not double due to an increase in the feed line attenuation and the related thermal noise contribution.

Once the theoretical analysis has been performed it is not difficult to generate a large number of graphs comparing the system performance and cost as the different parameters are varied; for example see Figs. C-13 to C-16. This type of study is hard to interpret simply due to the large number of curves necessary. A more desirable approach used here was to arrange this multiparameter problem into a format in which a computer could be utilized to compare and analyze a large number of cases and present the reduced results in a manner which could be readily used.

The computer program is listed in Appendix II. It requires input data for the following parameters:

1. Range in Au
2. Data Rate
3. Phase shifter loss and cost
4. Feed line loss and cost
5. Amplifier temperature and cost
6. Number of subarrays desired
7. Element cost

The first two input data remain fixed during a given computer run. The last five component and system characteristics represent the parameters to be varied; several values of each may be entered to determine the variation of the total array size and cost with that parameter.

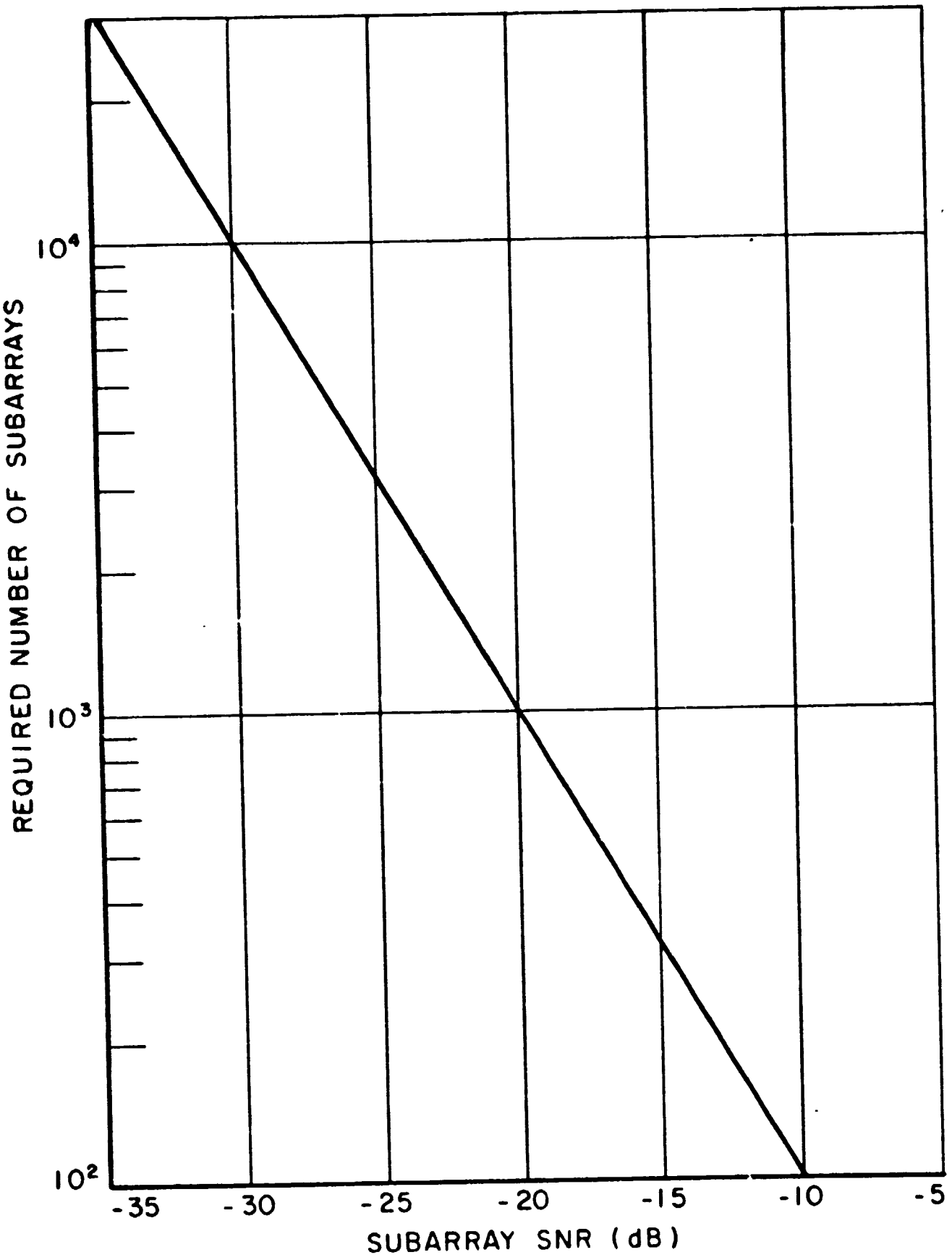

Fig. C-12. Required number of subarrays vs subarray SNR.

TABLE C-II
REQUIRED APERTURE SIZE TO PRODUCE 10 dB SNR

	Feed line loss	Phase shifter loss	Amplifier noise temperature	Number of subarrays	Required aperture - meters^2 For 2 Au	Required aperture - meters^2 For 4 Au
A. Parabolic dish (70% aperture efficiency) using 15°K maser					2,560 (190 ft. diameter)	10,240 (380 ft. diameter)
B. Dense array of dipoles over a ground plane						
loss-less	0 dB/ft	0 dB	15°	------	1,800	7,200
wave-guide	0.015	0	15	1,000	2,100	10,000
	0.015	0.25	15	10,000	3,380	13,300
	0.015	0.25	15	1,000	3,800	16,500
	0.015	0.50	15	1,000	5,000	23,200
	0.015	0.50	50	1,000	7,600	32,000
	0.015	0.50	100	1,000	11,800	48,500
	0.015	0.50	.500	1,000	47,000	185,000
strip-line	0.18	0	15	1,000	20,000	
	0.18	0.25	15	1,000	25,400	
	0.18	0.25	50	10,000	10,500	67,500
	0.18	0.50	15	1,000	32,000	
	0.18	0.50	50	10,000	12,500	84,500

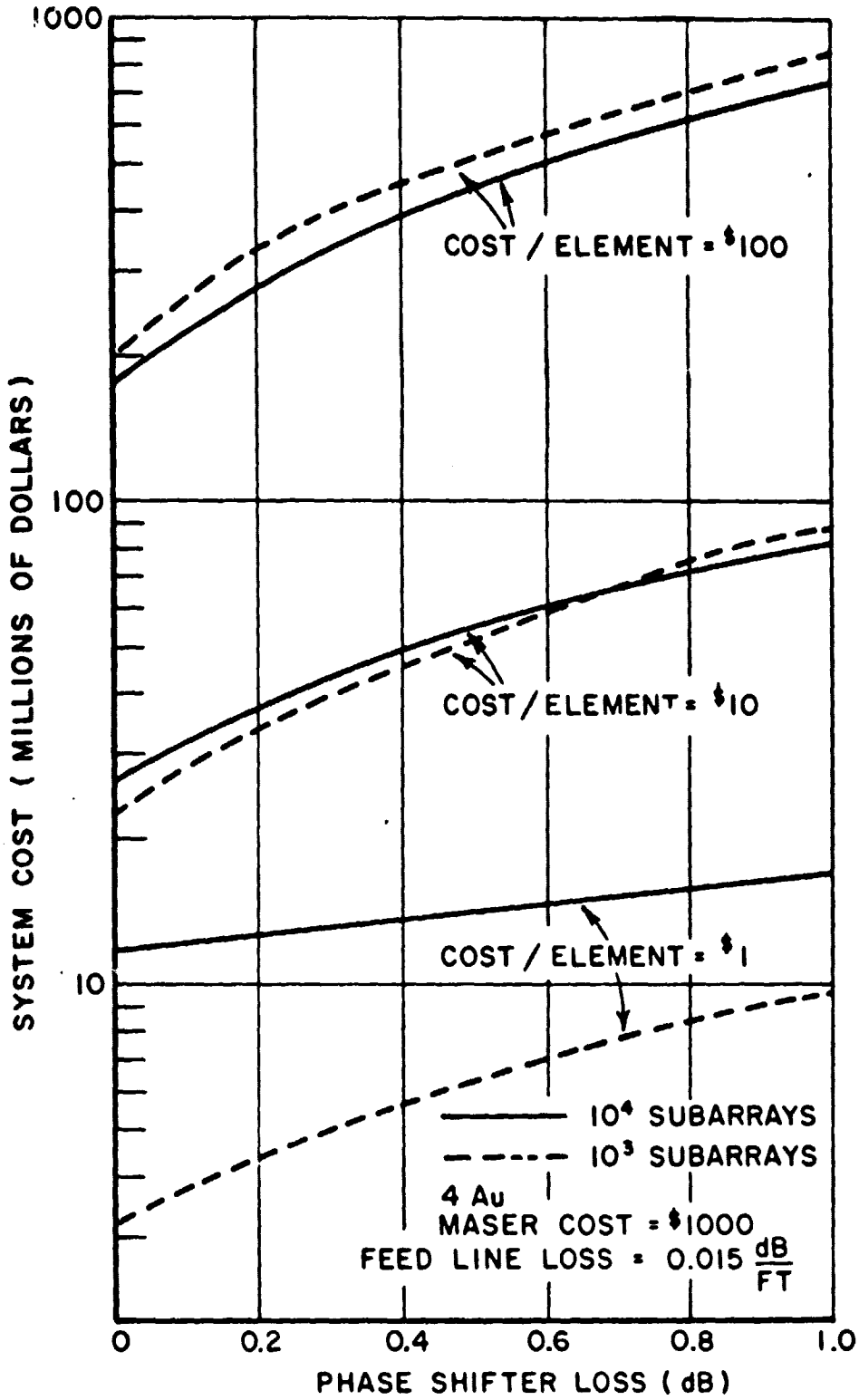

Fig. C-13. System cost vs phase shifter loss.

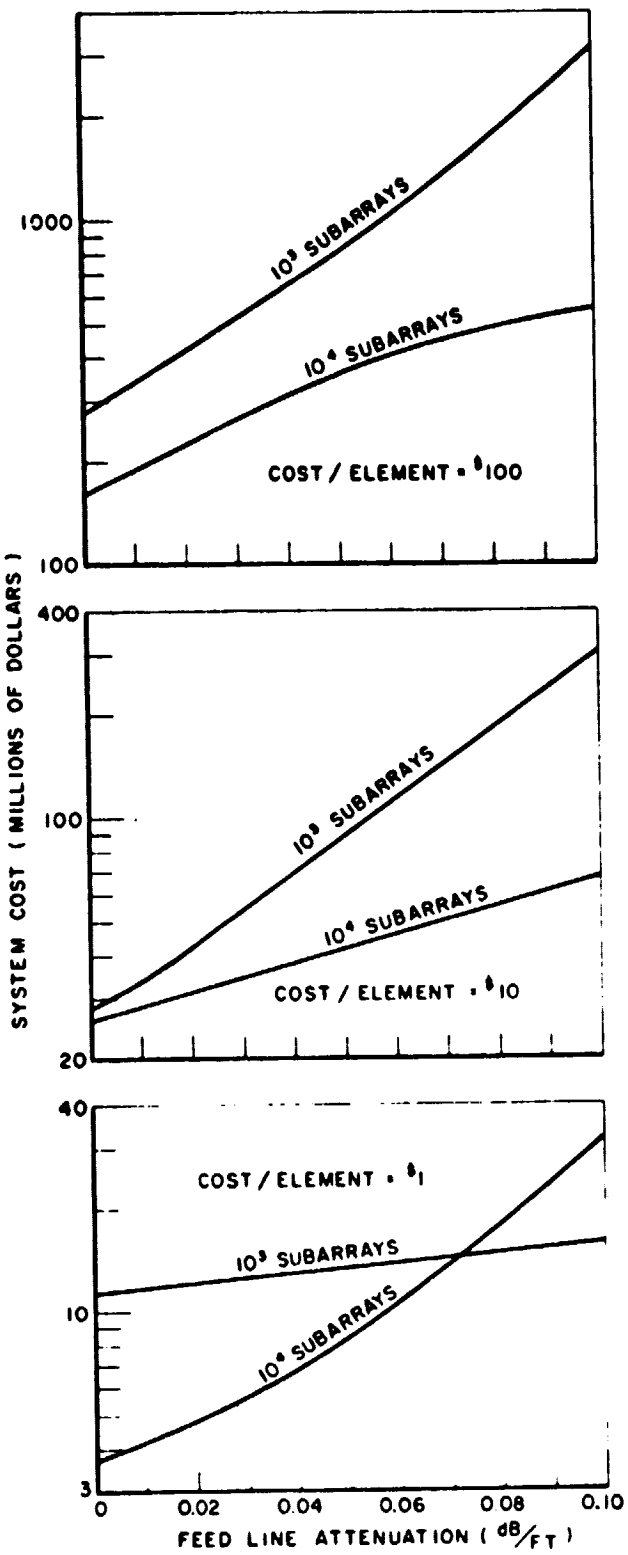

Fig. C-14. System cost vs attenuation of feed line. Computed for 4Au, Maser cost = $1000, 0.25 dB phase shifter loss.

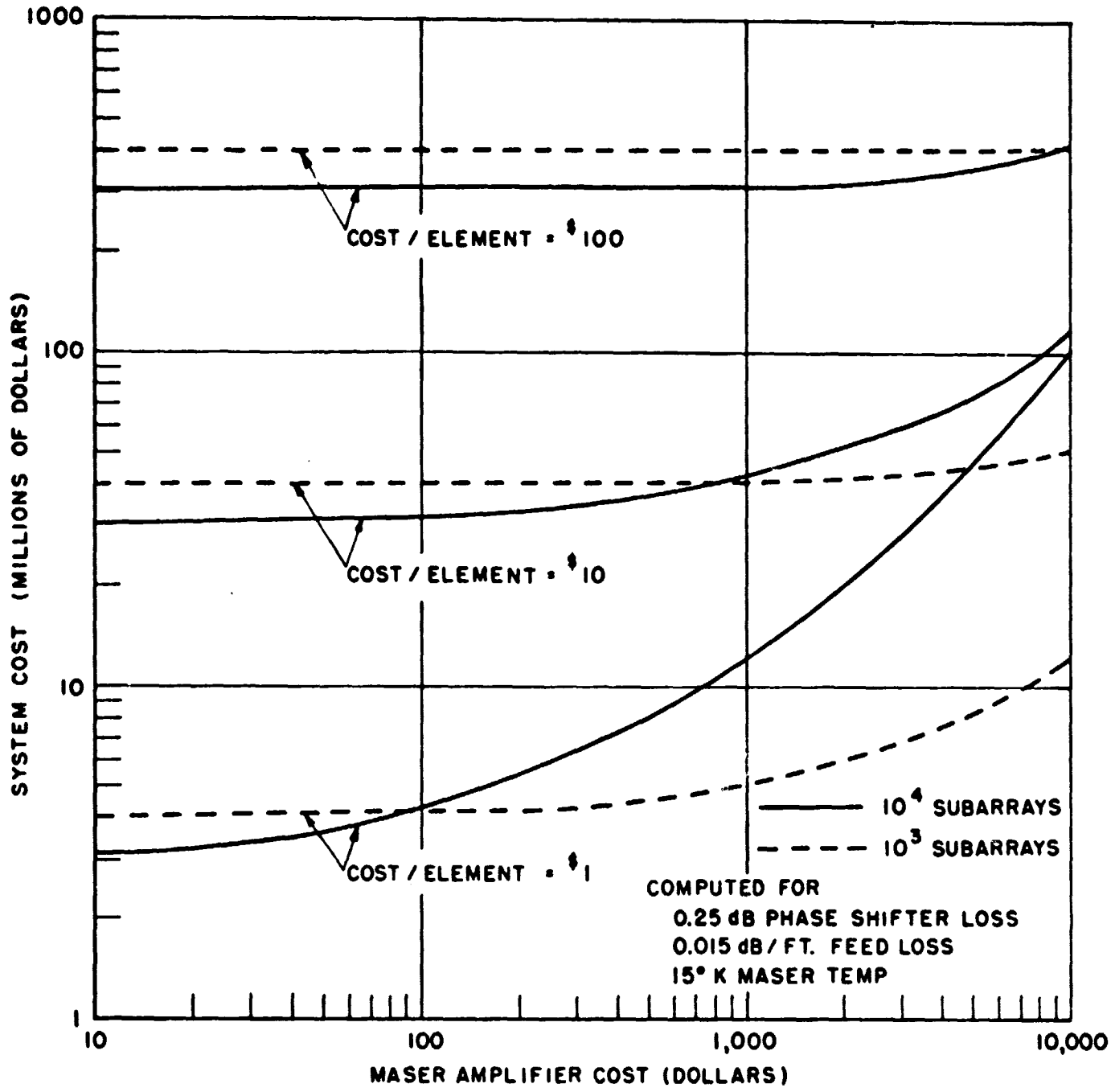

Fig. C-15. System cost vs maser amplifier cost.

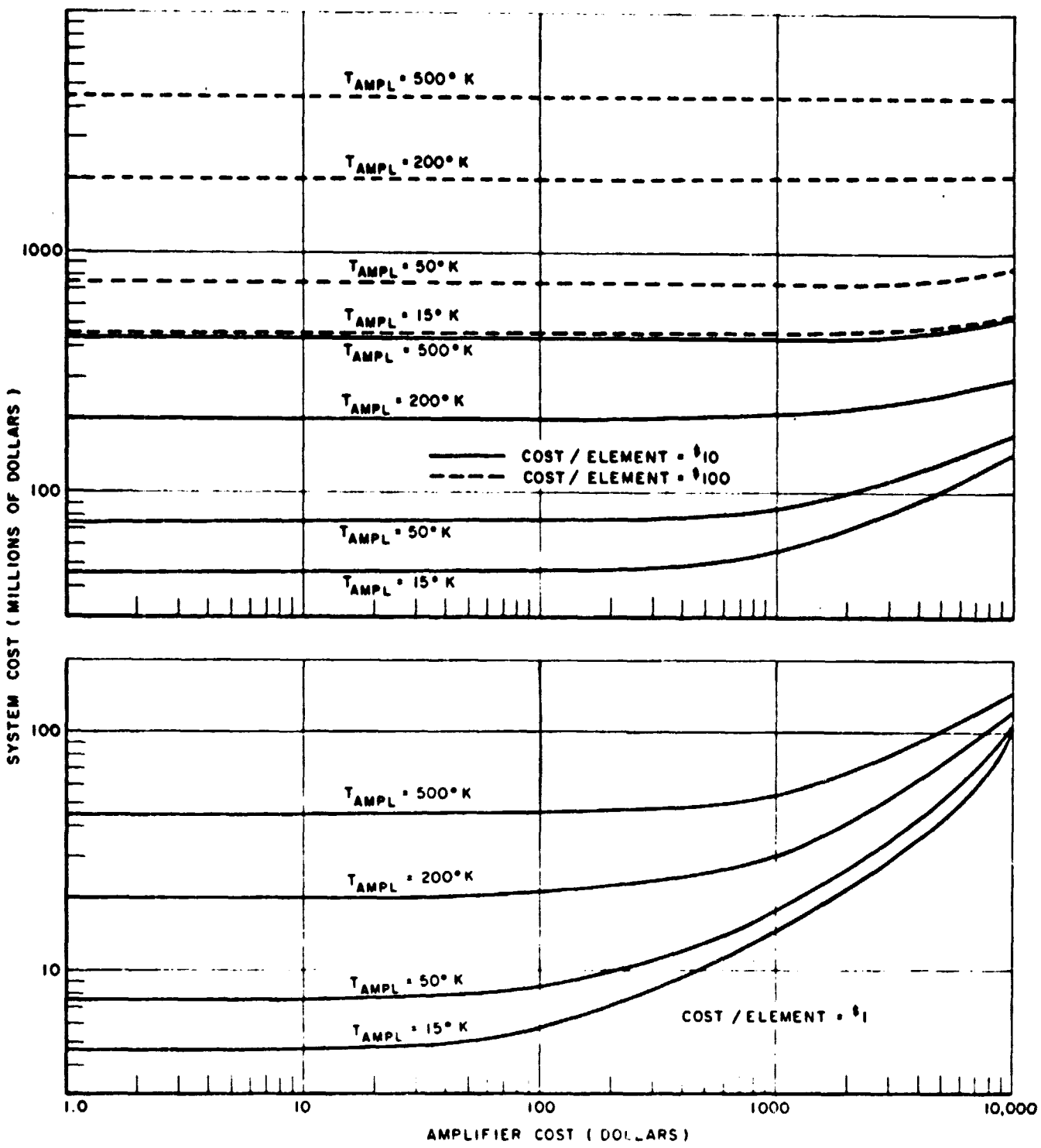

Fig. C-16. System cost vs subarray amplifier cost for various amplifier noise temperatures. Computed for 4Au, 0.5 dB phase shifter loss, .015 dB/feet feed loss, 10^4 subarrays.

To illustrate how the program might be used, consider the following example. Figure C-17 shows the input data selected; the fixed value of 2 Au and 10^6 bits per second were chosen. Two choices for phase shifters were entered, a ferrite device with .25 dB insertion loss at a cost of $20 and a diode type with .75 dB loss but costing $5. The choices for the feed system were a waveguide network (.05 dB/ft) costing $5/element and a stripline one (.15 dB/ft) costing only $0.5/element. Two amplifiers were considered, a 15°K maser at a cost of $10,000 and a 50°K paramp at $1,000. To determine how sensitive the cost was to subarray size, arrays composed of 1,000 and 5,000 subarrays were considered. The maximum number of subarrays permitted is bounded, as discussed previously, by requiring sufficient SNR at each subarray to maintain phase lock. For the model discussed here the maximum is about 20,000. The fixed element cost was set at $5/element and $50/element. This includes the cost of all the components not considered above, such as IF amplifiers, control circuitry, etc. Obviously the choice of lowest element cost will result in the lowest overall cost; the purpose of selecting several choices is to study some intangible factors. For example, the first choice might be the minimum possible element cost, the second might be for a system with automatic error detection circuitry to detect and locate system malfunctions such as component failures. For the 5 parameters listed above, each having two possible choices, there are $32 = 2^5$ distinct ways of constructing the array to obtain the specified error rate or output signal to noise ratio. The computer then calculates the required number of elements and the total cost for each of these systems and displays the output in the increasing cost format shown in Fig. C-17. Referring to this figure it can be seen that for the selected input data the most economical array would be obtained by using the .75 dB phase shifter, a waveguide feed, a maser amplifier, the $5 element cost, and 1,000 subarrays. It is interesting to observe that using these same values except increasing the number of subarrays to 5,000 would have produced a more efficient system which contained 20% less elements but cost almost twice as much. The size reduction is due to the individual subarray being smaller so that the cumulative effect of feed line loss is less; the increase in cost is due to the increase in required number of expensive masers. Another perhaps surprising observation is that the economically best three systems all utilized the .75 dB phase shifter rather than the higher performance .25 dB one. This is due of course to the difference in cost ($5 vs. $20).

Initially it was believed that the use of stripline would not be possible due to its large attenuation factor (.15 dB/ft.). It can be seen, however, that the third best system utilizes a stripline feed network. Even though this system requires considerably more elements (nearly twice as many) the total cost is only slightly more than optimum.

```
COST ANALYSIS FOR S BAND PHASED ARRAY OF DIPOLE ELEMENTS

ENTER DISTANCE IN AU
2
ENTER DATA RATE IN MEGABITS PER SECOND
1
ENTER NUMBER OF CHOICES FOR EACH COMPONENT
2
ENTER PHASE SHIFTER LOSS(DB) AND COST($)
  CHOICE   1
.25,20
  CHOICE   2
.75,5
ENTER FEED LINE LOSS(DB/FT) AND COST/ELEMENT
  CHOICE   1
.05,5
  CHOICE   2
.15,.5
ENTER AMPLIFIER TEMP AND COST
  CHOICE   1
15,10000
  CHOICE   2
50,1000
ENTER NUMBER OF SUBARRAYS DESIRED
  CHOICE   1
1000
  CHOICE   2
5000
ENTER FIXED COST PER ELEMENT
  CHOICE   1
5
  CHOICE   2
50
   FOR THE ABOVE PARAMETERS THE POSSIBLE SYSTEM CONFIGURATIONS AND THEIR
 COST ARE:
```

PHASE SHIFTER LOSS (DB)	$	AMPLIFIER TEMP	$	FEED LINE DB /FT	$	ELEMENT COST	NUMB S.A.	REQUIRED NO.ELEM	TOT COST MILL $
0.75	5	15	10000	0.05	5.0	5	1000	2252000	43.78
0.75	5	50	1000	0.05	5.0	5	5000	2760000	46.40
0.75	5	50	1000	0.15	0.5	5	5000	3945000	46.42
0.25	20	15	10000	0.05	5.0	5	1000	1310000	49.30
0.75	5	50	1000	0.05	5.0	5	1000	3262000	49.93
0.25	20	50	1000	0.05	5.0	5	5000	1810000	59.30
0.25	20	50	1000	0.05	5.0	5	1000	2201000	67.03
0.25	20	50	1000	0.15	0.5	5	5000	2750000	75.12
0.75	5	15	10000	0.15	0.5	5	1000	6341000	76.58
0.75	5	15	10000	0.05	5.0	5	5000	1840000	77.60
0.75	5	15	10000	0.15	0.5	5	5000	2825000	79.66
0.25	20	15	10000	0.05	5.0	5	5000	1180000	85.40
0.25	20	15	10000	0.15	0.5	5	5000	1720000	93.86
0.75	5	50	1000	0.15	0.5	5	1000	9039000	95.90
0.25	20	15	10000	0.05	5.0	50	1000	1310000	108.25
0.25	20	15	10000	0.15	0.5	5	1000	4138000	115.51
0.25	20	15	10000	0.05	5.0	50	5000	1160000	138.50
0.25	20	50	1000	0.05	5.0	50	5000	1813000	140.75
0.75	5	15	10000	0.05	5.0	50	1000	2252000	145.12
0.25	20	50	1000	0.15	0.5	5	1000	6220000	159.61
0.75	5	15	10000	0.05	5.0	50	5000	1840000	160.43
0.25	20	50	1000	0.05	5.0	50	1000	2201000	166.37
0.75	5	50	1000	0.05	5.0	50	5000	2760000	170.60
0.25	20	15	10000	0.15	0.5	50	5000	1720000	171.26
0.75	5	50	1000	0.05	5.0	50	1000	3262000	196.72
0.25	20	50	1000	0.15	0.5	50	5000	2750000	196.87
0.75	5	15	10000	0.15	0.5	50	5000	2825000	206.78
0.75	5	50	1000	0.15	0.5	50	5000	3945000	223.94
0.25	20	15	10000	0.15	0.5	50	1000	4138000	331.72
0.75	5	15	10000	0.15	0.5	50	1000	6341000	361.92
0.25	20	50	1000	0.15	0.5	50	1000	6221000	439.51
0.75	5	50	1000	0.15	0.5	50	1000	9139000	532.66

Fig. C-17. Typical example using computer analysis.

It should be emphasized that the comments on system cost in this example are dependent on the particular component values and element cost selected; these values were considered reasonable at this time but by no means exact. The significant contribution of the analysis and computer program is that given updated values of these components and desired data rate at any time in the future, the optimum way can be obtained to combine these components so as to minimize the total cost.

7) Subarray Components and Techniques

The optimum antenna system for the ground terminal is one that maximizes the signal-to-noise ratio under the practical constraints imposed by tolerance, reliability, noise environment, and cost. The antenna must have a low equivalent noise temperature and must provide a high-gain pattern which is steerable through a wide angle ($\pm 60^{o}$). It will be the purpose of this section to consider the circuit components and techniques appropriate to the design of a large phase array and to delineate their characteristics as parameters in determining subaperture size and performance characteristics. A phased array consists of radiating elements, a power distribution or collection network, a beam-steering or phasing system, and an optimal number of low noise preamplifiers. Each of these antenna components plays an important and interdependent role in the determination of the overall antenna performance. There exists a variety of beamsteering techniques applicable to a large antenna of phase array type; these include the use of a phase shifter at each element, and the use of a mixing scheme that translates a phase shift from the operating frequency to a convenient frequency band. Those areas in phased-array distribution and component technology that must be advanced to make the large arrays practical are to be discussed and delineated in this section. In addition, some consideration is being given to other types of scanning techniques in an effort to provide an optimum response to communication signals under a wide variety of environmental conditions.

a) Feed Systems The feed system or distribution network collects the signal from each of the radiating elements and phase shifters of the array and brings them to a common receiving port so that they combine in phase with a minimum of loss or distributes the energy to the individual radiating elements from the signal generator with proper phases and minimum loss in order to obtain a desirable radiation pattern. The distribution network largely and sometimes wholly determines the antenna aperture distribution; hence, it determines the antenna pattern, sidelobe level, and directivity. In the present study where the applicability of any particular overall system technique is determined by the various loss factors discussed above, the nature of the distribution network is most critical since it can shift the balance of effectiveness from one type of ground based system to another; a few tenths of dB/100' of loss in a transmission line can change the desirability of a particular technique since there are many hundreds of feet involved in the overall signal distribution. Distribution systems to be considered herein will include

those which are essentially optical and the several types of transmission lines as shown in Table C-III (see Ref. C-11). The various types of distribution networks to be evaluated in this phase scanned system can also apply to multiple-beam system where low-noise is an essential feature. At this stage in this study, it is already obvious that performance figure of merit of a large phased array will be largely determined by the characteristics of the distribution network and that further study and development beyond the present state-of-art in low loss transmission lines will be needed to satisfy the requirements of this program.

There are several distribution networks for feeding a phase array. The basic principles of each is briefly described as follows:

Constrained Series Figure C-18 shows several types of series feeds. In all cases the path length to each radiating element has to be computed as a function of frequency and taken into account when setting the phase shifters. The series feed lends itself to simple assembly techniques. Figure C-18a is an end-fed array. It is frequency sensitive and leads to more severe bandwidth restrictions than most other feeds. Figure C-18b is center fed and has essentially the same bandwidth as a parallel feed network (Ref. C-14). Sum and difference pattern outputs are available, but they have contradictory requirements for optimum amplitude distribution that cannot both be satisfied. As a result, either good sum or good difference patterns can be obtained, but no reasonable compromise seems possible that gives good sum and difference patterns simultaneously. At the cost of some additional complexity the difficulty can be overcome by the method shown under Fig. C-18c. Two separate center-fed feed lines are used and combined in a network to give sum and difference pattern outputs (Ref. C-15). Independent control of the two amplitude distributions is possible. For efficient operation the two feed lines require distributions that are orthogonal within each branch of the array, that is, in each branch the two feed lines give rise to patterns where the peak value of one coincides with a null from the other and the aperture distributions are respectively even and odd.

A very wide band series feed with equal path lengths is shown in Fig. C-18d. If the bandwidth is already restricted by the phase shifters at the aperture, very little advantage is obtained at the cost of a considerable increase in size and weight. The network of Fig. C-18e permits simple programming since each phase shifter requires the same setting. The insertion loss increases for successive radiators and the tolerances required for setting the phases are high. A modified series phase shifters technique, series-series feed system, has been investigated in Sec. 4C for feeding an array of subarrays. The signal to noise ratio (SNR) of individual subarray in terms of number of elements in the subarray, phase shifter loss, the fraction of power delivered to the phase shifters and the total effective noise temperature of the subarray has been obtained in Eq. (C-13). Curves of subarray SNR versus phase shifter temperature, which were computed from Eq. (C-13), for a 100-element subarray for each range, 1AU and 2AU are shown in Fig. C-22.

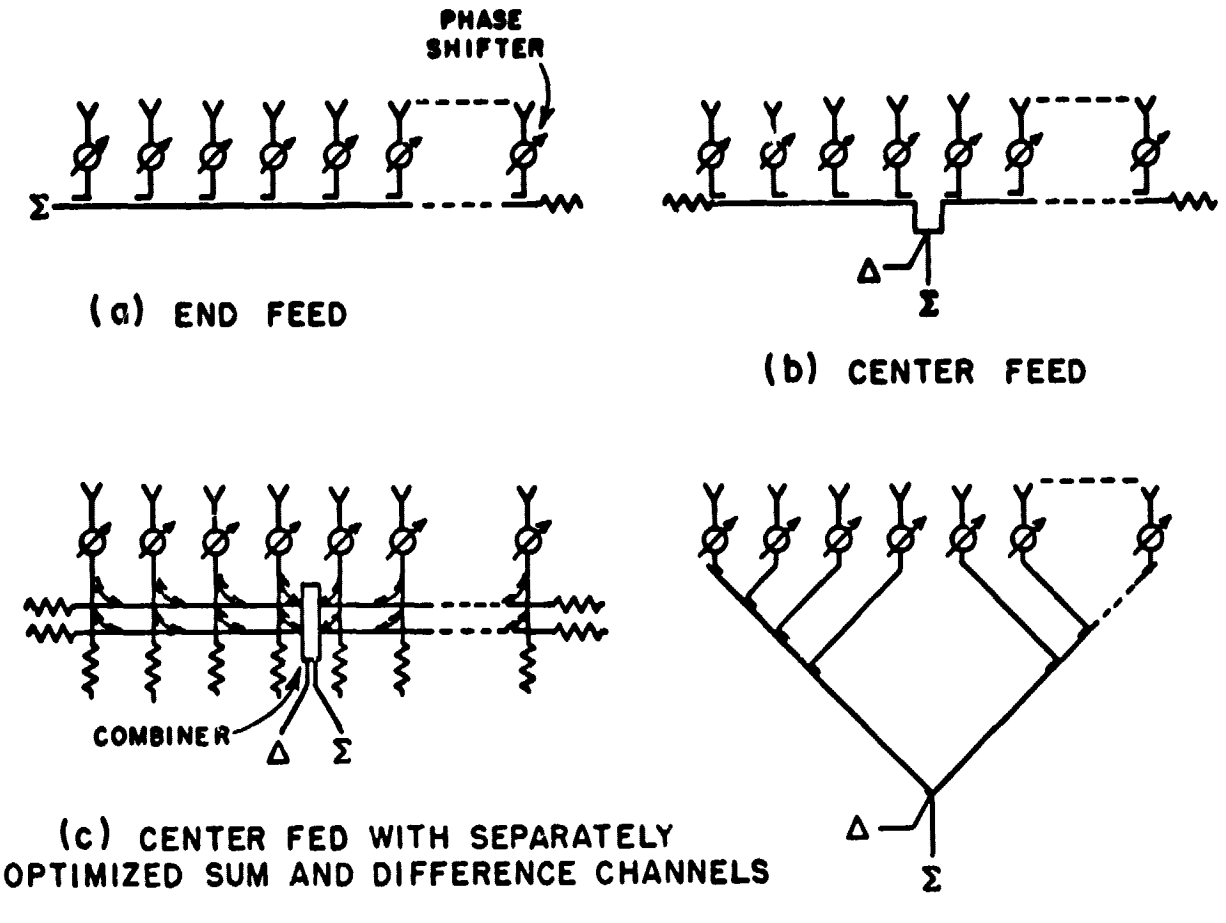

Fig. C-18. Series feed networks.

Parallel Feeds Figure C-19 shows a number of different parallel feed systems. They would usually combine a number of radiators into subarrays and the subarrays would then be combined to form sum and difference patterns.

Figure C-19a shows a matched corporate feed which is assembled from matched hybrids. The out-of-phase components of mismatch reflections from the aperture and of other unbalanced reflections are absorbed in the terminations. The in-phase and balanced components are returned to the input, and no power reflected from the aperture is reradiated. To break up periodicity and reduce peak quantization lobes (Ref. C-14), small additional phase shifts may be introduced in the individual lines and compensated by corresponding readjustments of the phase shifters. An equal length corporate feed system has also been investigated in Sec. 4C for feeding an array of subarrays. The

signal to noise ratio of individual subarray has been obtained in Eq. (C-15).

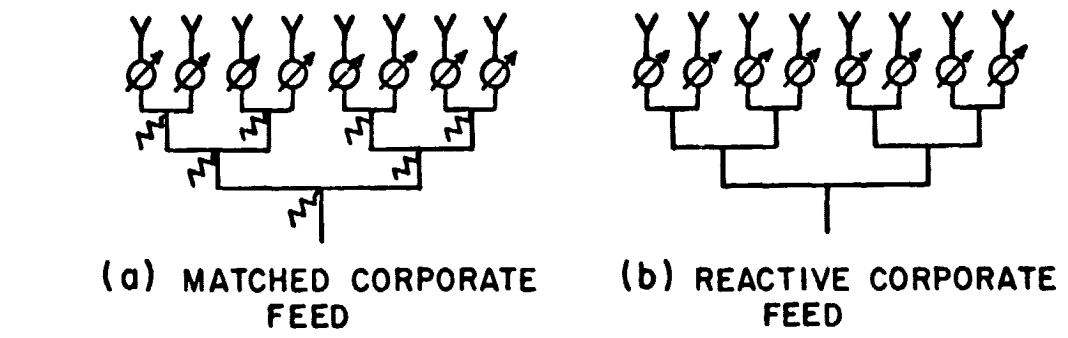

Fig. C-19. Parallel feed networks.

With nonreciprocal phase shifters the two-way path length is a constant, independent of the phase shifter setting. Under these conditions the performance of a reactive corporate feed is similar to that of the matched corporate feed. However, if additional phase shifts are added to the individual arms or if reciprocal phase shifters are used, then the out-of-phase components of the reflections due to the aperture m ;match will be reradiated (Ref. C-14). Figure C-19b shows a schemaiic layout for a reactive power divider in which wave-guides may be used. A stripline power divider is shown under Fig. C-19c. A constrained-optical power divider using an electromagnetic lens is shown under Fig. C-19d. The lens may be omitted and the correction applied at the phase shifters. With nonreciprocal phase shifting, a fraction of the power reflected from the aperture will then be re-radiated rather than returned to the input. The amplitude distribution across the horn is given by the wave-guide mode. It is constant with an E-plane horn as shown.

In this section of the report, transmission line feeding systems have been considered which to date are deemed appropriate for large phased arrays. From a manufacturing viewpoint strip-line is by far the most desirable type of transmission line because it is readily adaptable to mass producing techniques. However, its extremely high loss relative to coax and waveguide is due to dielectric losses rather ohmic conductor loss. One of the most useful low loss high frequency dielectrics is Teflon (polytetrafluoroethylene). Because pure Teflon has such a poor coefficient of thermal expansion it is usually mixed with glass or quartz; it is this additive which seriously degrades its attenuation properties. It is expected that considerable improvements will be made in dielectric materials and will make stripline devices more desirable.

TABLE C-III

	Attenuation in dB/100' at 2 GHz
Brass Waveguide	0.6
Rigid and Semi-rigid coax	1-2.5
Flexible coax - RG 20	6
Flexible coax - RG 9	12
Flexible coax - RG 58	35
Microstrip	19
Stripline (Triplate)	18

All subsequent calculations will be made using nominal values of feed line loss ranging from a lossless line to that of the coax.

Optical Feed Systems Phased array apertures may be used in the form of lenses or reflectors, as shown in Fig. C-20, where an optical feed system provides the proper aperture illumination. The lens has input and output radiators coupled by phase shifters. Both surfaces of the lens require matching. The primary feed can be optimized to give an efficient aperture illumination with little spillover (1 to 2 dB), for both sum and difference patterns. If desired the transmitter feed can be separated from the receiver by an angle α, as shown. The antenna is then rephased between transmitting and receiving so that in both cases the beam points in the same direction. The phasing of the antenna has to include a correction for the spherical phase front. To the first approximation this correction is

$$\frac{2\pi}{\lambda}\left[\sqrt{f^2 + r^2} - f\right] = \frac{\pi}{\lambda}\,\frac{r^2}{f}\left[1 - \frac{1}{4}\left(\frac{r}{f}\right)^2 + \cdots\right] .$$

With a sufficiently large focal length, the spherical phase front may be approximated by that of two crossed cylinders, permitting the correction to be applied simply with row and column steering commands. Correction of the spherical phase error with the phase shifter reduces peak phase quantization lobes (Ref. C-14). Space problems may be

encountered in assembling an actual system, especially at higher frequencies, since all control circuits have to be brought out at the side of the aperture.

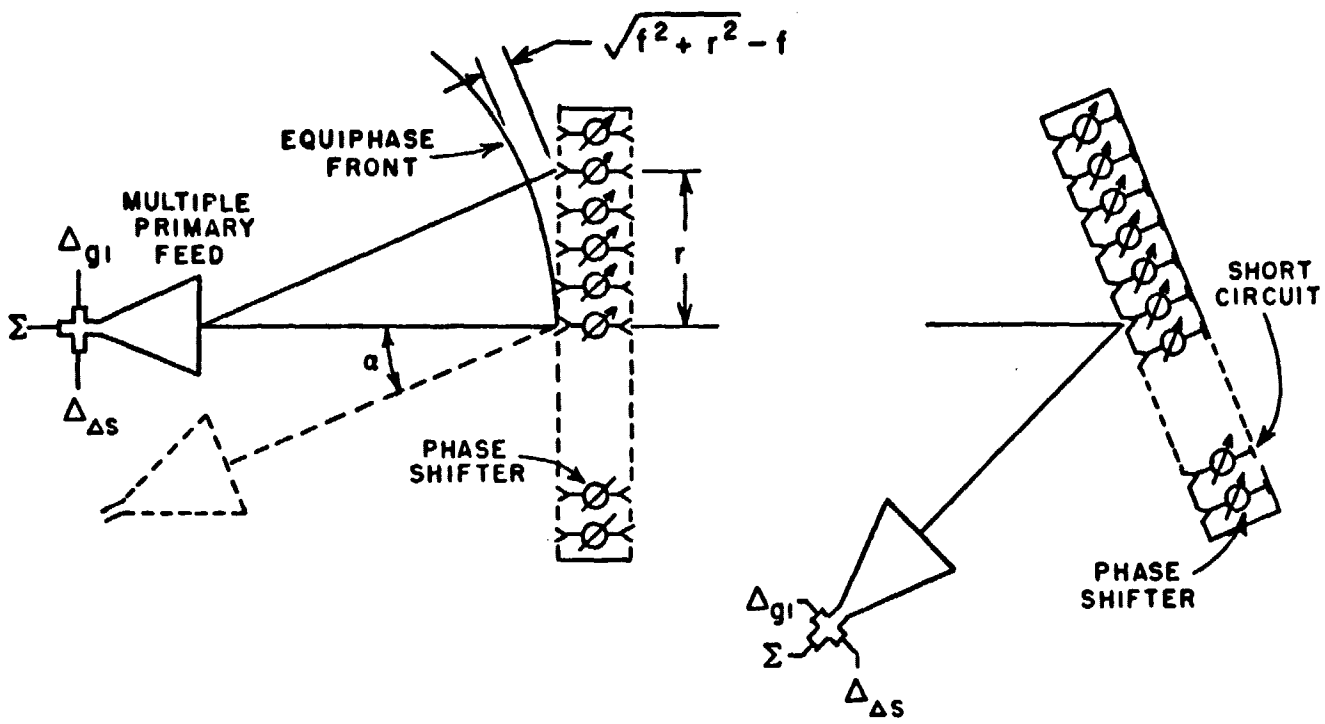

(a) LENS (b) REFLECTOR

Fig. C-20. Optical feed systems.

Multiple beams may be generated by adding further primary feeds. All the beams will be scanned simultaneously by equal amounts in sin θ.

The phased array reflector shown in Fig. C-20B has general characteristics similar to those of the lens. However, the same radiating element collects and reradiated after reflection. Ample space for phase shifter control circuits exists behind the reflector. To avoid aperture blocking, the primary feed may be offset as shown. As before, transmit and receive feeds may be separated and the phases separately computed for the two functions. Multiple beams are again possible with additional feeds.

The phase shifter must be reciprocal so that there is a net controllable phase shift after passing through the device in both directions. This rules out nonreciprocal phase shifters and this type of device.

b) Scanning Techniques There are several techniques for electronically scanning a beam presently being employed in various systems for diverse applications in both radar and communications. Since the basic objectives of this program may require implementation of a combination of these techniques, the basic principles of each is described briefly below:

Phase Scanning. This is the principle technique discussed in this subsection. Here the beam of an antenna points to a direction that is normal to the phase front. In phased arrays this phase front is adjusted to steer the beam by individual control of the phase of excitation of each radiating element. This is indicated in Fig. C-21a. The phase shifters are electronically actuated to permit rapid scanning and are adjusted in phase to a value between 0 and 2π. With an inter-element spacing s, the incremental phase shift ψ between adjacent elements for a scan angle θ_o is

$$\psi = \frac{2\pi}{\lambda} \; s(\sin \theta_o).$$

If the phase ψ is constant with frequency, then the scan angle θ_o is frequency dependent such that $(\sin \theta_o)/\lambda$ is constant.

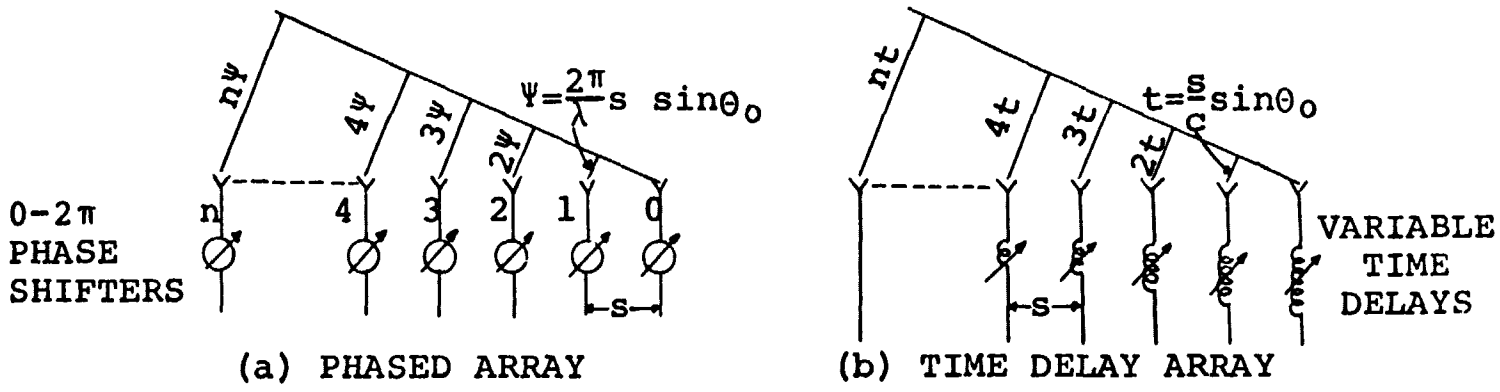

(a) PHASED ARRAY (b) TIME DELAY ARRAY

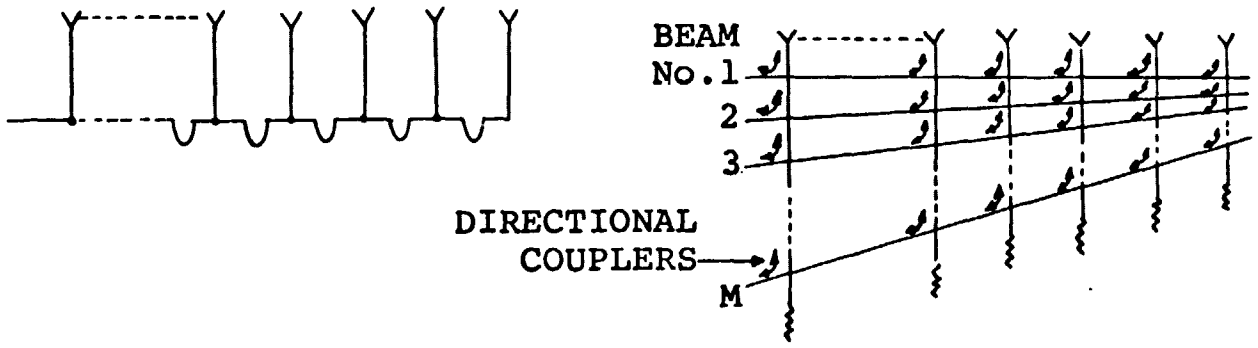

(c) FREQUENCY SCANNED ARRAY (d) MULTI-BEAM TYPE ARRAY

Fig. C-21. Generation of scanned beams.

Time Delay Scanning. The simple discussion above indicates that phase scanning is fundamentally frequency sensitive. Time delay scanning is independent of frequency. Delay lines are used instead of phase shifters, as shown in Fig. C-21b, providing an incremental delay from element to element of $t = s/c \sin \theta_o$. Individual time delay circuits (Ref. C-14) are normally too complex to be added to each radiating element. A reasonable compromise may be reached by adding one time delay network to a subarray of elements that have phase shifters. This type of compromise may provide a lower loss factor for the entire system.

Frequency Scanning. Frequency rather than phase may be used as the active parameter to exploit the frequency sensitive characteristics of phase scanning. Figure C-21c shows the arrangement. At one particular frequency all radiators are in phase. As the frequency is changed, the phase across the aperture tilts linearly, and the beam is scanned. This type of scanning may be used for "fine tuning" of the scan angle.

IF Scanning. When receiving, the output from each radiating element may be heterodyned (mixed) to an IF frequency. All the various methods of scanning are then possible, including the beam switching system described below, and can be carried out at IF where amplification is readily available and lumped constant circuits may be used. Equivalent techniques of mixing may be used for transmitting.

Beam Switching. With lenses or reflectors, a multiplicity of independent beams may be formed by feeds at the focal surface. Each beam has substantially the gain and beamwidth of the whole antenna. Allen (Ref. C-16) has shown that there are efficient equivalent transmission networks that use directional couplers and have the same collimating property. A typical form after Blass (Ref. C-17) is shown in Fig. C-21d. The beams may be selected through a switching matrix requiring (M-1) SPDT switches to select one out of M beams. The beams are stationary in space and overlap at about the 4 dB points. This is in contrast to the previously discussed methods of scanning, where the beam could be steered accurately to any position. The beams all lie in one plane. Much more complexity is required for a system giving simultaneous beams in both planes.

C) RF Phase Shifters. Beam steering for a conventional phased array requires some type of phase shifting device at each element. The primary requirements for such a device are that it be capable of 360 degrees of phase shift and that it has an extremely low insertion loss, preferably less than 0.1 dB. In addition these devices must be relatively inexpensive since their requisite number is proportional to the total aperture size, be capable of being packaged to fit within the array element spacing, and be temperature insensitive to ambient environments.

At present, there is no phase shifting device that will meet all of these requirements. Typically, electronic phase shifters such as ferrite and diode devices have insertion losses on the order of 0.5 dB. While this loss does not greatly reduce the incoming signal strength, it does contribute considerable noise and consequently seriously degrades the SNR which influences the required aperture size. As shown in Fig. C-22 which was computed from Eq. (C-13) (series-series model) considerable improvement in SNR is possible by cooling the device. This seems like a particularly feasible approach for the diode type of phase shifters where a Peltier cooling device could be incorporated as an integral part of a semiconductor ship. Several commercial manufacturers are presently developing and manufacturing Peltier cooling devices for inclusion in a diode phase shifter and for direct attachment to the semiconductor.

The devices that are presently available for phase arrays fall into three general groups which require consideration and some critical observation. A preliminary discussion of these groups, their advantages and disadvantages is given below and will be updated as new pertinent information becomes available:

Diode Phase Shifters - Digital diode phase shifters are small, lightweight devices that are insensitive to temperature and can be switched from one phase setting to another in a few nanoseconds. Two types of digital phase shifters are in current use. One uses a transmission line structure in which different susceptances are switched across the line to produce incremental phase shift. The other design configuration is a reflection structure that may be converted to a transmission component by the employment of a 3 dB coupler or a circulator. Diode phase shifters are, at present, somewhat costly because of the cost of the diodes and their mounting structure. P-i-n diodes are typically used as the control elements because of their high power handling capability. Since high power is not of prime concern in a receiving system, other arrangements of solid state materials may be more desirable although to date there has been no stimulus for such analysis and design. The engineers of the Texas Instrumental Corporation who are involved in the MERA module and system design report that they have been able to produce IC phase shifters with 1.2 dB insertion loss as the average value of a large group with 1.5 dB as a maximum value.

Ferrite Phase Shifters - Ferrite phase shifters (Ref. C-12) are typically waveguide size, moderate in weight, somewhat temperature sensitive, can be switched from one phase setting to another in a few microseconds, and require significant drive energy. They are somewhat costly because of the cost of the ferrite material. Two general configurations are available. One uses a transverse magnetizing field; the second uses a longitudinal magnetizing field. The former is reciprocal only for certain configurations while the latter is intrinsically reciprocal, a property desirable in arrays to be used for both transmission and reception. Phase shifters that use longitudinal magnetization also

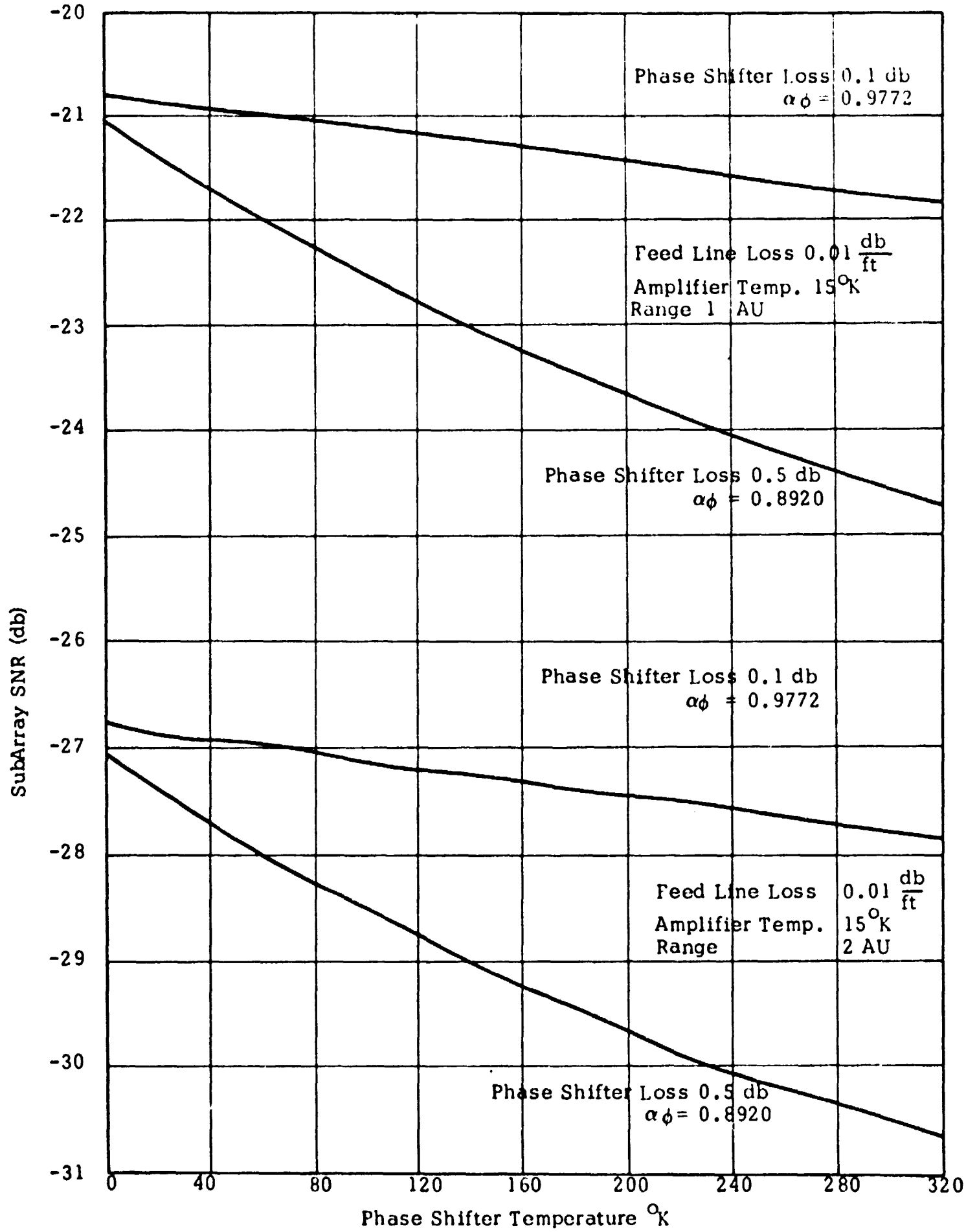

Fig. C-22. SNR vs phase shifter temperature for a 100 element subarray.

produce greater phase shifts at lower levels of applied magnetic field than do those that use transverse magnetization. General characteristics of ferrite phase shifters that affect spacecraft scanning applications are reciprocity impedance matching, frequency dependence of phase shifts, temperature sensitivity, and hysteresis effects. Weight can also be a great problem with ferrite phase shifters for a space-borne array with large numbers of elements. However, weight is only a secondary problem in a ground array compared to the temperature effects.

Novel Devices - There are several new devices which are not being developed whose progress bears some observation. Ferroelectric phase shifters are quite small and light weight. They are, at present, extremely temperature sensitive, due to the sensitivity of the ferroelectric crystal, and they have very high insertion loss characteristics. Since they are still in the experimental stages, production costs are unknown. At present, it appears that a major improvement will be required in the basic crystal before these devices can be considered for use in an array. As in the case of the ferroelectric phase shifter, the plasma phase shifter is still in the experimental state. It is moderate in size and weight with a negligible temperature sensitivity. The insertion loss is comparable to that of the ferrite and diode phase shifters, but a significant reduction may be possible. At the present time, it is not a low cost device and requires significant drive energy; both factors are due to the need for the generating and sustaining of a plasma.

The high loss associated with the electronic phase shifting device can be eliminated or reduced by either mechanically scanning the subarrays, by using mechanical phase shifting devices such as a line stretcher, or by some form of simple air filled guide which may employ a multi-moding technique to properly gather the signals from numerous input ports. Each of these schemes needs further study and experimentation to develop the low loss feed system required by a high data rate communication link.

From the preceding equations it can be shown that one of the most important components which influence the required aperture size is the phase shifters. Electronic phase shifters such as ferrite and diode devices typically have insertion losses in the order of 0.5 dB instead of the more desirable 0.1 dB. While this loss does not greatly reduce the incoming signal it does contribute considerable noise and consequently seriously degrades the SNR. As shown in Fig. C-22 for a typical set of parameters, considerable improvement in SNR is possible by cooling. This seems particularly feasible for the diode type phase shifters where a Peltier cooling device could be an integral part of the semiconductor chip. The Peltier cooling effect is a thermo-electric phenomenon in which heat is absorbed or generated by current passing through a semiconductor junction. Several companies (Ref. C-13) are presently developing and manufacturing Peltier cooling devices for inclusion in the diode case and for direct attachment to the semiconductor chip. These problems will require further study and work is now in progress to examine

the results using parameters that are more closely related to values which are possibilities for the future.

Time Delay Networks Figure C-23a shows a time delay network that is digitally controlled by switches. The total delay path length that has to be provided nondispersively amounts to 'a sin θ_{max}'' where θ_{max} is the maximum scan angle for the aperture 'a'. The smallest bit size is about $\lambda/2$ or λ, with the precise setting adjusted by an additional variable phase shifter. A 1^{o} beam scanned 60^{o}, for example, requires a time delay of 6 or 7 bits, the largest being 32 wavelengths, as well as an additional phase shifter. The tolerances are tight, amounting in this case to a few degrees out of about 20,000, and are difficult to meet. Problems may be due to leakage past the switch, to a difference in insertion loss between the alternate paths, to small mismatches at the various junctions, to variations in temperature or to the dispersive characteristics of some of the reactive components. Painstaking design is necessary. The switches may be diodes or circulators. Leakage past the switches may be reduced by adding another switch in series in each line. The difference in insertion loss between the two paths may be equalized by padding the shorter arm. The various problems are comprehensively assessed and analyzed by Temme and Betts (Ref. C-18).

Figure C-23b shows another configuration that has the advantage of simplicity. Each of the switchable circulators connects either directly across (counterclock wise) or via the short-circuited length. Isolation in excess of 30 dB is required, and the higher insertion loss of the longer path cannot easily be compensated. Each time delay network would therefore, precede a final power amplifier on transmitting and follow a preamplifier on receiving or a special design which is as yet unavailable.

Only the edge elements or edge subarrays of the antenna require the full range of time delay. The center does not need any time delay, only a biasing line-length. The amount of delay required increases as the edge of the aperture is approached. This is shown in Fig. C-24.

A further method of providing delay is possible by translating the problem from the microwave domain and delaying at IF since the insertion loss of time delay circuits is usually too high for most practical systems at RF.

I-F Phase Shifting Techniques. Because of the modular nature of the electronically steered systems being considered for this study, it will be possible to employ I-F phase shifting techniques. These techniques (Ref. C-1) offer several advantages as compared with R-F phase shifting techniques. First, requirements on the phase-shifting components may be relaxed as compared with requirements on corresponding R-F components. In addition, since the phase shifting for reception is performed after frequency translation and I-F amplification, losses in the phase shifters do not degrade system noise figure nor do they contribute to

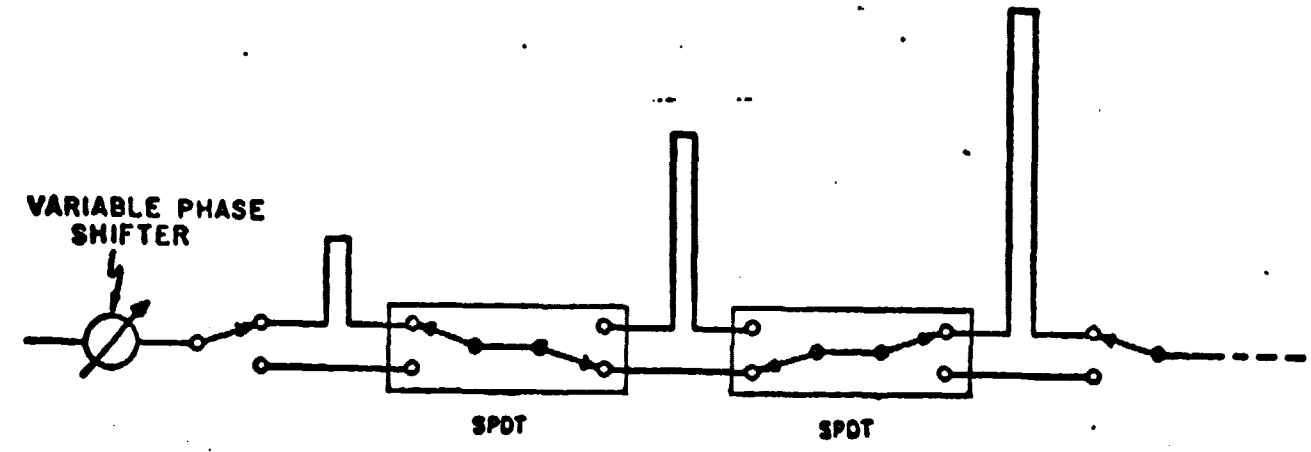

(a) TIME DELAY BY CHOOSING UPPER OR LOWER PATHS

(SPDT = SINGLE-POLE, DOUBLE-THROW SWITCH)

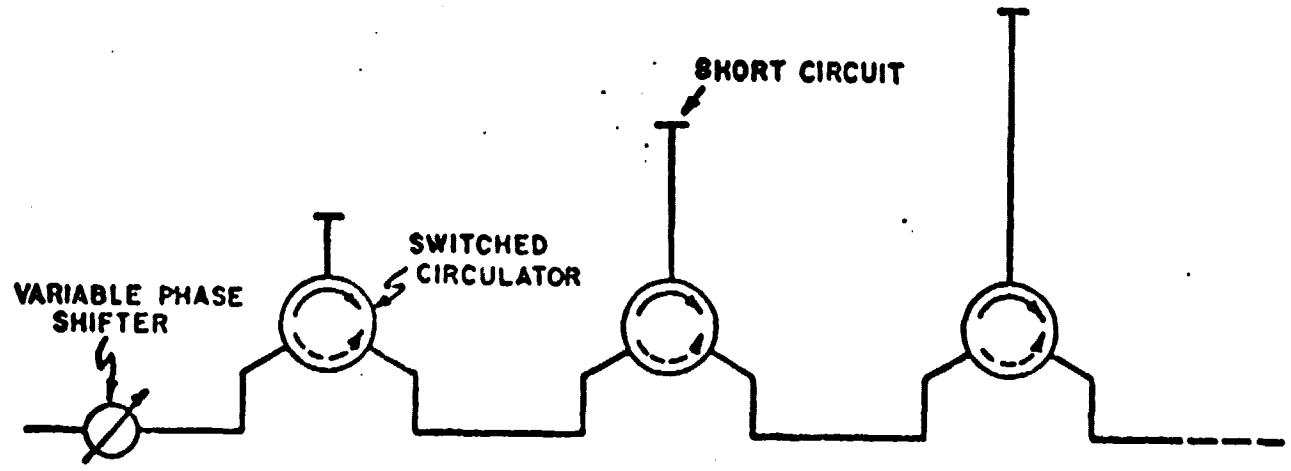

(b) TIME DELAY USING SWITCHED CIRCULATORS

Fig. C-23. Time delay configurations.

reduced system gain as would R-F phase shifters without individual R-F preamplifiers. The phase shifting for transmission can be done at low power levels with I-F phase shifters so that the power handling capabilities and losses of the phase shifters do not present problems. Typically, each complete moduie includes an antenna element, an R-F diplexer, a mixer, an I-F amplifier, and a phase shifter for reception; for transmission a similar set of components is required with the addition of a high-power R-F source. A number of configurations are possible to accomplish the desired performance characteristics but each requires I-F phase shifting devices. These devices are discussed in the following paragraphs.

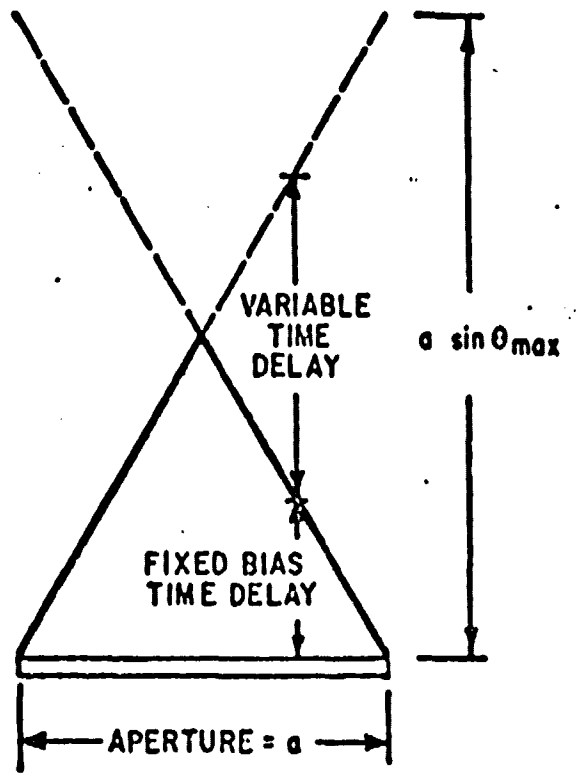

Fig. C-24. 'Variable' and 'Fixed Bias' time delay for an aperture.

The simplest type of I-F digital phase shifter is that composed of discrete sections of delay lines that can be switched in and out with electronically controlled single-pole, double-throw switches. Such a device is illustrated in Fig. C-23a. The various delay lines could be distributed or lumped parametric types depending on the particular frequency ranges being used. The 180° phase step is obtained merely by reversing the polarity of the line connections at that point.

d) Other Solid-State Components. During the past years, technical literature has reported significant improvement in solid-state devices and circuitry for electronically steered arrays. Typically, improvements have been effected in phase shifters, I-F amplifiers, microwave power sources, mixers, filters, and circulators.

Filters. Excellent filters are commercially available in the frequency range up through X-band and beyond. These include filters employed in communication systems; for example, bandpass (nominally flat), band rejection, diplexers, and high Q stabilizing cavities. In these higher frequency ranges the structures may be waveguide, strip transmission line, coaxial, or microstrip; but for space applications, the small, lightweight strip transmission line coaxial

devices, or microstrip, are most attractive. The performance of the latter, in terms of loss, needs improvement to be competitive with waveguide filters.

Preamplifiers There are two possibilities for the preamplifier that lend themselves to microstrip application: tunnel diode amplifiers (TDA's) and transistor amplifiers. With the present state-of-the-art at 2 to 10 GHz and above, the TDA is slightly lower in noise figure than available transistors. Since a TDA must use a circulator, a 0.5 dB insertion loss must be added to the noise figure to give a value of 4.5 dB and perhaps 30 dB of gain. In comparison present day transistors can give a noise figure of 5.2 dB and 20 dB of gain.* At present, at 1 GHz, transistors have 3.5 dB noise figures, but manufacturers (KMC Corporation and NEC) anticipate that devices with better noise figures will be available within a year. Such devices would give a receiver noise figure of 4.4 dB at S-band. A transistor amplifier can be fabricated into a smaller package than the TDA due to the use of microcircuit lumped elements. The TDA uses at least one circulator which, with present technology, has a minimum size of about 1 inch square. Thus, on a size and weight and future performance comparison, the transistor amplifier is the preferred device.

At X-band a tunnel diode amplifier will give the best noise figure. However, because a mixer is simpler, lighter in weight, and lower in cost and has a competitive noise figure, it is anticipated that it will remain the preferred component at the higher frequencies for several years.

Mixers The element that most determines the design of the receiver is the mixer. Present conventional balanced mixers have produced single sideband noise figures of less than 5 dB at S-band. However, this value represents carefully matched low loss conditions which may be hard to achieve in mass production in microstrip.

An alternative design for the conventional mixer with a low-noise preamplifier is the image enhancement mixer. Recently at MIT** an S-band image enhancement mixer was measured with less than a 3 dB single sideband noise figure and 0 dBm saturation level. The local oscillator power and complexity of this device is greater than that of the conventional mixer. A local oscillator drive of 50 mw was reported;

---

* Nippon Electric Co., SM153 Gallium Asenide Schottky Barrier Diode. I-F amplifier noise figure assumed to be 1.5 dB.

**R.P. Rafuse and D. Steinbrecher as reported in Sprint, MIT Quarterly Progress Report and by private communication.

this figure compares with 1 or 2 mw for normal operation. This type of mixer will need further development before its merits can be fully evaluated.

As the integrated circuit technology advances, solid-state devices are being developed for integration into array antennas to form and phase beams and also for amplification. Microstrip transmission circuits have been developed that contain various microwave circuit elements such as circulators, switches as well as amplifiers, mixers, and multipliers (Ref. 19). With these devices, systems become possible where many relatively low power transmit amplifiers are used and distributed over the aperture with each amplifier connected to a radiating element. The expected advantages of integrated antennas include high reliability and low cost, simple low voltage power supplies for the RF amplifiers and a system which is simple and light in weight and yet capable of operating with relatively high RF power.

e) Summary Since the objectives of this present program are completely dependent upon adequate phase shifting devices and techniques, a continuing effort will be made to assess the performance parameters of the present state-of-art devices as well as to evaluate the potential of newly discovered structures. The listing shown in Table C-IV describes the nominal performance parameters of various genetic types of phase shifters at X-band frequencies since these devices are readily available and extensively used in radar systems. As may be seen from the table, many of the devices have relatively high insertion losses for the present communication application. These large loss values are due partly to the universal requirements of fast switching speed and high power handling capacity as dictated by radar application. Neither high-speed nor high-power capability are necessary for a ground based communication system, and consequently it can be expected that special designs of the above devices may be available with a substantially lower loss than the values of .6 to 3.0 dB for 360° of phase shift as shown in Table C-IV. However, for the present studies a nominal insertion loss value of .5 dB shall be used until analysis and the appropriate experimental hardward are available to reduce the insertion loss to the desired value.

The results for phase shifters that are designed primarily for use at X-band are given only as a temporary expedient until precise descriptions of the corresponding devices operating at S-band frequencies can be obtained. In Table C-V, a listing of commercially available S-band phase shifters is given with only some of the pertinent performance characteristics. More information will become available as these devices are employed in various array applications. Most of the electronically controlled phased arrays in current operation or in the planning stage are for use in radar systems where power handling capability is one of the primary concerns. The cost and electrical performance of phase shifters specifically designed for use in communication receiving arrays is as yet quite difficult to obtain. Table C-VI presents a summary of a recent article in Microwaves (April '69) concerning the cost and performance of

TABLE C-IV
MICROWAVE PHASE SHIFTERS (MAY 1968)

Characteristic	Ferrite Longitudinal Field, Digital, Reciprocal	Ferrite Transverse Field, Digital, Nonreciprocal	Ferrite Longitudinal Field, Digital, Reciprocal	P-I-N Diode Transmission Digital (Stripline)	P-I-N Diode Reflection Digital - One Port Device	P-I-N Diode Reflection Digital - with 3-db Coupler
Frequency	X-band	X-band	X-band	X-band	X-band	X-band
Phase Shift (Maximum)	360° continuous	360° 22.5° steps (4-bit)	360° 22.5° steps (4-bit)	360° 22.5° steps (4-bit)	360° 90° steps (2-bit)	360° 90° steps (2-bit)
Figure of Merit	600°/db	500°/db	350°/db	100°/db	100°/db	200°/db
Temperature Sensitivity	5°/°C	1°-3°/°C	5°/°C	Negligible	Negligible	Negligible
Excess Noise Temperature	0° K	0° K	0° K	Negligible	Negligible	Negligible
Control Power	0.1 watt	3 by 10^{-4} watt-sec.	10^{-3} watt-sec	0.1 watt	0.05 watt	0.1 watt
Time Constant	100 μsec.	2-10 μsec.	2-10 μsec.	0.2-10 μsec.	0.2-10 μsec.	0.2-10 μsec.
Size (inches)*	6 by 1 by 1/2	5 by 1 by 1/2	7 by 1 by 1/2	10 by 1 by 1/2	1 by 1 by 0.025	2 by 1 by 0.025
Weight	2-1/2 oz + waveguide	2-1/2 oz. + waveguide	5 oz. + waveguide	1-1/2 oz.	1/2 oz.	1 oz.
Disadvantages	1. Requires magnetic shielding 2. Requires temperature stabilization 3. Requires continuous holding power	1. Nonreciprocal 2. High current driver	1. High current driver 2. Requires temperature stabilization	1. Requires large numbers of diodes 2. Difficult to package 3. Susceptible to burnout	1. Susceptible to burnout 2. High loss for large number of phase bits	1. Susceptible to burnout 2. High loss for large number of phase bits
Range of frequencies at which practical devices can be built	2 to 50 GHz	2 to 40 GHz	2 to 20 GHz	0.1 to 10 GHz	2 to 18 GHz	2 to 18 GHz

* Assumes device slips into solid-state array.

TABLE C-V.

Characteristic	MA*-8356 05X Diode Digital	MA-8356 151X Diode Digital	MA-8356 251X Diode Digital	MA-8356 451X Diode Digital	MA-8356 851X Diode Digital	MA-8356 8525 Diode Digital
Frequency	S-Band	S-Band	S-Band	S-Band	S-Band	S-Band
Phase Shift (Maximum)	22.5° 22.5° steps	45° 22.5° steps	90° 22.5° steps	180° 22.5° steps	360° 22.5° steps	360° 5.6° steps
Figure of Merit (Maximum VSWR) in db)	2.3	2.3	2.3	2.3	2.3	1.75
Temperature Sensitivity	Negligible	Negligible	Negligible	Negligible	Negligible	Negligible
Excess Noise Temperature	Negligible	Negligible	Negligible	Negligible	Negligible	Negligible
Control Power	+5V at 200mA -200V at 1mA	+5V at 400mA -200V at 1mA	+5V at 800mA -200V at 1mA	+5V at 1.6A -200V at 1mA	+5V at 3A -200V at 1mA	+5V at 3.4A -200V at 1mA
Time Constant	0.4 μs	0.4 μs	0.4 μs	0.4 μs	0.4 μs	0.5 μs
Size						
Weight						
Disadvantages						
Range of Frequencies at which practical devices can be built	2.9-3.1GHz	2.9-3.1GHz	2.9-3.1GHz	2.9-3.1GHz	2.9-3.1GHz	2.0-4.0GHz

* MA - Microwave Assiciates

TABLE C-VI
SURVEY OF PHASE SHIFTER COST AND PERFORMANCE
(Data taken from April 1969 Microwaves)

Source of information	T.M. Hyltin Texas Instruments	J.F. White Microwave Assoc.	G.T. Roome Syracuse University Research Corp.	D.H. Temme MIT Lincoln Lab	G. Harrison Sperry Microwave Div.
Type of Phase Shifter	Diode Micromin	Metal Housed Diode	Planar Ferrite	Waveguide Ferrite	Waveguide Ferrite
Cost of diodes or ferrite materials	$8.00 (for 16 diodes)	$80.00 (16 diodes and bypass capacitors)	$4.80	$20.00	not given
Packaging, housing substrate, board	$10.00	$39.00	$6.00	$10.00	not given
Driver	$ 4.50	$45.00	$30.00	$50.00	$90.00
Yield, labor, testing	$27.50	$18.00	not given nor included in cost estimate	$18.00	not given
Estimated cost for one	$50.00 (based on 10,000 units)	$182.00 (based on 1000 units)	$38.25 (based on 1000 units)	$98.00 (based on 1000 units)	$150.00 actual cost (4000 units manufactured)
Frequency	S, C, Ku	not given	not given	S-K	C
Insertion loss	not given	not given	<2 dB	.5 - 1.0 dB	not given
Power handling capability	peak 200W ave 5 W	peak 25 KM	peak 100 W	Peak 100 KW ave 1 KW	Peak 3 KW

phase shifters. The values given are not those presently available but represent a best estimate by an expert in each company about what can be made available if the need presents itself.

8. Preliminary Considerations of Subsystem Organizations

This study has demonstrated that the required array size and cost is extremely sensitive to the phasing and feeding components. The critical part of the feed network is at the subarray level. The problem is how to combine and phase shift the individual elements to form a subarray output. Any attenuation and noise which occurs after the subarray amplifier is relatively unimportant.

After considerable study of the various possibilities described in the previous subsections, it became apparent that a typical receiving system organization would require certain specialized characteristics. Thus Fig. C-25 shows a simplified diagram of a characteristic receiving system which can be used independently or in conjunction with an adaptive mode to provide for periodic interference from a large noise source or from coherent interfering signals. Course scanning of each subarray would probably be achieved by computer programming for two reasons:

1. The desired look angle is usually known quite accurately or can be determined by raster scanned search techniques or by using information from only one portion of the available aperture.

2. The SNR at the output of each element in the subarray of a large array would be considerably below the threshold of any adaptive combining scheme.

The output of each subarray is amplified by a low noise device such as a maser or paramp to reduce the noise degradation due to the feed lines and the signal processing equipment which follows it. Each amplified subarray is then multiplied by a complex weighting coefficient (amplitude and phase) before being combined to produce the array output. The value of the weighting coefficients could either be determined by the open loop techniques (computer program) or by closed loop feedback techniques such as phase locking, minimizing mean square error or any such operational techniques. The choice, of course, depends on the array environment. For example, if undesired or interfering signals were present, the proper choice would be the adaptive mode using the LMS technique as described in Section IV-D to generate array nulls in the direction of the interference. Finally, the array output is decoded or detected to recover the desired information.

A corporate feed network has been studied and the need for low loss transmission feed lines was demonstrated in this subsection. Stripline, one of the most appealing materials from the cost aspect since it is ideal for mass production was shown to seriously degrade the subarray performance.

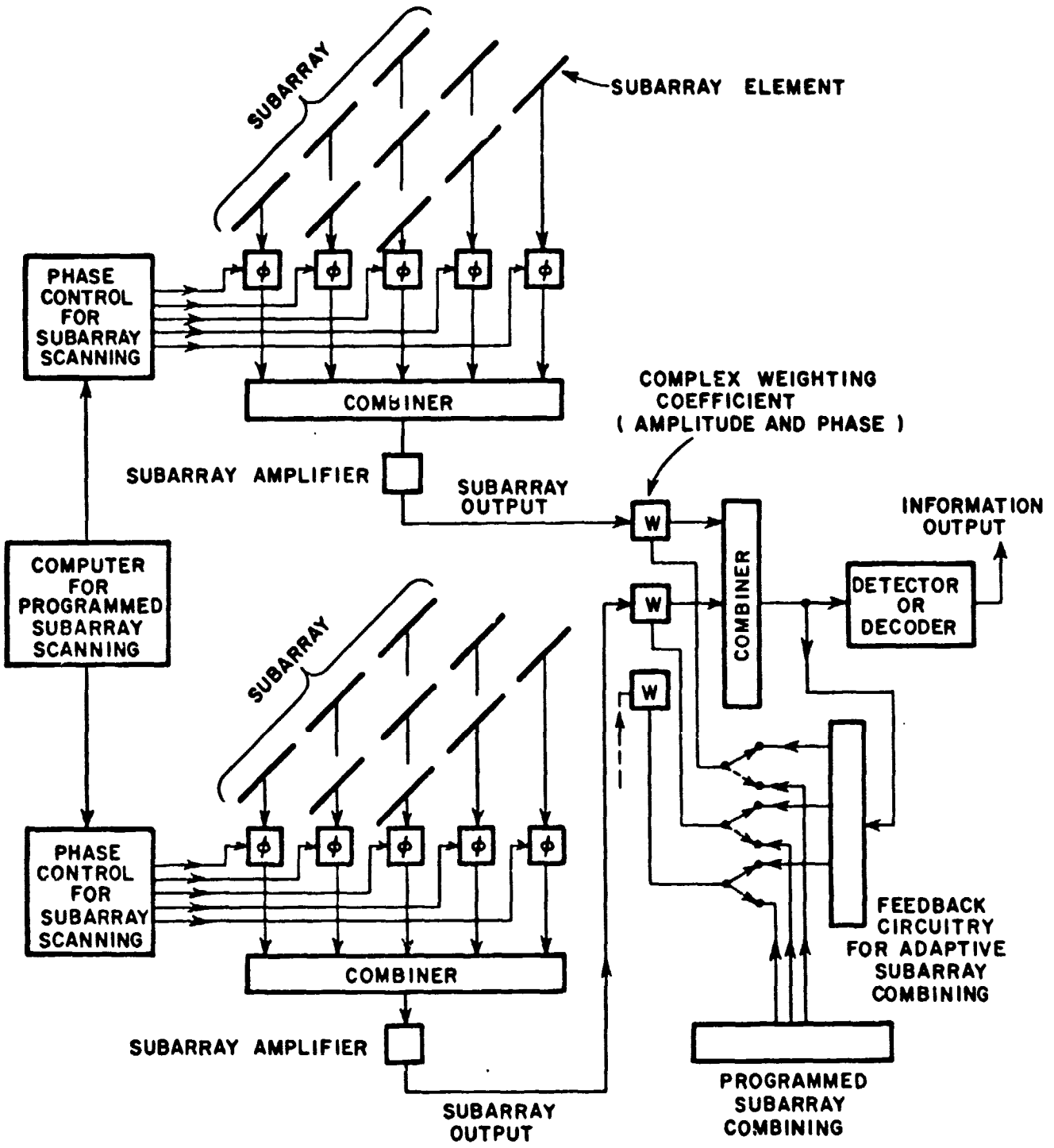

Fig. C-25. Block diagram of receiving array.

An alternate type of feeding and phasing arrangement which might eliminate some of this problem is the reflector feed shown in Fig. C-26. Each subarray would have a horn which is essentially an optical feed to receive the energy scattered by the subarray elements. The scattered waves are focussed at the collecting horn by phase shifters behind each element. For example, if the antenna elements were open ended waveguides the phase shift could be obtained by turning on the proper diode switch (see Fig. C-27) to produce a variable length short. This reflect array technique is being employed in many of the modern phased array radars.

To design a phase shifting technique for dipole elements is considerably more difficult since any impedance changing scheme will detune the dipole and greatly reduce the amplitude of the scattered wave. Active devices might be used to solve this problem but the large noise contribution from any of these devices would probably make this approach uncompetitive with the corporate feed scheme. Additionally, their fabrication is more complicated and consequently more costly.

An analysis of the various studies and inputs that have been conducted in this subsection bring to light many problems that still need solution. The problem of limiting the noise (or attenuation) in a system that has to be distributed over vast amount of real estate is still a difficult one to decide on how to proceed. It is to be hoped that the solution will be reached or that some invention or technique will be forthcoming which will permit a design to circumvent this difficulty. However at present, only more conceptual effort is called for at this stage. Consequently, it is one of the purposes of this program to investigate all recent developments in both components and techniques in an effort to solve the subarray distribution problem.

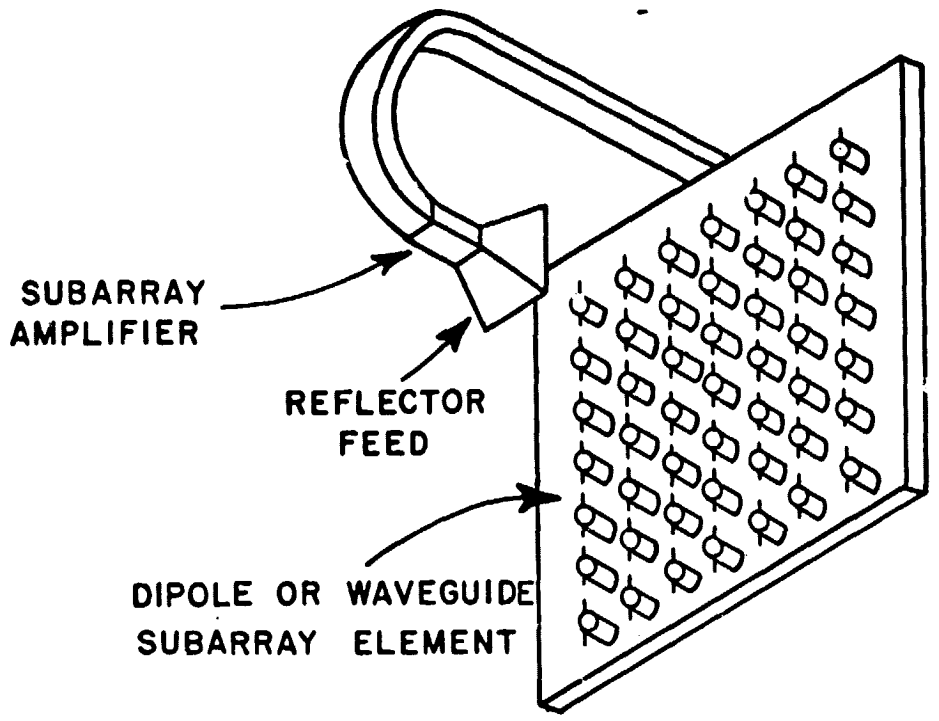

Fig. C-26. Reflector subarray.

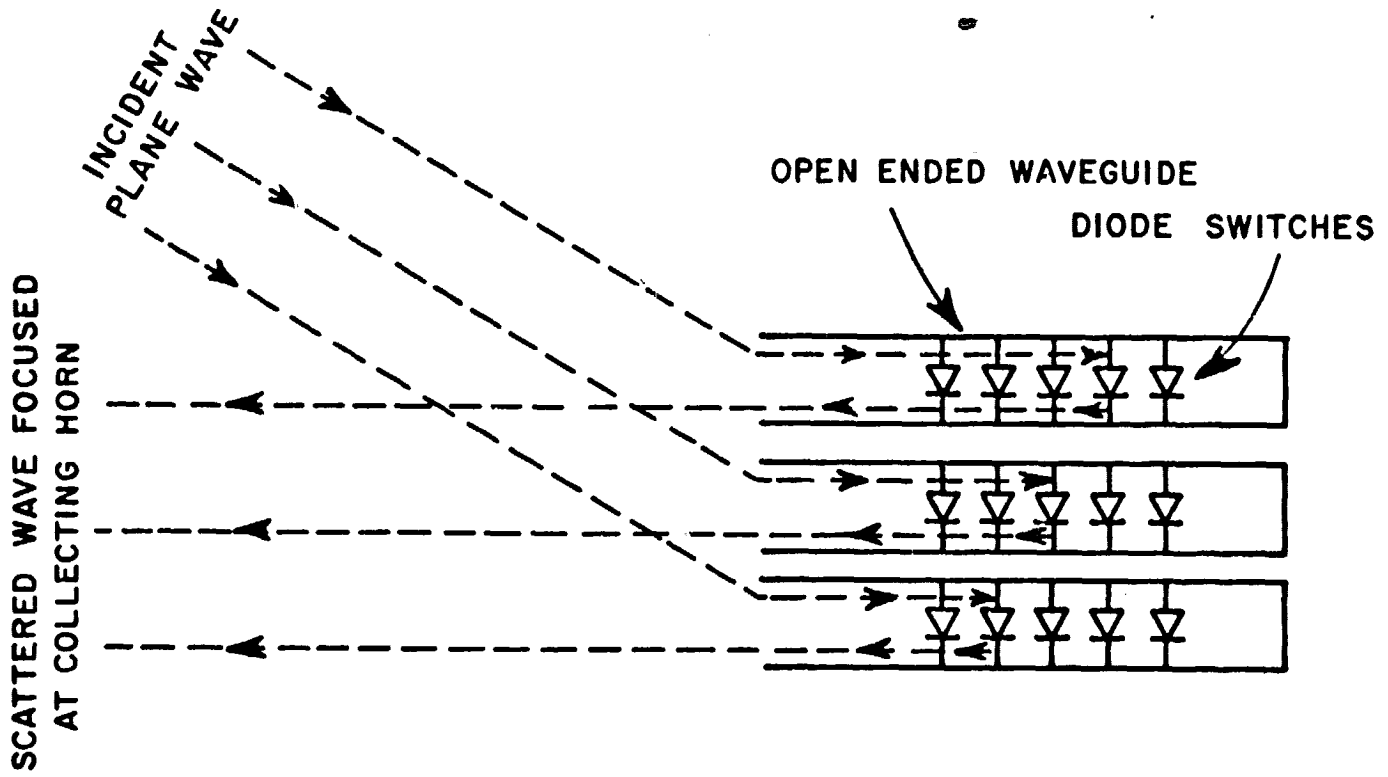

Fig. C-27. Scheme for phase shifting.

APPENDIX I
RELATIONSHIP BETWEEN GAIN AND SIZE FOR THE DIPOLE ANTENNA MODEL

To calculate the gain of the two dimensional array shown in Fig. A1 it is convenient to use the concept of array multiplication, that is the total pattern can be calculated as

$$F_T = F_E F_X F_y F_Z$$

where

F_E = element pattern of a single dipole

F_X, F_Y = array factor for an array of isotropic elements along the X, Y axis

F_Z = array factor for two isotropic elements along the Z direction.

For $D_x = D_y = \lambda/2$ and $D_z = \lambda/4$ the resulting expressions are:

$$F_E = \frac{\cos(\pi/2 \sin\theta \cos\phi)}{\sqrt{1 - \sin^2\theta \cos^2\phi}}$$

$$F_Z = \sin(\pi/2 \cos\theta)$$

$$F_X = 1 + 2 \sum_{k=1}^{(N_o-1)/2} \cos(K\pi \sin\theta \cos\phi)$$

$$F_Y = 1 + 2 \sum_{k=1}^{(N_o-1)/2} \cos(K\pi \sin\theta \sin\phi)$$

where

N_o = number of elements on a side (assumed odd).

The power density $S = F_T^2$ and the directivity is

$$D = \frac{S(\theta = 0)}{\frac{1}{4\pi} \int_0^{2\pi} \int_0^{\pi/2} S(\theta,\phi) \sin\theta \, d\theta \, d\phi} .$$

The effective aperture $A_e = \frac{\lambda^2 D}{4\pi}$.

Defining the physical aperture is somewhat arbitrary, for example, a single dipole has zero physical area. However for large arrays each element occupies on the average $\lambda^2/4$ area, hence the total physical aperture is defined as $A_p = N_o^2 \lambda^2/4$. Figure A2 shows the relationship between A_e and A_p. Note that the effective collecting aperture rapidly approaches the physical size.

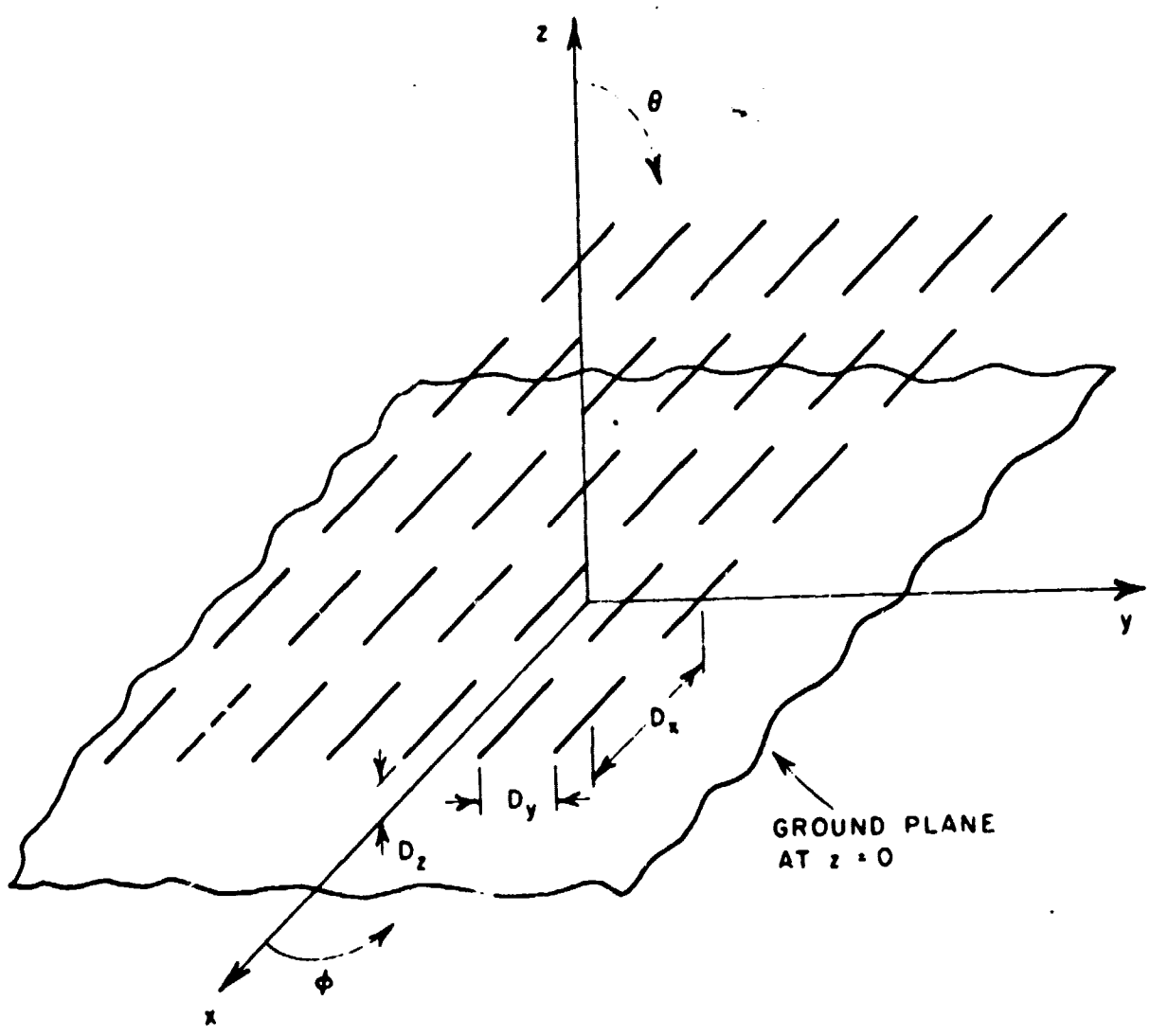

Fig. A1. Dipole array model.

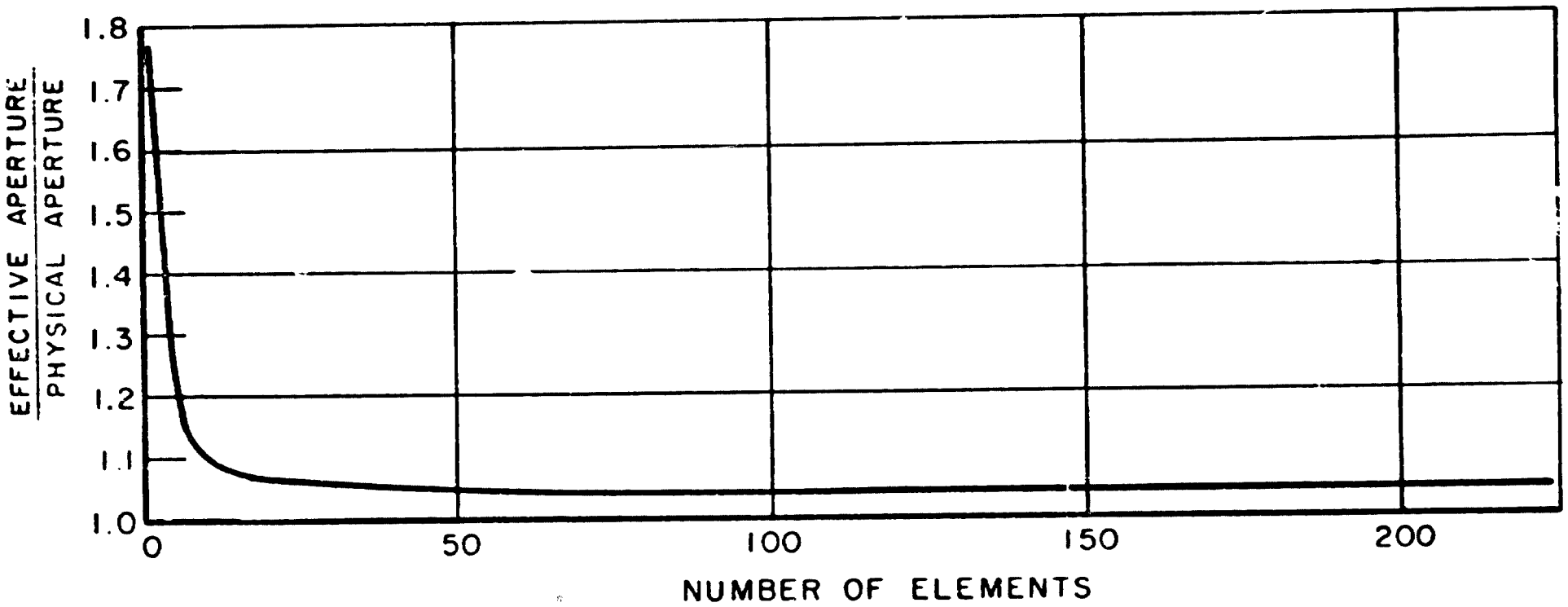

Fig. A2. Relationship between physical aperture and electrical aperture.

APPENDIX II
COMPUTER PROGRAM

This appendix includes a listing of the computer program discussed in the report. A simplified flow diagram is included to show the order in which the data is entered, calculation are performed, and reduced data is displayed.

No particular attempt was made to minimize the computer execution time; casual programming was used throughout for simplicity. The example discussed in the report with 32 possible system configurations required two minutes (about $5) using a commercial time sharing computer.

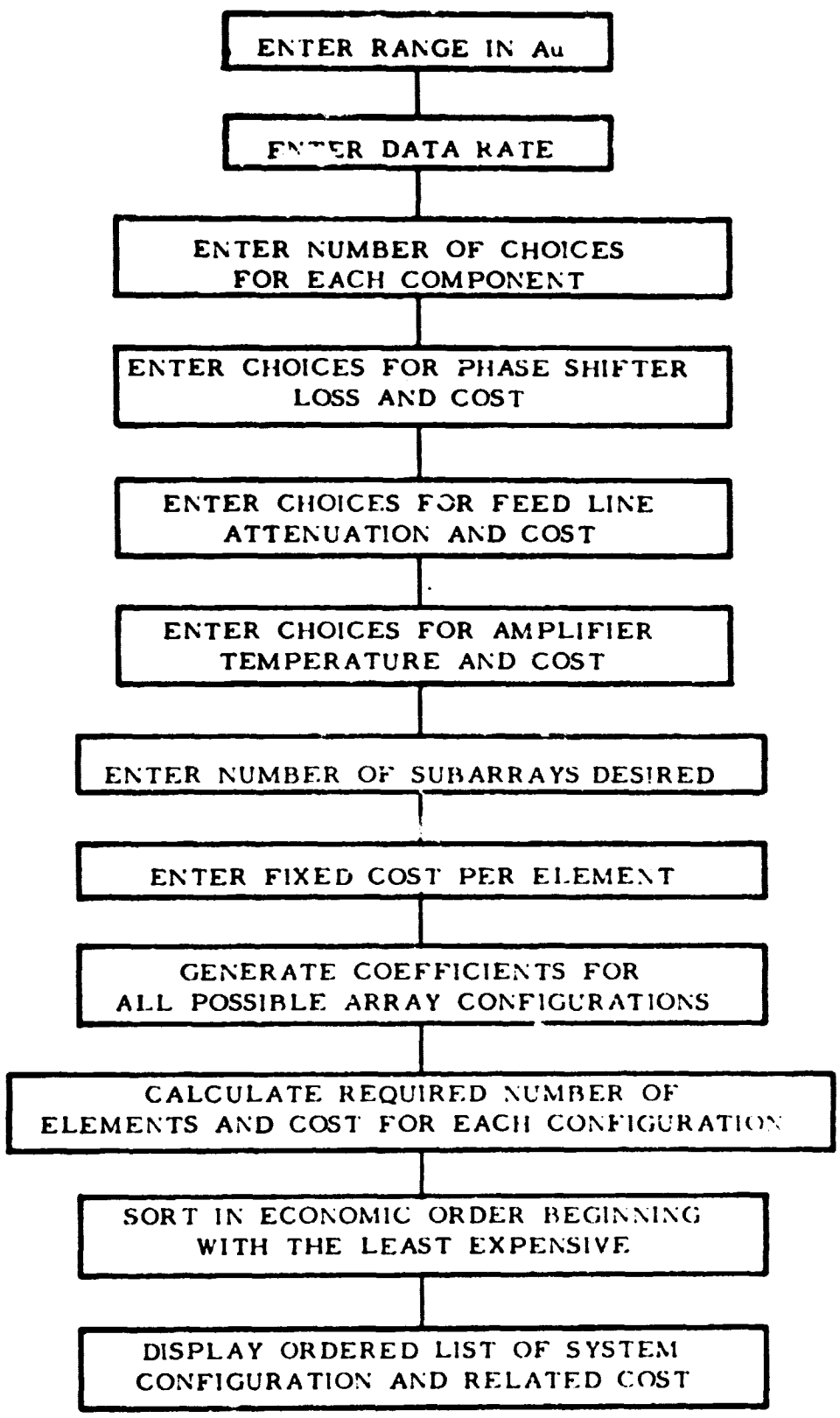

Fig. A3. Simplified flow diagram of computer listing.

```
 1.      C:COST OF PLANAR RECEIVING ARRAY OF DIPOLES FOR VARIOUS PARAM.
 2.      C: COMPUTED FOR 50 WATTS TRANSMITTER, 30 FOOT DISH
 3.      C: MAX BIT ERROR PROB=10**-5 (10 DB SNR)
 4.      DISPLAY['COST ANALYSIS FOR S BAND PHASED ARRAY OF DIPOLE ELEMEN
         TS"]
 5.      DISPLAY['     "]
 6.      DIMENSION PSLDB(5),CPS(5),DBPF(5),TAMP(5),CAMP(5),NSA(5)
 7.      DIMENSION LL(5),IFC(5),FEC(5),SNR(99),COST(99),CFL(5)
 8.      DIMENSION IC(99),NELEM(99)
 9.      99 FORMAT(F5.2,2I4,I9,F5.2,F4.1,I7,I10,I12,F9.2)
10.      DISPLAY['ENTER DISTANCE IN AU"]-
11.      ACCEPT[AU]
12.      DISPLAY['ENTER DATA RATE IN MEGABITS PER SECOND"]
13.      ACCEPT[DR]
14.      DISPLAY['ENTER NUMBER OF CHOICES FOR EACH COMPONENT"]
15.      ACCEPT[NC]
16.      TANT=9
17.      DISPLAY['ENTER PHASE SHIFTER LOSS(DB) AND COST($)"]
18.      DO 10 I=1,NC
19.      DISPLAY['  CHOICE",I]-
20.      10 ACCEPT[PSLDB(I),CPS(I)]
21.      DISPLAY['ENTER FEED LINE LOSS(DB/FT) AND COST/ELEMENT"]
22.      DO 15 J=1,NC
23.      DISPLAY['  CHOICE",J]-
24.      15 ACCEPT[DBPF(J),CFL(J)]
25.      DISPLAY['ENTER AMPLIFIER TEMP AND COST"]
26.      DO 20 K=1,NC
27.      DISPLAY['  CHOICE",K]
28.      20 ACCEPT[TAMP(K),CAMP(K)]
29.      DISPLAY['ENTER NUMBER OF SUBARRAYS DESIRED"]
30.      DO 25,L=1,NC
31.      DISPLAY['  CHOICE",L]
32.      25 ACCEPT[NSA(L)]
33.      DISPLAY['ENTER FIXED COST PER ELEMENT"]
34.      DO 26 M=1,NC
35.      DISPLAY['  CHOICE",M]
36.      26 ACCEPT[FEC(M)]
37.      DISPLAY['   FOR THE ABOVE PARAMETERS THE POSSIBLE SYSTEM CONFIG
         URATIONS AND THEIR COST ARE:"]
38.      DISPLAY['     "]
39.      DISPLAY['  PHASE      AMPLIFIER     FEED      ELEMENT      NUMB      RE
         QUIRED     TOT"]
40.      DISPLAY[' SHIFTER                    LINE       COST       S.A.      NO
         .ELEM     COST"]
41.      DISPLAY['-------------------------------------------------------
         --------------"]
42.      DISPLAY['LOSS    $     TEMP    $    DB    $    "]
43.      DISPLAY['(DB)                        /FT
                 MILL $"]
44.      NV=1
45.      DO 5 MM=1,5
46.      5 LL(MM)=1
47.      6 I=LL(1)
```

```
      J=LL(2)
      K=LL(3)
      L=LL(4)
      M=LL(5)
      DSNR=10.*ALOG10(10./NSA(L))
      FLL=1.-PBFF(J)*.23*.22
      TO=290
      PST=290
      A=-168-20*ALOG10(AU)-PSLDB(I)
      BK=(1.38*10**-23)*(.5*DR*10**6)
      PSL=EXP(-2.3*PSLDB(I)/10)
      N=10
   30 SUM=0
      II=N/10
      DO 35 NK=1,N-
   35 SUM=SUM+FLL**(NK-1)-
      Z=(FLL/(N*N))*SUM*SUM
      SIG=A+10*ALOG10(N*N)-10*ALOG10(1/Z)-
      TNOS=10*ALOG10(BK*(TO*(1-Z)+PST*(1-PSL)*Z+TANT*PSL*Z+TAMP(K)))+
     30
      SNR(II)=SIG-TNOS
      IF(SNR(II)-DSNR) 40,42,45
   40 N=N+10
      GO TO 30
   45 SLOPE=((10*II)**2-(10*(II-1))**2)/(SNR(II)-SNR(II-1))
      YINTERCEPT=(10*II)**2-SLOPE*SNR(II)
      NELEM(NV)=SLOPE*DSNR+YINTERCEPT
      GO TO 50
   42 NELEM(NV)=N*N
   50 COST(NV)=(NELEM(NV)*(CPS(I)+CFL(J)+FEC(M))+CAMP(K))*NSA(L)
      IC(NV)=NV
      NV=NV+1
      IF(NV.GT.NC**5) GO TO 90
      CALL COMB(LL,NC,5)
      GO TO 6
   90 CONTINUE
      CALL TPLSORT(1,COST,IC,NELEM,1,NC**5)
      CONTINUE
      DO 91 NV=1,NC**5-
      DO 92 MM=1,5
   92 LL(MM)=1
      IZ=1
   95 I=LL(1)
      J=LL(2)
      K=LL(3)
      L=LL(4)
      M=LL(5)
      IF(IZ.EQ.IC(NV)) GO TO 94-
      CONTINUE
      CALL COMB(LL,NC,5)
      IZ=IZ+1
      GO TO 95
   94 CONTINUE
```

```
      91 WRITE(1,99) PSLDB(I),CPS(I),TAMP(K),CAMP(K),DBPF(J),CFL(J),F
     EC(M),NSA(L),NELEM(NV)*NSA(L),COST(NV)/10**6
      CONTINUE
      END
      SUBROUTINE COMB(LL,I,J)
      IJ=1
      9 LL(IJ)=LL(IJ)+1
      IF(LL(IJ).LE.I) RETURN
      LL(IJ)=1
      IJ=IJ+1
      IF(IJ.GT.J) RETURN
      GO TO 9
      END
         SUBROUTINE TPLSORT(KODE,SEEDS,FOLLO,TAKE,JAX,LAX)
      C:   IF KODE=1,ASCENDING SORT.  IF KODE=2,DESCENDING SORT.
      C:  SEEDS IS THE ARRAY TO BE SORTED.-
      C:  FOLLO AND TAKE ARE TWO ARRAYS WHICH ARE TO BE REARRANGED
      C:  ACCORDING TO THE NEW ORDER OF SEEDS, SO THAT THE PROPER ITE
     MS
      C: WILL STILL BE CORRECTLY ASSOCIATED WITH SEEDS.
      C:  JAX IS BEGINNING LOCATION TO SORT FROM.
      C:  LAX IS END LOCATION TO SORT TO.
      IF(LAX.EQ.1) RETURN
          IF(JAX.GT.0)GOTO7
           JAX=1
        7  IF(KODE.LT.1.OR.KODE.GT.2)GOTO6
          DO 1 JO=JAX,LAX-1
          DO2 KI=JO+1,LAX
          GOTO(3,4)KODE
         3    IF(SEEDS(JO).LE.SEEDS(KI))GOTO2
          5      SAVE=SEEDS(JO)-
           SEEDS(JO)=SEEDS(KI)-
         SEEDS(KI)=SAVE
           TEMP=FOLLO(JO)
           FOLLO(JO)=FOLLO(KI)
           FOLLO(KI)=TEMP
        HOLD=TAKE(JO)-
        TAKE(JO)=TAKE(KI)
         TAKE(KI)=HOLD-
         GOTO2
         4    IF(SEEDS(JO).LE.SEEDS(KI))GOTO5
         2 CONTINUE
         1  CONTINUE
         RETURN
        6   DISPLAY['ILLEGAL CODE IN CALLING SEQUENCE."]
            DISPLAY['                    KODE=",KODE]-
          STOP
         END-
```

REFERENCES

C-1. Bailin, L.L. and Hamren, S.D., "Some Fundamental Limitations Large Antennas," in preparation.

C-2. Lindsey, W.C., "Phase Shift Keyed Signal Detection With Noisy Reference Signals," IEEE Trans. Aerospace and Electronic Systems, p. 393, July, 1966.

C-3. Oliver, B.M., "Thermal and Quantum Noise," Proc. IEEE 53, 5 pp. 436-454, 1965.

C-4. Riegler, R.L., "Microwave Radiometric Temperatures of Terrain," Report 1903-2, ElectroScience Laboratory, The Ohio State University Research Foundation; prepared under Contract NSR-36-008-027, National Aeronautics and Space Administration, Washington, D.C., June 31, 1966.

C-5. Wulfsberg, Karl N., "Apparent Sky Temperatures at Millimeter Wave Frequencies," Physical Sciences Research Papers No. 38, Air Force Cambridge Research Laboratories, July, 1964.

C-6. Siegman, E.A., "Thermal Noise in Microwave Systems," Microwave Journal, March, 1961.

C-7. Final Report, Advanced Deep Space Communication Study, Report No. P67-15, Hughes Aircraft Company, January, 1967.

C-8. Schwartz, Bennet, and Stein, Communication Systems and Techniques, McGraw-Hill Book Co., Inc., 1966.

C-9. Gardner, F.M., Phase Lock Techniques, John Wiley and Sons, Inc., 1966.

C-10. Martin, B.D., "The Pioneer IV Lunar Probe: A Minimum Power FM/PM Systems Design," Report 32-215, Jet Propulsion Laboratory, March, 1962.

C-11. Reference Data for Radio Engineers, ITT, p. 615, 1963.

C-12. Kummer, W.H., Feeding and PHase Scanning, Microwave Scanning Antennas, Vol. III, Chap. 1, R.C. Hansen, ed., Academic Press, 1966.

C-13. "Semiconductors Keep Cool Via Peltier," EDN Magazine, p. 56, a Cahners Publication, December, 1967.

C-14. Cheston, T.C. and Frank, J., "Array Antenna," Technical Memorandum TG-956, Applied Physics Laboratory, Johns Hopkins University, March 1968.

C-15. Lopex, A.R., "Nonopulse Networks for Series Feeding an Array Antenna," Digest 1967, IEEE International Symposium on Antenna and Propagation, Ann Arbor, Michigan.

C-16. Allen, J.L., "A Theoretical Limitation on the Formation of Lossless Multiple Beams in Linear Arrays," IRE Trans., Vol. AP-9, pp. 350-352, July 1961.

C-17. Blass, J., "The Multidirectional Antenna: A New Approach to Stacked Beams," 1960 IRE Trans., Vol. AP-9, pp. 350-352, July 1961.

C-18. Allen, J., et al., "Phased Array Studies," MIT Lincoln Laboratory Technical Report No. 381, pp. 299-318, March 1965.

C-19. Digest, International Symposium, PGMTT, Boston, 1967, Sessions V and VI.

D. ADAPTIVE ARRAYS

1) Introduction

An investigation of adaptive arrays is being pursued in this program because an array, composed of either dishes or small elements, can offer improved performance, and perhaps lower cost, over a single large dish antenna. This section briefly discusses the theory, experimental results, and application of the LMS adaptive array. A more complete discussion can be found in a separate report (Ref. D-4) which is to be considered a portion of this program and, consequently, this report.

Previous to this study there were two ways to combine the outputs of the subarrays in order to form an array pattern:

1) A programmed technique in which the required phase shift for each subarray is calculated from known ephemeris data.

2) A phase lock technique in which all of the subarrays are automatically made to have the same phase at the carrier frequency so that coherent combination can be achieved.

A third way has now been suggested, the LMS approach, which offers some additional improvement not possible with the above two techniques. If an interfering signal (or signals) is present in the environment of the array (for example in the sidelobes, near field, etc.) the LMS technique will automatically phase the subarrays in such a manner to direct a null of the array pattern at the interference. In principle this null pointing is also possible with programmed combining but not feasible since the array geometry, mutual coupling, and direction of interference is not usually known with sufficient accuracy.

Phase lock and LMS are both "self steering" techniques since they point the array main beam in the direction of the desired signal but they perform quite differently in the presence of the interfering signals. In fact, a phase lock system makes no attempt to reject interference, it merely aligns the phase of the carrier signal from each subarray before adding them.

2) Theoretical Description of an Adaptive Array

An "adaptive antenna" may be defined as one that modifies its own pattern, frequency response, or other parameters, by means of internal feedback control, while the antenna is operating. Such automatic control of the antenna characteristics may be used (1) to exclude interfering signals from the output of the antenna, or (2) to maintain antenna performance in the presence of a changing near-field environment, as explained below. Other uses for such antennas are also discussed in subsection IV-D.

The work to date in this area has concerned an adaptive array as shown in Fig. D-1 and is based on a feedback algorithm for least mean square error (LMS) as discussed originally by Short (Ref. D-1) and also by Widrow, et al. (Ref. D-2, D-3). In the basic form of such an antenna, $x_1(t), \cdots, x_n(t)$ represent the signals received from the individual elements of the array. These signals are multiplied by weighting coefficients, $w_1, \cdots, w_n$ and then added together to produce the array output $s(t)$. In order to control the weighting coefficients w_i, the output signal is compared with a "desired signal" $d(t)$ to produce an error signal $\varepsilon(t) = d(t) - s(t)$. (The question of how $d(t)$ is obtained is discussed below.) The error signal $\varepsilon(t)$ along with the signals $x_1(t), \ldots, x_n(t)$ are used as inputs to a feedback system which adjusts the weighting coefficients w_i. The feedback operates in such a way as to minimize $\varepsilon^2(t)$, i.e., to make the output of the array approximate the desired signal $d(t)$ as closely as possible, in a minimum squared error sense. The operation of the fedback loop may be described as follows: since the output from the array is (see Fig. D-1)

$$s(t) = \sum_i w_i x_i(t)$$

the error signal is

$$\varepsilon(t) = d(t) - \sum_i w_i x_i(t)$$

and hence the "squared error" is

$$\varepsilon^2(t) = d^2(t) - 2d(t) \sum_i w_i x_i(t) + \sum_i \sum_j w_i w_j x_i(t) x_j(t)$$

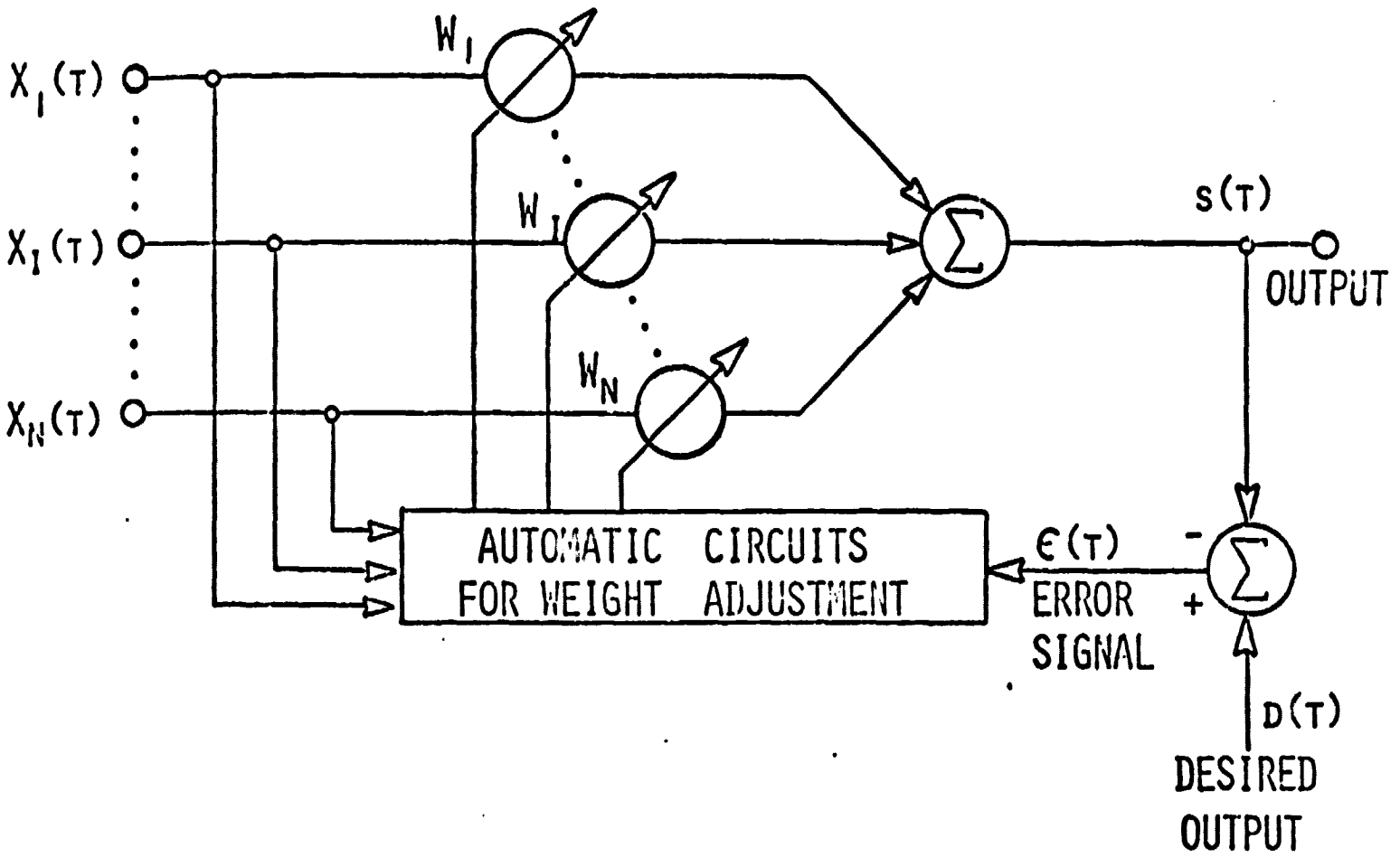

BASIC ADAPTIVE FEEDBACK SYSTEM

Fig. D-1.

$\epsilon^2(t)$ is always a positive quantity and may be used as a performance criterion for the array. The lower ϵ^2, the better is the array adjustment. At any given time, ϵ^2 is a quadratic function of the weights w_i, so the surface defined by plotting ϵ^2 versus the w_i's is a "bowl-shaped" surface with a well-defined minimum. The value of w_i can be adjusted to keep the array operating near the bottom of the bowl, i.e., to minimize ϵ^2. To do this, w_i is adjusted according to a steepest descent method by computing the gradient of ϵ^2 with respect to the w_i, and moving the w_i in the maximum downhill direction.* Specifically, compute $\nabla(\epsilon^2)$ from

$$\nabla(\epsilon^2) = \frac{\partial \epsilon^2}{\partial w_1}\,\hat{w}_1 + \frac{\partial \epsilon^2}{\partial w_2}\,\hat{w}_2 + \cdots + \frac{\partial \epsilon^2}{\partial w_n}\,\hat{w}_n$$

*Comparison of the work of Shor (Ref. D-1) and Widrow (Ref. D-3) also shows that this is identical to a steepest-ascent optimization of signal-to-noise ratio.

and then adjust each w_i so that

$$\frac{dw_i}{dt} = k_s \nabla_i(\varepsilon^2) = k_s \frac{\partial \varepsilon^2}{\partial w_i}$$

where k_s is a negative constant. Thus, if $\frac{\partial \varepsilon^2}{\partial w_i}$ indicates a large sensitivity of ε^2 to w_i, w_i is changed quickly to move toward the bottom of the bowl. If $(\partial \varepsilon^2)/(\partial w_i)$ is very small, w_i changes very slowly.

Since

$$\nabla_i(\varepsilon^2) = 2\varepsilon \nabla_i \varepsilon = -2\varepsilon X_i$$

the feedback rule is actually

$$\frac{dw_i}{dt} = -2k_s \, \varepsilon(t) X_i(t)$$

or

$$w_i(t) = -2k_s \int_0^t \varepsilon(t') \, X_i(t') dt' + w_i(o)$$

3) Summary of Experimental Results

One type of adaptive array which automatically rejects undesired or interfering signals has been studied and experimentally implemented. The complete description of this system and the measured data obtained are presented in a separate report (Ref. D-4). The array behavior is controlled by an adaptive feedback system, whose operation is based on a steepest descent minimization of error.

A two element S-band array of this type was built and the report discusses its experimentally measured antenna patterns for various desired and interfering signals. Its transient response behavior as well as the relationship of the received signal and reference signal spectral properties to the array behavior is also discussed.

The results show that such an antenna system is capable (within certain basic constraints) of automatically rejecting interfering signals under a wide variety of conditions. No a priori information concerning the angles of arrival or the detailed spectral properties (except the carrier frequency of the desired signal) are required.

4) Possible Applications for Adaptive System

Although the prime motivation for studying adaptive arrays with respect to high performance communication systems has already been mentioned, it is certainly worthwhile to consider how such an antenna type can be used in other applications. Since it is a versatile technique, it needs some further consideration before its total value is clearly understood. A number of applications have occurred to the workers on this program, and as the behavior of these antennas becomes clearer and the performance characteristics become more definitive, more applications become apparent. These applications are worth discussing because they provide the motivation and justification for working in this portion of the program. However, it has now become apparent that adaptive arrays have versatility which can be employed successfully in other areas. Consequently, this subsection will be devoted to a qualitative description of some of the areas where adaptive antennas appear to be useful.

The first and perhaps most important application of adaptive antennas will be as a "design tool" for conformal arrays--for arrays whose elements must be placed on a curved surface. In practice, it is difficult to design the phasing networks for a conformal array (particularly if the antenna beam must be electronically scanned) because the element patterns and mutual impedances are different for each element. Adaptive antennas offer a possible solution to this problem. A conformal array can be built on the surface on which it is to be used, and then by going through a special test procedure, while the antenna is operated in an adaptive mode, the optimum set of weighting coefficients can be found. The test procedure would consist of illuminating the antenna with a test signal from various directions in space, while using the same test signal for the desired signal d(t). The adaptive feedback will find, for each direction of illumination, the best set of weighting coefficients. In other words, the antenna will design its own aperture distribution. The coefficients found can be stored and used later in a normal scanning mode.

A second use for adaptive antennas is in situations where the antenna is subject to a changing near-field environment, and it is necessary to recalibrate or readjust the pattern of the antenna during such changes. There are many examples of this. For instance, antennas used for aircraft control around airports must have patterns which are accurately known. After such an antenna is installed and operating, it may happen that at a later date airport officials would like to put up a new building, but are unsure what effect the presence of the building may have on the antenna pattern. If the antenna could be operated in an adaptive mode, it could be recalibrated periodically as the building is being constructed, using a test procedure similar to the one outlined above.

A third use for adaptive antennas is for communication antennas that are resistant to jamming and other forms of interference. By

providing a "desired signal" d(t) and a test signal on each element of the array with a phase corresponding to a given "lock angle", an adaptive antenna has the property that it receives signals from the desired direction, but tends to form nulls on signals arriving from other directions. (This behavior is described by Widrow, et al., Ref. D-3). If an interfering signal appears from a certain direction, the weighting coefficients in the array readjust themselves to form a null in that direction.

As a fourth possibility, the same technique as used for anti-jamming antenna above can also be used to eliminate low-angle clutter from a radar antenna. The requirement for operating an antenna at low elevation angles results in a difficult pattern synthesis problem, namely, the synthesis of a main beam with a nonsymmetric sidelobe structure. The sidelobes on the "ground" side must be minimized at the expense of the "sky" sidelobes. The adaptive array achieves the desired characteristics in an optimum way by minimizing the undesired power return from wherever it may arrive and at the same time maximizing the desired signal.

Many other possibilities exist. It is clear that the applications for adaptive arrays, although of a special nature, are sufficiently numerous that study in this area is worthwhile.

REFERENCES

D-1. S.W.W. Shor, J. Acous. Soc. Am., Vol. 39, No. 1, Jan. 1966, pp. 74-78.

D-2. B. Widrow, "Adaptive Filters I: Fundamentals," Techn Report No. 6764-6, December 1966; prepared under Contract No. DA-01-021, AMC-90015(Y), U.S. Army Materiel Command, NIKE-X Project Office, Redstone Arsenal, and under Contract NOBsr-95038, Naval Ship System Command, Dept. of the Navy.

D-3. B. Widrow, P.E. Mantey, L.J. Griffiths, B.B. Goode, Proc. IEEE, Vol. 55, No. 12, December 1967, pp. 2143-2159.

D-4. R.L. Riegler and R.T. Compton, "An Adaptive Array for Interference Rejection," ElectroScience Laboratory Report 2522-4, in preparation.